DISS. ETH NO. 24917

Towards improving joint replacement:

Which characteristics of design and activity govern joint kinematics in total knee arthroplasty?

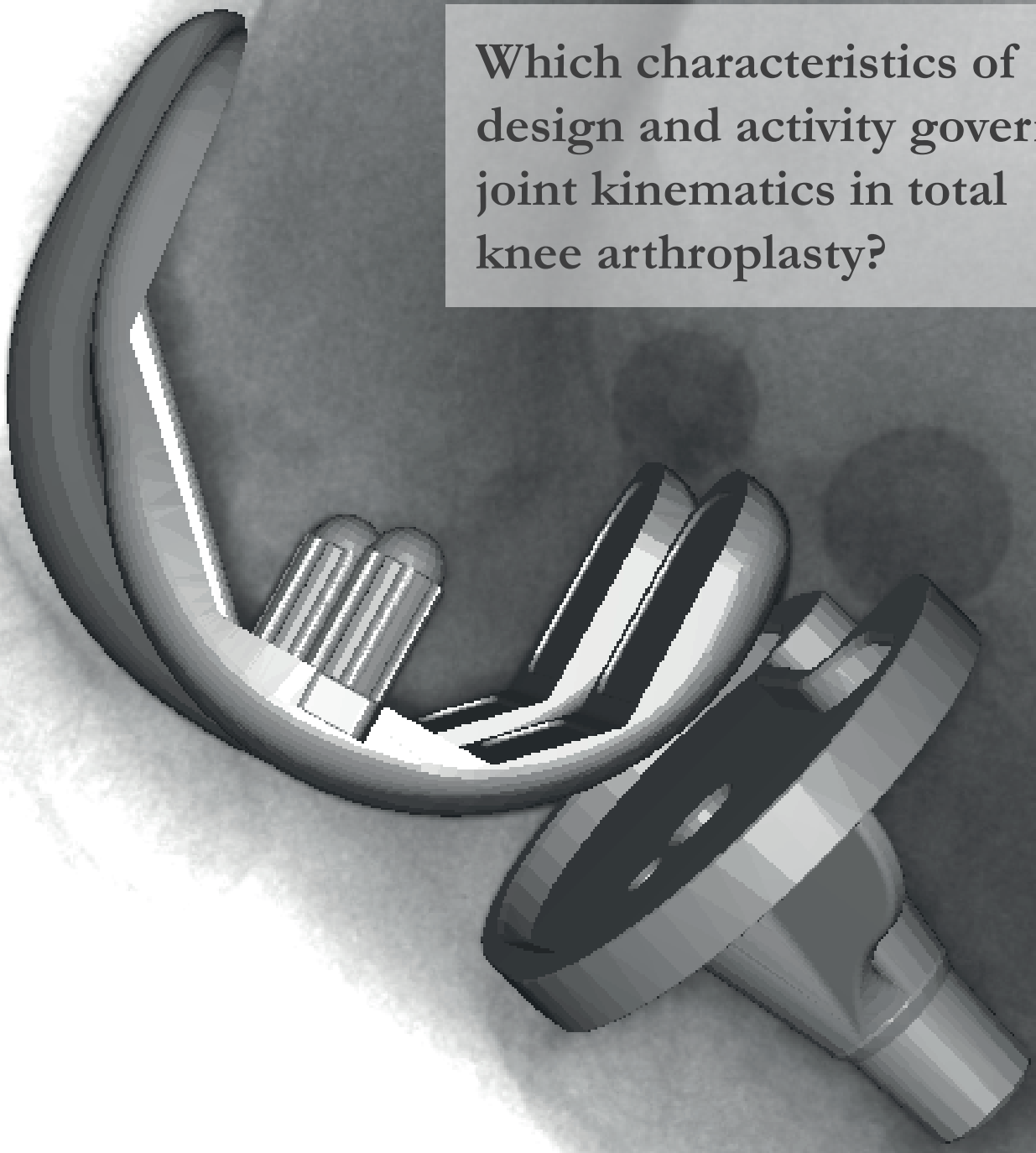

Pascal Schütz

2018

DISS. ETH NO. 24917

Towards improving joint replacement: Which characteristics of design and activity govern joint kinematics in total knee arthroplasty?

A thesis submitted to attain the degree of

DOCTOR OF SCIENCES of ETH ZURICH
(Dr. sc. ETH Zurich)

presented by

PASCAL SCHÜTZ
MSc ETH HMS, ETH Zurich
born on 16.05.1985
citizen of Luzern, LU

accepted on the recommendation of

Prof. Dr. William R. Taylor, examiner
Dr. Renate List, co-examiner
Prof. Dr. Kamiar Aminian, co-examiner

2018

Statement of originality

I hereby confirm that I am the sole author of the written work here enclosed and that I have compiled it in my own words. Corrections of form and content were partially written with the support of the supervisors.

Pascal Schütz

Acknowledgements

I want to express my gratitude to all the people who have contributed to this work and supported me during all the years of my dissertation. They have laid the foundation of this project, advised me during the process, helped with the measurements or inspired me in interesting discussions and provided an enjoyable work environment.

I had the privilege to work with a unique technology allowing new insights into knee motion. Many people were involved in the development and construction of the moving fluoroscope and subsequent data analysis. Therefore, I want to thank Prof. Dr. Edgar Stüssi, Prof. Dr. Stephen Ferguson, Prof. Dr. William R. Taylor, Dr. Hans Gerber, Dr. Monika Zihlmann, Dr. Mauro Foresti, Dr. Renate List, Jaqueline Stucki, Marco Hitz and Peter Schwilch for their contribution to the development of the moving fluoroscope. Particular thanks go to Hans, Marco and Peter for their technical support during the measurements of my project.

Furthermore, I want to thank Barbara Postolka and Marina Hitz who contributed with their master thesis to my project and supported me during the complex measurements. These measurements were only possible with the help of many people. Special thanks to Michi Angst, Karin Schnüriger, Stefan Plüss, Michi Plüss, Thomas Zumbrunn and all the students who supported me during the measurements and post-processing of the data.

I would also like to thank all the subjects who participated in the studies, as well as Dr. med. Reto Grünig, PD Dr. med. Sandro Fucentese, PD Dr. med. Peter Koch, Christel Ilg, Uta Bonitz, Nathalie Kühne and Michel Schläppi for supporting the recruitment of the subjects. For the good cooperation, I want to thank all the involved people from the Charité-Universitätsmedizin Berlin. Then I much appreciated the support and enthusiasm of Prof. Dr. med. Michael A. R. Freeman and Prof. Dr. med. Vera Pinskerova for this project. The funding from DePuy Synthes (Johnson and Johnson), Medacta International, Commission for Technology and Innovation (CTI) Switzerland and RMS Foundation made the different studies possible.

Most of all I want to express my gratitude to Dr. Renate List, Prof. Dr. William R. Taylor, PD Dr. Dr. Silvio Lorenzetti and all my colleagues in the movement biomechanics group for their big support during the time at the institute.
Bill and Renate gave me the opportunity to conduct the PhD in the clinical biomechanics group and working with them has always been a pleasure and very inspiring. The way Renate is doing scientific work has motivated me from the very first day - detailed in planning and precise in conducting measurements to acquire high quality data, self-reflecting and critical during data analysis and always open to collaborations and new ideas. Combined with her empathy when working with patients or colleagues, she has always been an example for me. Sincere thanks to you Renate, for your cordial cooperation, valuable inputs and discussions and especially providing me always great support.
I would like to thank Bill, who has been my supervising professor, for his confidence and support. I have learned a lot from his experience, his passion for writing and visionary ideas. He has always asked the relevant questions and pointed out the key points of a study regarding clinical application and came up with new ideas. His input and support added significant quality to this work. In addition, I really appreciated his open door for problems and his support regarding my career.
Many thanks also to Silvio, who has supported me during my first steps at the institute and later during my PhD, especially with a good cooperation regarding lab issues.

Renate, Bill and Silvio have always created a great atmosphere in the group, with organising generous sport or social group events as well as with their warm manner to lead the group. Every single group member contributed to the extremely enjoyable time. I especially want to thank Dr. Navrag Singh, Dr. Roland Zemp, Dr. Florian Schellenberg, Dr. Niklas Ignasiak, Stefan Plüss, Florian Vogl, Michi Angst, Barbara Postolka, Hamed Hosseini Nasab, Marina Hitz, Karin Schnüriger and Lynn Ellenberger for their general support, valuable inputs, interesting discussions and for having made work a memorable experience.

Finally, I want to cordially thank my beloved family for their personal and financial support during my journey. Together with all my friends they have established the basis to always find energy, also during difficult times. A special thank goes to Martina who has always been there for me, during exciting as well as stressful times of my dissertation. Beside the emotional support, she has also provided practical support with proofreading of the manuscript – thank you!

Abstract

The knee is a highly complex joint in the human body and a perfect interaction between the joint structures is needed in order to ensure a high degree of functionality throughout a range of activities of daily living as well as recreational and sports activities. Knee disorders such as osteoarthritis can therefore affect patients through limiting range of motion and producing pain in the joint, leading to immobility and restricting independent living. Total knee arthroplasty (TKA) has become a standard surgical procedure to relieve pain and restore function to the tibio-femoral joint, with the aim to allow a return to active life. However, some 16-30 % of TKA patients are known to be unsatisfied with their implant function during knee bending and gait activities. To provide good functionality in performing daily activities, reproduction of healthy tibio-femoral kinematics could provide a crucial route towards improving implant designs, particularly with regard to reducing instability, maintaining a sufficient range of joint motion, and avoiding overloading of the surrounding soft tissue structures. Here, quantifying the *in vivo* joint kinematics can allow an evaluation of critical measures of joint functionality in an objective manner, but until now, the relative role of implant design and patient activity on governing implant kinematics *in vivo* throughout dynamic gait activities remains unknown.
This thesis therefore directly targets an understanding of the role of implant design and patient activity, and thereby aims to lay the foundations for understanding the mechanisms underlying instability, range of motion, and soft tissue overloading.

With the development of the moving fluoroscope at the Institute for Biomechanics, ETH Zürich, it is now possible to evaluate the *in vivo* tibio-femoral motion of implant components throughout complete cycles of dynamic activities, including level walking, downhill walking and stair descent. Such technology opens perspectives for investigating joint kinematics without errors due to soft tissue artefact, and has been utilised in this thesis for understanding the influence of different implant designs on joint kinematics during a range of activities of daily living. To ensure that the use of such technology does not influence subjects' movement, and is therefore appropriate for the

study design, possible effects of the moving fluoroscope on gait patterns was initially investigated in a study including subjects walking, both with and without the moving fluoroscope. The results established that healthy subjects walked with a decreased gait velocity with the moving fluoroscope, which became comparable to the self-selected gait speeds reported in subjects after TKA. Importantly, the resulting subjects' gait characteristics were comparable to those during unimpeded slow walking. As a result, it was concluded that the methodology was appropriate for examining joint kinematics in TKA cohorts.

In a first patient study, sitting and rising from a chair as well as level walking and stair descent, were investigated and the characteristics of activity were identified as an important factor governing the implant kinematics. The results presented in this study showed that flexion angle alone, as in knee bending activities, cannot fully explain tibio-femoral TKA kinematics during gait activities. Therefore, beside activities with continuous flexion, gait activities should be included in a complete evaluation of implant design.

In order to understand the effect of implant design on the more complex kinematic behaviour during gait activities, five different types of implant designs were then investigated. Although implant design was clearly able to constrain joint kinematics through e.g. high levels of congruency, individual differences between the subjects were clearly observed under unconstrained conditions. Here, additional subject specific factors such as implantation, soft tissue constraints, and muscle activity, also seemed to play an important role in governing the kinematics, particularly when freedom was allowed by the implant design. These subject-specific datasets are now actively being used as a basis for driving numerical simulations in the form of musculoskeletal and finite element models, and aim to provide an avenue for elucidating the relative importance of soft tissue structures and muscle activity for guiding joint kinematics.

Validation of the accuracy of such models is extremely challenging for the biomechanics community. One of the only ways validation can currently be achieved is direct comparison of the predicted forces against measured internal joint contact forces, but access to such data has been astonishingly difficult. In attempt to not only foster a new understanding of how *in vivo* knee joint kinematics and contact forces are interlinked – and thereby impact biomechanical interpretation of any new knee replacement design – but also provide opportunities for worldwide biomechanical collaboration, this thesis lays the foundation for making comprehensive datasets of human kinematics and kinetics available. Here, a collaborative effort with the Charité – Universitätsmedizin Berlin, Germany, has created the "Comprehensive Assessment of the Mus-

culoskeletal System" (CAMS-Knee) datasets, which are now becoming available for public release. To create these unique datasets of the lower limb musculoskeletal system, measurements of six subjects with instrumented knee implants, synchronized with a moving fluoroscope and other measurement techniques (including whole body kinematics, ground reaction forces (GRF), video data, and electromyography (EMG) data) for multiple complete cycles of five activities of daily living, were performed. These data thereby provide state-of-the-art access for validation of biomechanical models and for further understanding of the factors driving implant kinematics.

In conclusion, the presented thesis has successfully investigated characteristics of activity and implant design and their role in governing *in vivo* TKA kinematics during daily activities. For the first time the TKA kinematics of different implant designs were analysed throughout complete cycles of level walking, downhill walking and stair descent. This body of work clearly shows that joint kinematics during dynamic gait activities cannot be explained by knee flexion angle alone, and that characteristics of activity and implant design play a dominant role.

Zusammenfassung

Das Knie ist ein hochkomplexes Gelenk im menschlichen Körper und benötigt ein perfektes Zusammenspiel der verschiedenen Gelenksstrukturen, um einen hohen Grad an Funktionalität während verschiedener Alltags-, Freizeit- und sportlichen Aktivitäten zu ermöglichen. Entsprechend gross sind daher die Auswirkungen von Knieproblemen, wie beispielsweise bei Osteoarthritis. Kniebeschwerden limitieren Betroffene in ihrem Bewegungsumfang, verursachen Schmerzen und können ein unabhängiges Leben durch Immobilität stark einschränken.
Knie-Totalendoprothesen sind daher zu einem chirurgischen Standardeingriff geworden, um von Schmerzen zu befreien und die Funktionalität des tibio-femoralen Gelenks wiederherzustellen. Ziel der Prothesen ist dabei, dass Betroffene zu einem unabhängigen und aktiven Leben zurückkehren können. Trotzdem sind 16-30 % der Patienten nicht zufrieden mit der Funktion ihres Implantats während alltäglicher Bewegungen wie Kniebeugen und sonstigen Gangaktivitäten.
Um eine gute Funktionalität bei der Ausführung von Alltagsaktivitäten zu ermöglichen, ist die Nachbildung der gesunden tibio-femoralen Kinematik ein wichtiger Ansatz, um Implantat-Designs zu verbessern, speziell um Instabilität zu reduzieren, die Gelenkbeweglichkeit hinreichend zu erhalten und Überbelastungen der umliegenden Weichteilstrukturen zu verhindern. Hier kann die Quantifizierung der *in vivo* Gelenkskinematik eine objektive Beurteilung von kritischen Messgrössen für die Gelenksfunktionalität ermöglichen. Bislang fehlen allerdings Untersuchungen zum Einfluss von Implantat-Design und Patientenaktivität auf die Gelenksbewegung *in vivo* während dynamischer Gangaktivitäten.

Diese Doktorarbeit hat daher zum Ziel, Erkenntnisse über den Einfluss von Implantat-Design und unterschiedlichen Alltagsbewegungen auf die Gelenkskinematik zu liefern, um Mechanismen besser zu verstehen, welche zu Instabilität, eingeschränktem Bewegungsumfang und Überbelastung der Weichteilstrukturen führen können.

Um den Einfluss verschiedener Implantat-Designs auf die Gelenksbewegung zu untersuchen,

wurde das „Moving Fluoroscope“ verwendet, eine Technologie, die am Institut für Biomechanik der ETH Zürich entwickelt wurde. Sie ermöglicht, die tibio-femorale Bewegung der Implantat-Komponenten während kompletter Zyklen von dynamischen Gangaktivitäten *in vivo* zu messen, einschliesslich Gehen auf ebener Fläche, Abwärtsgehen und Treppe hinuntersteigen. Diese Technologie eröffnet neue Perspektiven auf die Untersuchung der Gelenkskinematik ohne Fehler aufgrund von Weichteilartefakten.
Um sicher zu stellen, dass sich das „Moving Fluoroscope“ für das Studiendesign eignet und die Bewegung der Probanden nicht beeinflusst, wurde eine initiale Gangstudie durchgeführt. Dabei wurden mögliche Effekte des „Moving Fluoroscope“ auf die Gangmuster von Probanden bei Wiederholungen mit und ohne „Moving Fluoroscope“ untersucht. Die Resultate zeigten, dass sich gesunde Probanden bei Wiederholungen mit dem „Moving Fluoroscope“ mit reduzierter Ganggeschwindigkeit bewegen, die jedoch vergleichbar ist mit Ganggeschwindigkeiten von Patienten mit Knieprothesen in anderen Studien. Wichtig, die resultierenden Gangmuster der Probanden mit dem „Moving Fluoroscope“ waren vergleichbar mit Mustern bei unbeeinflusstem, langsamem Gehen. Aufgrund dieser Resultate wurde das methodische Vorgehen mit dem „Moving Fluoroscope“ für geeignet befunden, um die Gelenkskinematik bei Probanden mit Knieprothesen zu untersuchen.

In einer ersten Studie wurden Bewegungsabläufe mit einem Stuhl (Aufstehen und Absitzen) untersucht sowie Gehen auf ebener Fläche und Treppe hinuntersteigen. Die Merkmale der Aktivitäten wurden als wichtige Faktoren identifiziert, welche die Implantat-Kinematik beeinflussen. Die Resultate zeigten, dass der Flexionswinkel alleine, wie dies bei Kniebeugeaktivitäten gefunden wurde, die tibio-femorale Implantatkinematik während Gangaktivitäten nicht vollständig erklären kann. Deshalb sollten zukünftig neben Aktivitäten mit kontinuierlicher Flexion auch Gangaktivitäten in eine komplette Überprüfung von Implantat-Designs eingeschlossen werden.

Um den Effekt von Implantat-Design auf das komplexere kinematische Verhalten während Gangaktivitäten zu verstehen, wurden anschliessend fünf verschiedene Implantat-Design-Typen untersucht. Obwohl das Implantat-Design die Kinematik klar einschränken konnten, durch z.B. hohe Kongruenz, wurden unter uneingeschränkten Bedingungen Unterschiede zwischen den verschiedenen Probanden beobachtet. In diesem Fall scheinen zusätzliche probandenspezifische Faktoren wie die Ausrichtung bei der Implantierung, Weichteilstrukturen und Muskelaktivität auch eine wichtige Rolle zu spielen bei der Führung der Kinematik, speziell, wenn Bewegungsfreiheit durch das Implantat-Design erlaubt wird.

Um diese relative Wichtigkeit probandenspezifischer Faktoren bei der Steuerung der Gelenkskinematik zu ergründen, können die erhobenen probandenspezifischen Datensätze über die vorliegende Doktorarbeit hinaus als Inputdaten für numerische Simulationen in Form von muskuloskelettaler Modellierung und finiter Elemente-Modellierung verwendet werden. Die Validierung der Genauigkeit von solchen Modellen ist allerdings eine grosse Herausforderung in der Biomechanik. Der direkte Vergleich der berechneten Kräfte mit gemessenen internen Kontaktkräften im Gelenk ist eine der wenigen Möglichkeiten, wie eine solche Validierung durchgeführt werden kann. Der Zugang zu solchen Daten war bislang allerdings sehr schwierig.

Hier bot die Zusammenarbeit mit der Charité – Universitätsmedizin Berlin, Deutschland, eine einzigartige Möglichkeit, einen Datensatz mit internen Kräften (instrumentierte Knieprothese) synchron mit der Gelenksbewegung aufzuzeichnen. Die in diesem Zusammenhang als weiterer Aspekt dieses Doktorats erhobenen Daten ermöglichen eine Validierung von biomechanischen Modellen und ein vertieftes Verständnis der Faktoren, welche die Implantat-Kinematik steuern. Für diesen Datensatz wurden Messungen mit sechs Probanden mit instrumentierter Knieprothese für mehrere komplette Zyklen von fünf Alltagsaktivitäten durchgeführt, synchronisiert mit dem „Moving Fluoroscope“ und anderen Messtechniken (inklusive Ganzkörperkinematik, Bodenreaktionskräften, Videoaufnahmen und Elektromyographie-Daten).
Der erstellte «Comprehensive Assessment of the Musculoskeletal System» (CAMS-Knee) Datensatz des muskuloskelettalen Systems der unteren Extremitäten soll ein neues Verständnis der Interaktion von *in vivo* Gelenkskinematik und Kontaktkräften fördern und für die Öffentlichkeit verfügbar werden. Damit legte diese Doktorarbeit die Basis, um umfangreiche Datensätze menschlicher Kinematik für eine weltweite biomechanische Zusammenarbeit zur Verfügung zu stellen.

Zusammenfassend kann gesagt werden, dass die Merkmale von Aktivität und Implantat-Design sowie deren Rolle bei der Steuerung der *in vivo* Implantat-Kinematik während Alltagsaktivitäten erfolgreich untersucht wurden. Zum ersten Mal wurde die Implantat-Kinematik von unterschiedlichen Implantat-Designs während kompletter Gangzyklen (Gehen auf ebener Fläche, Abwärtsgehen und Treppe hinuntersteigen) analysiert. Diese Arbeit hat klar gezeigt, dass die Gelenkskinematik nicht alleine durch den Flexionswinkel des Knies erklärt werden kann und dass die charakteristischen Merkmale von Aktivität und Implantat-Design eine wichtige Rolle spielen.

Contents

List of Figures

List of Tables

Abbreviations

A-P	Anterior-posterior
ASI	Absolute symmetry index
BMI	Body mass index
BW	Body weight
CAD	Computer-aided design
CAMS	Comprehensive Assessment of the Musculoskeletal System
CMC	Coefficient of multiple correlation
CoP	Centre of pressure
CR	Cruciate retaining
CT	Computed tomography
EMG	Electromyography
f	Female
FluMo	Moving Fluoroscope
GCA	Geometric center axis
GRF	Ground reaction force
KOOS	Knee injury and osteoarthritis outcome score
lat	Lateral
LED	Light-emitting diode
LSD	Least significant differences
m	Male
max	Maximum
med	Medial
min	Minimum
MRI	Magnetic resonance imaging
MVC	Maximal voluntary contraction
p-d	Proximo-distal
PS	Posterior-stabilized
ROM	Range of motion
RSA	Radiostereometric analysis
SD	Standard deviation
SPM	Statistical parametric mapping
TKA	Total knee arthroplasty
TTL	Transistor-transistor logic
UC	Ultra-congruent
VAS	Visual analog scale
WOMAC	Western Ontario and McMaster Universities osteoarthritis index

Chapter 1

Introduction and motivation

The knee is a highly complex joint in the human body. A perfectly balanced cooperation between rigid bones, covered by cartilage to minimise friction, passive soft tissue structures guiding and constraining the joint movement and the active muscles driving the knee joint motion is needed to perform a variety of demanding activities. Both, a large range of motion in all six degrees of freedom and stabilisation during impact situation is required to perform the activities of daily life as well as recreational and sports activities. Any problem with the knee joint therefore affects the subject seriously.

With age the prevalence of knee osteoarthritis increases and beside age, obesity, abnormalities in joint shape, injury and physical activity were identified as risk factors [1, 2]. Osteoarthritis is a degenerative disease of the joint cartilage and the underlying subchondral bones and is associated with severe pain. Functional limitations and pain in the knee joint lead to immobility and restrict the ability of a person to successfully complete the tasks of daily living. In a later stage of osteoarthritis total knee arthroplasty (TKA) has become a standard surgical procedure to relieve pain and restore the function of the tibio-femoral joint [3–5]. A well-functioning joint after TKA is essential for independent living and for a good quality of life. Nowadays, the elderly population stays in general longer active and expects to return to higher levels of activity [6] and therefore increases the requirements for TKA regarding functionality.

In TKA, as in every orthopaedic procedure, patient satisfaction is the ultimate goal. However, still 15-20 % of primary TKA patients were not satisfied with the outcome [7–9] due to pain or impairments in joint function. Regarding function during daily activities, 16-30 % were not satisfied with their outcome depending on the activity [7]. While pain and joint function were important for patient satisfaction, the main reasons leading to early failure in TKA and possible

revision surgery were aseptic loosening, excessive wear of the polyethylene inlay and instability [10].

To avoid early failure and provide good functionality in performing daily activities, reproduction of healthy tibio-femoral kinematics could provide a crucial route for allowing a large range of motion without overloading the surrounding soft tissue structures [11, 12]. While patient satisfaction is highly subjective and driven by expectations of the patient [7], TKA kinematics can provide objective measures, to understand the underlying mechanisms leading to early failure or unsatisfactory outcomes in general, and to iteratively improve surgical techniques as well as the development of innovative implant designs, with the goal of mimicking healthy knee kinematics.

Therefore, the tibio-femoral kinematics including condylar motion has been excessively investigated in TKA as well as healthy knees, as a function of knee flexion angle, during activities including continuous flexion or extension [5, 12–31]. It remains unclear whether the description of condylar motion as a function of flexion is also valid for dynamic gait activities with a change in loading condition and movement direction. Imaging techniques, like videofluoroscopy, allow an accurate assessment of condylar motion with an appropriate measurement frequency to measure dynamic tasks. However, due to the limited field of view of static system the assessment of knee joint kinematic is limited to highly restricted knee bending motions or the analysis of only a portion of the whole movement. This technological limitation is the reason for the lack in knowledge about the kinematic behaviour of the knee throughout complete cycles of gait activities. However, the most frequent and challenging activities in daily life, causing difficulties for subjects with knee disorders [7] or knee implants [6], like stair descent [32, 33] or downhill walking [34, 35] should be included in a complete assessment of the healthy knee and to evaluate a TKA.

With the development of dynamic systems [36, 37] like the moving fluoroscope [37–39], developed at the Institute for Biomechanics, it's now possible to evaluate the tibio-femoral motion of the implant components, with the needed accuracy, during full cycles of dynamic level walking, downhill walking and stair descent.
The moving fluoroscope consists of a conventional C-arm mounted on an automated trolley (Figure 1.1), controlled by a wire sensor attached to the knee of the subject, allowing real time tracking of the knee in horizontal and vertical direction [37, 39]. The videofluoroscopic system acquires images of the knee with a frequency of 25Hz, while the moving fluoroscope is following the knee motion during the gait activity. The acquired two dimensional fluoroscopic images are

then corrected for distortion and the projection parameters of the fluoroscopic system is determined based on images of a calibration device [38]. The 3D geometry of the implant is then fitted to the 2D fluoroscopic image, using a registration algorithm, to determine pose and orientation of the implant components [39–41].
With single plane videofluoroscopy, translations in medio-lateral direction cannot be analysed with the required accuracy (out of plane error up to 3mm). However, the the small ranges found in studies investigating TKA kinematics or healthy knee kinematics during complete gait cycles using dual plane fluoroscopy [36, 42] showed, that main translation occurs in the anterior-psterior (A-P) direction, suggesting that in terms of translation, analysis in the sagittal plane is sufficient for gait activities.
The moving fluoroscope technology provides unique access to *in vivo* implant kinematics throughout complete cycles of dynamic gait activities. Using this technology, the impact of the activity on TKA kinematics as well as the ability of implant designs to govern the implant motion can now be investigated in patient studies.

Therefore, with the goal of providing a better understanding of the factors driving the *in vivo* kinematics in TKA, including complete cycles of dynamic gait activities, this doctoral thesis includes the following aims:

- **Aim 1:** Investigating the influence of the moving fluoroscope on gait characteristics.
- **Aim 2:** Examination of task dependency including activities with continuous knee flexion and gait activities.
- **Aim 3:** Kinematic evaluation and comparison of TKA designs during level walking, downhill walking and stair descent.
- **Aim 4:** Acquisition of a comprehensive data set including simultaneous measurement of TKA kinematics and internal joint forces.

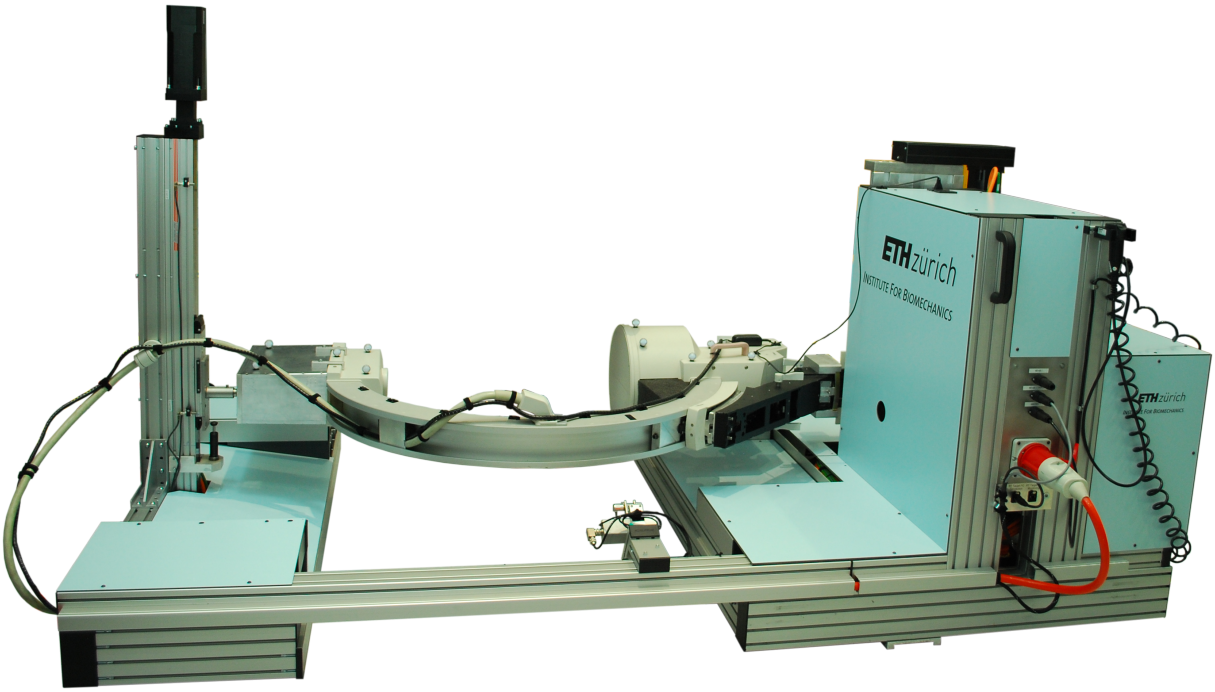

Figure 1.1: Moving fluoroscope used to track the knee throughout complete cycles of gait activities. Figure adapted from List et al., 2017 [37].

1.1 Outline of the thesis

This thesis is structured into **9 chapters**. **Chapters 3 to 6** are based on peer-reviewed scientific articles, published or submitted to an international scientific journal.

Chapter 2 provides information about different measurement methods to analyse tibio-femoral kinematics and conventions to describe knee motion. In addition, an overview of current findings about the kinematics of the healthy knee as well as TKA kinematics of different implant designs is presented.

The possible influence of distracting factors, associated with the moving fluoroscope, on the gait characteristics of subjects when walking with the moving fluoroscope, is analysed in **chapter 3**.

Chapter 4 shows the ability of the moving fluoroscope to investigate kinematics including condylar motion during chair sitting, level walking and stair descent and points out the importance of analysing complete cycles of gait activities in a complete evaluation of total knee arthroplasty design.

Based on these findings, the impact of the design concept on the implant kinematics during level walking, downhill walking and stair descent is examined in **chapter 5**.

Interindividual differences found in the results between the subjects suggest other factors related to soft tissue structures to be involved in governing the tibio-femoral kinematics. To investigate the role of soft tissues, namely ligaments and muscles, musculoskeletal modelling is necessary. The collected data presented in **chapter 4 and 5** can be used as input data for modelling, but validation of these models remains a challenge due to unknown internal forces.

To include internal forces in a comprehensive dataset, an instrumented implant was measured with the moving fluoroscope. The methodology and exemplarily results were presented in **chapter 6**. This comprehensive dataset can now be used for validation in modelling as well as for a variety of scientific questions.

In **Chapter 7**, the findings of the studies presented in the previous chapters are summarized and the collective results discussed. Limitations of the thesis and implications for future studies are discussed in **chapter 8**, before presenting the conclusions in (**chapter 9**).

Chapter 2

Kinematics of the tibio-femoral joint

This section contains background information about measurement methods and description of tibio-femoral kinematics as well as an overview of the current findings in the literature regarding healthy and implant knee kinematics.

2.1 Evaluation of tibio-femoral kinematics

2.1.1 Measurement technologies

In human movement science, motion capture is the most employed tool to analyse full body kinematics and joint kinematics [43–48]. Reflective or active skin markers on the body segments are tracked to determine relative motion between the segments. Using this technique, tibio-femoral kinematics have been investigated in subjects with healthy knees as well as in subjects with a knee replacement [32, 49–51]. Due to relative motion between the skin marker and the underlying bones [46, 52], this technique is limited in its accuracy. The described skin movement artefacts limit the analysis of ab/adduction, internal/external and A-P translation in the human knee joint [53–56]. Different approaches to reduce skin movement artefacts have been proposed and evaluated [52, 56–64]. These include numerical, functional and geometrical approaches to reduce the effect of skin marker motion relative to the underlying skeletal structures [46, 62]. However, the motion of the skin is extremely complex and the achieved accuracy still not sufficient to access the subtle changes in axial rotations in the transverse plane, ab/adduction in the frontal plane and especially condylar A-P motion relative to the tibial plateau [62]. For

a complete understanding of the tibio-femoral joint kinematics other methods are needed to provide a reasonable accuracy.

In cadaveric studies [27, 28] condylar motion during flexion has been studied, but was limited by the absence of muscular contraction and physiological loading patterns.

Bone pins, directly screwed into the bone and captured with a motion capture system, allow to measure the motion of the bones *in vivo*, without soft tissue artefacts, during activities of daily living [42, 54]. This highly invasive technique cannot be applied to a larger study population due to ethical reasons and it remains unclear if the bone pins and the anaesthesia might lead to altered motion patterns.

Imaging techniques like magnetic resonance imaging (MRI) [28, 30, 31], radiostereometric analysis (RSA) [65] and fluoroscopy [12, 29, 66, 67] were successful in analysing tibio-femoral motion including condylar motion *in vivo*, without soft tissue artefacts, in weight bearing and non weight bearing situations in subjects with healthy knees as well as knee replacements. Single plane [12–14, 17, 18, 18, 19, 22, 22, 24, 26, 29, 39, 66, 68] and dual-orthogonal [36, 55, 56, 67] videofluoroscopy provide sufficient measurement frequency to measure dynamic movements in addition to quasi dynamic flexion. With a subsequent 2D/3D registration of the 3D pose of either the surface models of the implant components or the bone models (segemented computed tomography (CT)/MRI scans) of the healthy knee based on the 2D fluoroscopic images and the projection parameters of the fluoroscopic system, the tibio-femoral kinematics can be comprehensively analysed [38, 39, 66, 67]. A drawback of all imaging systems including videofluoroscopy is the limited field of view, only allowing highly restricted movements or capturing only a portion of the activity [39]. In particular, complete cycles of gait activities, including high acceleration of the knee joint and changing muscle activation, cannot be analysed with static C-arm systems [38].

To overcome this limitation of a static image intensifier, dynamic systems have been developed [36, 37, 69]. The moving fluoroscope at the Institute for Biomechanics allows tracking of the knee joint throughout complete cycles of level walking, downhill walking and stair descent [37]. This unique technology now allows to address important questions for a better understanding of the tibio-femoral joint during gait activities and to provide valuable information about the *in vivo* performance of TKA during functional activities of daily living.

2.1.2 Definitions and mathematical conventions

To describe the tibio-femoral kinematics of the human knee joint flexion/extension in the sagittal plane, internal/external rotation in the transversal plane and ab/adduction in the frontal plane were used. For clinical interpretation most studies investigating tibio-femoral joint rotations are using the conventions described by Grood and Suntay [70], whereas, depending on the scientific question, cardan sequences or a helical axis approach with subsequent decomposition of the attitude vector, are also used to determine intersegmental rotations [47, 71].

For a complete kinematic description of tibio-femoral motion, the relative translations of the medial and lateral femoral condyles to the tibial plateau were described [72]. With the goal to quantify mainly anterior-posterior translation as well as possible lift off, condylar motion was described using centre points of circles fitted to the geometry of the condyles [28, 73], points on axes defined based on bony landmarks [67] or contact/closest points of the femoral condyles relative to the tibial plateau [28, 29, 66].

Both, the tibio-femoral rotations as well as the condylar translations are very sensitive to their definitions [28, 67, 74]. Here, different definitions can lead to differences in magnitudes of the kinematics due to crosstalk between the parameters [67]. In contrast to knee implants with known constructional geometries, definition of axes and contact/closest points in healthy knees are more challenging due to the individual anatomies [75–77].

As the description of tibio-femoral translation is strongly influencing the resulting translations [67, 74], the definitions should be taken into account when comparing different studies and for interpreting the results. Ideally, the results should be presented using the most common definitions to allow comparison to other studies.

2.2 Kinematics of the healthy tibio-femoral joint

In general, in studies investigating tibio-femoral kinematics with increasing or decreasing active or passive joint flexion, the lateral condyle was found to translate posterior with increasing flexion while the medial condyle only showed minimal anterior-posterior translation resulting in an internal tibial rotation with increasing flexion [12, 27–31]. For flexion angles from full extension to 120° flexion, lateral ranges of translations about 20mm were reported, whereas the medial condyle showed translations about only 2mm [28, 30]. The magnitudes of the condylar

translations varied between the studies, possibly due to different definitions or type of knee bending activity, but all of them found in average larger ranges of lateral translation, resulting in a medial centre of rotation. However, large inter-subject variations were found during deep knee bending and chair sitting with an observed reversed pattern with a lateral center of rotation and external tibial rotation with increasing flexion for single subjects [66].

While knee bending activities are well researched, there is very limited information available about tibio-femoral kinematics, including condylar motion, during gait activities. Only a few studies investigated condylar motion during the loaded stance phase of dynamic gait activities [66, 67]. Komistek and co-workers [66] investigated the condylar motion based on contact points during the stance phase of overground walking and during stair descent (one step to ground level) and Kozanek and co-workers [67] analysed the stance phase of treadmill walking. Komistek and co-workers [66] found almost no translation for the medial condyle (0.9mm) and slightly larger translation for the lateral condyle with posterior translation from heelstrike to 66 % of the stance phase (8.4mm), followed by an anterior translation until toe-off (4.2mm). In contrast, the study of Kozanek and co-workers [67] found a significantly larger range of translation for the medial condyle (points on transepicondylar axis: 9.7mm/ geometric center axis: 17.4mm) compared to the lateral condyle (points on transepicondylar axis: 4.0mm/ geometric center axis 7.4mm).

The axial rotation during the stance phase of gait measured by bone pins [42, 54], and the stance phase of treadmill walking measured with fluoroscopy [67] is described as initial tibial internal rotation after heel strike, followed by a slight tibial external rotation to a neutral postion in midstance before rotating internal again prior to toe-off. In contrast Komistek and co-workers [66] reported tibial external rotation from heel strike up to 33 % of stance phase, internal rotation from 33 %-66 % of stance phase and again external rotation until toe-off.
The unloaded swing phase was only investigated in the study of Lafortune and co-workers [42], using bone pins. They found a tibial external rotation up to 75ms before heel strike prior to the initiation of internal rotation. Average ranges of tibial rotation were found from 5°-11.3° during stance and swing phases of gait and different kinematic coupling of tibial rotation with flexion was observed depending on the loading condition [42].

Interestingly, the latter bone pin study [42] reported anterior-posterior translation of the femur relative to the tibia throughout the complete gait cycle and described tibial posterior translation of the femur with flexion and anterior translation during extension. The tibia relative to the femur translated 3.6mm posterior during stance and 14.3mm posterior during swing phase and

direct kinematic coupling between flexion and A-P translation was found [42].

For stair ascent (one step) and stair descent (one step) tibial internal rotation about 4.9 to 7.8° was found with increasing flexion [65, 66]. Both studies showed posterior translation for the lateral condyle (3.9mm [66]/3.4mm [65]) and anterior translation of the medial condyle (2mm [66]/5.5mm [65]) with increasing flexion but with different tendencies of a medial [66] or lateral [65] centre of rotation.

It remains unclear whether this controversial findings, especially during functional gait activities, occur due to different activities, execution of the motion tasks, different methods (including definitions of the axes and condylar motion) or differences between subjects, namely limb alignment, differences in soft tissue structure and muscle activation.

2.3 Kinematics of total knee arthroplasty

The majority of the studies investigating the *in vivo* kinematics of the femoral and the tibial components of total knee replacements focussed on weight bearing and non-weight bearing knee bending activities, such as deep knee bend, lunge or squatting activities as well as step up, step down activities [5, 13–26]. In those activities, the internal/external rotation, ab/adduction, condylar A-P translations and condylar lift off with increasing or decreasing flexion angles were analysed mainly using fluoroscopy to evaluate the performance of TKA designs in comparison to the healthy knee kinematics during weight bearing and non-weight bearing flexion as presented by Pinskerova and co-workers [28].

Different TKA design features and surgical procedures were proposed with the goal to guide the tibia-femoral motion towards replication of the kinematics found for natural knees with tibial internal rotation and lateral rollback with increasing flexion, while the medial condyle only exhibits minimal A-P translation [12, 27–31].

Two types of interfaces between the polyethylene inlay and the metal tibial component exist. In fixed-bearing designs, the inlay is fixed to the tibial tray and the geometry of the inlay guides tibial rotation. In contrast, in mobile-bearing designs the inlay can freely rotate around a medial centre of rotation and rotational behaviour is thought to be limited by the surrounding soft tissue structures only. Studies investigating the differences between fixed- and mobile-bearing designs with increasing flexion found similar patterns in A-P translation and rotation for both bearing

types [21, 78]. Another study found no differences in A-P translation but more internal tibial rotation with a pattern more similar to the natural knee for a posterior-stabilized mobile-bearing design in comparison to the fixed bearing version using the same femoral component [18]. It has been reported that decoupling of the translation and rotation in rotating platform knees could be beneficial to reduce polyethylene wear [79–81].

In TKA, two surgical techniques, retention or resection of the posterior cruciate ligament, are performed [82, 82–84] and corresponding designs are available. Mainly in posterior cruciate ligament retaining implants, "paradoxical" anterior movement of the condyles was observed during flexion compared to posterior cruciate ligament resecting implants [13–19, 68, 85]. To guide the kinematics towards the found natural movement, despite a resected posterior cruciate ligament, specific design features or different conformities between the condyles and the geometry of the inlay were presented. The cam-post mechanism in posterior-stabilized designs [14, 19, 23, 25], a gradually reducing radius of the condyles [16, 85] or a highly constrained medial compartment [24–26, 86, 87] should prevent "paradoxical" anterior movement of the condyles and should guide the kinematics towards the pattern found for the healthy knee, with a stable medial condyle and posterior translation of the lateral condyle with flexion, resulting in an internal rotation of the tibia around a medial pivot.

The posterior stabilized designs showed in general posterior translation with increasing flexion for the lateral condyle, but more pronounced for larger flexion angles when interaction of the cam-post mechanism occurs. For smaller flexion angles and the medial condyle the average results vary between the studies [13, 14, 18, 19, 25] as well as between loaded and unloaded conditions [19]. Some studies observed anterior movement of the condyles between 0-50° [25] and 30-90° flexion [14]. These findings were in line with a study comparing the effect of a bicruciate stabilized design with anterior and posterior cam-post feature, showing no posterior translation for flexion angles without cam-post engagement [12].

For a design with a gradually reducing radius, posterior translation of the lateral condyle with increasing flexion was reported [16, 85]. Pfitzner and co-workers [16] found anterior movement of the medial condyle during loaded and unloaded flexion, whereas Takagi and co-workers [85] observed medial posterior translation during passive flexion, but less in magnitude compared to the lateral condyle and therefore resulting in a medial pivot motion [85].

Medial pivot designs with highly congruent medial compartments showed only minimal medial condylar translation and lateral posterior translation with increasing flexion resulting in the

intended internal rotation of the tibia and a medial pivot motion [15, 24–26, 86].

As found for healthy knees, variations in tibio-femoral kinematics between the single subjects were observed [24]. It was shown, that several designs can replicate the pattern of healthy knee kinematics during activities with continuously increasing/decreasing flexion, but for all designs smaller magnitudes of lateral A-P translation and tibial internal rotation were found.

Two studies investigated whether the kinematic behaviour of an implant is altered during dynamic gait activities compared to activities including continuous flexion [13, 73]. They compared the stance phase of gait to a deep knee bend [13] or a step-up activity [73] with continuously increasing flexion. Significantly different kinematic behaviour between the stance phase of gait, including phases of flexion and extension, and the task with continuous flexion were observed. For a posterior-stabilized design, "paradoxical" anterior translation of the lateral condyle and a reversed rotation pattern were observed during gait, whereas for deep knee bend all subjects exhibited lateral posterior translation with flexion [13]. Banks and co-workers found significant differences between the stance phase of gait and a step-up task depending on the implant design [73]. Two studies examined TKA kinematics during complete cycles of treadmill walking [55, 88] in a posterior-stabilized knee replacement, but only Guan and co-workers investigated overground walking [88]. For complete cycles of overground walking in a posterior-stabilized implant they found similar patterns of A-P translation for both condyles except for the medial condyle during early stance, which exhibited more posterior translation than the lateral condyle [88]. The A-P translation changed direction several times and not only due to changes in flexion angle. Here, the interaction of loading and unloading with flexion angle could drive the condylar motion. These results show the importance of analysing complete cycles of gait activities for a complete evaluation of a total knee arthroplasty.

Chapter 3

Influence of the moving fluoroscope on gait patterns

adapted from:

Marina Hitz, Pascal Schütz, Michael Angst, William R. Taylor, Renate List
Institute for Biomechanics, ETH Zürich, Switzerland

PlosOne, vol.13, e0200608, 2018
DOI: 10.1371/journal.pone.0200608
open access

Keywords

Machine human interaction, videofluoroscopy, gait analysis, gait symmetry, ground reaction force, tibiofemoral kinematics

3.1 Abstract

Videofluoroscopic analysis can provide important insights for the evaluation of outcome and functionality after total knee arthroplasty, allowing the *in vivo* assessment of tibiofemoral kinematics without soft tissue artefacts. To enable measurement of the knee throughout activities of daily living such as gait, robotic systems like the moving fluoroscope have been developed that follow the knee movement and maintain the joint in front of the image intensifier. Since it is unclear whether walking while being accompanied by moving fluoroscope affects normal gait, the objective of this study was to investigate the influence of the moving fluoroscope on gait characteristics in healthy subjects. In addition, the impact of the motors' noise was analysed.

By means of skin markers analysis and simultaneous measurement of ground reaction forces, gait characteristics when walking with and without the moving fluoroscope as well as with and without ear protectors in combination with the moving fluoroscope, were obtained in young (n=10, 24.5y ± 3.0y) and elderly (n=9, 61.6y ± 5.3y) subjects during level gait and stair descent. Walking with the moving fluoroscope significantly decreased gait velocity in level gait and stair descent over the respective movement without the fluoroscope. Statistical analysis including gait velocity as a covariate, resulted in no differences on the ground reaction force parameters. However, some kinematic parameters (ankle, knee and hip ranges of motion, minimal knee angle in late stance phase, maximal knee angles in stance and swing phase) seemed to be modified by the presence of the moving fluoroscope, but statistical comparison was limited due to velocity differences between the conditions. Wearing ear protectors to avoid the influence of motor sound during walking with the moving fluoroscope caused no significant difference.

Walking with the moving fluoroscope has been shown to decrease gait velocity and small alterations in kinematic parameters were observed. Therefore, gait and movement alterations due to the moving fluoroscope cannot completely be excluded. However, based on the absence of differences in ground reaction force parameters (when adjusted for velocity within ANCOVA), as well as based on the comparable shape of the angular curves to the slow control condition, it can

be concluded that changes in gait when walking with the moving fluoroscope are small, especially in comparison to natural slow walking. In order to allow assessment of joint replacement with the moving fluoroscope, including an understanding of the effects of joint pain, clinical analyses can only be compared to gait activities showing similarly reduced velocities. Importantly, the reduced gait speeds observed in this study are similar to those observed after total knee arthroplasty, suggesting that analyses in such subjects are appropriate. However, the moving fluoroscope would likely need to be optimized in order to detect natural gait characteristics at the higher gait velocities of healthy young subjects.

The moving fluoroscope can be applied for comparisons between groups measured with the moving fluoroscope, but care should be taken when comparing data to subjects walking at self-selected speed without the moving fluoroscope.

3.2 Introduction

Videofluoroscopy in combination with 2D/3D registration allows an accurate quantification of 3D joint motion free of soft tissue artefact and has thus become a well-accepted imaging technique for the acquisition of kinematic information of single joints during functional movement tasks. Research using single plane videofluoroscopic analysis [37–39, 89–92], as well as dual orthogonal fluoroscopy [36, 88, 93], has provided valuable information on the three-dimensional motion of total knee arthroplasties (TKAs) and healthy knees. However, due to the limited field of view of the stationary image intensifier, static systems can only be applied for the analysis of highly restricted movements [94, 95]. To overcome these limitations mobile devices, such as the robotic radiographic imaging platform [69, 96], the mobile fluoroscopy system [97], the mobile biplane X-ray imaging system [36] and the moving fluoroscope [37–39, 98] have all been developed to allow the tracking of the knee during complete gait cycles of level gait, stair and ramp walking.

The moving fluoroscope consists of a fluoroscopic unit mounted on a moving trolley that moves with the subject in real-time, and which is controlled by a wire sensor attached to the knee. When the subject's knee moves, the moving fluoroscope then follows the joint in real time, in both the horizontal and vertical directions, such that the knee remains in the field of view of the image intensifier. Although the ability of the moving fluoroscope to keep the knee in the field of view of the image intensifier has been demonstrated [37], it still remains unknown whether the physical presence of the moving fluoroscope and the sound of the moving fluoroscope's motors and the

visual information from the laboratory may have an influence on the time-distance, kinetic and kinematic parameters of a subject when being tested. Here, as the auditory and motor systems, as well as premotor regions, are known to interact, and especially sounds can have the ability to influence our motor behaviors [99], the noise of the fluoroscope could influence the subject's gait. As a result, although each subject is provided sufficient time and practice trials to become accustomed to the moving fluoroscope prior to testing, distractions caused by proximity to the large dynamic device could still result in unnatural or disturbed gait patterns.

Yamokoski and Banks [96] have tested the influence of their close-up robot tracking system on gait and found that the dynamic robot tracking caused significant changes in several parameters, such as stride length, ankle sagittal plane rotation as well as anterioposterior and mediolateral ground reaction forces, although the differences were small and not clinically relevant.

Previous research has shown that rhythmic sensory cues affect temporal dynamics in human gait, but the influence of auditory signals on gait parameters is known to be larger than visual rhythmic cues [100]. However, the reported effects of metronomic cueing on gait velocity and stride length are not consistent [100, 101]. Furthermore, the influence of auditory stimuli seems to be age dependent: In elderly subjects the structure of gait variability can be manipulated using auditory stimulation, as opposed to young people, who seem to dedicate less attentional resources to auditory stimuli [102]. Although rhythmic sensory cues such as music or a metronome affect some parameters of gait, it remains unclear whether the motor sounds of the moving fluoroscope have an impact on natural human gait.

To assess if the moving fluoroscope influences natural gait patterns, the objective of this research project was to analyse the impact of the moving fluoroscope on the gait characteristics, specifically the time distance parameters, whole body kinematics, and ground reaction forces, of young and elderly subjects. Additionally, the impact of an acoustic masking intervention with ear protectors was tested. It was hypothesized that none of the kinematic and the ground reaction force parameters differ between conditions.

3.3 Materials and methods

3.3.1 Subjects

Overall 19 subjects participated in the study, comprising of ten subjects between 20 and 35 years old (24.5y ± 3.0y, five male and five female, BMI 22.0 ± 2.3) and nine subjects older than 55 years (61.6y ± 5.3y, six male and three female, BMI 25.9 ± 4.0)(no drop-outs). An elderly and a young age group were included due to age dependency of the influence of auditory stimuli [102]. Recruitment took place between January and June 2016 using public placards, verbal announcements in different sports and music clubs, as well as in lectures of the study program Health Sciences and Technology. Inclusion criteria were the two defined age ranges and the ability to perform the motion tasks. Subjects with actual significant problems, such as current pain, current injuries of the lower extremities or implants in the lower extremities were excluded from this study, as well as subjects who had already experienced walking with the moving fluoroscope. The study was approved by the ethics committee of ETH Zurich, Switzerland (EK-2015-N-68) and all subjects provided written informed consent prior to participation in the study.

3.3.2 Data acquisition

The subjects performed two different motion tasks, level gait and stair descent, with and without the moving fluoroscope. Within the moving fluoroscope condition, trials including an acoustic masking intervention were performed. The order of the tasks and intervention were randomized for all subjects, such that for each subject the first task (level gait or stair descent) was randomly selected and for each task it was randomly determined whether the ear protectors were worn or not after the first control condition.

To familiarize the subjects with the device, three level gait practice trials with the moving fluoroscope were performed. Before and after performing a task including the moving fluoroscope, control trials without the moving fluoroscope were recorded at a self-selected gait speed (control 1, control 2). Between the control measurements, the condition with the moving fluoroscope (FluMo) and the intervention condition with the moving fluoroscope and an acoustic intervention (FluMo intervention) were performed. For each of the conditions and tasks, five valid gait cycles were conducted. A gait cycle was considered valid when each force plate was hit once only. In addition, the subjects were asked to perform two slow level gait trials (slow control condition)

after the second level gait control condition. The slow walking trials were also based on a self-selected gait speed, with subjects requested to walk relatively slower (resulting in an average velocity reduction of 30.3 ± 11.4 % to the Control 1 and 24.6 ± 12.6 % to the Control 2 conditions, with velocity changes for all subjects ranging from a reduction of 56.4 % to an increase of 5.2 % in comparison to the two control conditions, n.b. only a single subject exhibited a velocity increase).

Whole body kinematics were assessed using an opto-electronic motion capture system (VICON MX system, Oxford Metrics Group, UK) consisting of 22 infrared cameras and 55 reflective skin markers according to the IfB marker set [47]. Five force plates (Kistler, Instrumentation, Winterthur, Switzerland) embedded but decoupled from the surrounding floor of the movement analysis laboratory were used to measure the ground reaction forces [37, 39]. Additionally, a three step staircase was instrumented with two mobile force plates (Kistler, Instrumentation, Winterthur, Switzerland) [37]. Kinematic and ground reaction force data were recorded simultaneously at 100 Hz and 2000 Hz respectively.

The moving fluoroscope consists of a fluoroscopic unit (BV Pulsera, Philips Medical Systems Switzerland) mounted on a stand-alone robot that follows the knee in the horizontal and vertical directions in real-time, and which is controlled by a wire sensor attached to the knee such that the knee always remains in the field of view of the image intensifier [37]. Since the aim of this study was purely to assess possible kinematic changes in the subject's interaction with the fluoroscope, no X-ray radiation was involved in this study.

For the acoustic intervention, an ear protector (3M PELTOR WS Alert XP) with a built-in Bluetooth function was used. In order to communicate with the participants, the ear protector was connected via Bluetooth to a microphone. To completely drown any sound of the moving fluoroscope's motor, white noise was constantly played in the ear protectors.

3.3.3 Data processing

Time distance parameters

Gait events were defined based on the ground reaction forces with a threshold of 25N. The step length (based on the distance the heel marker moved between two consecutive heel strikes) and the cadence of both legs (ipsilateral: leg of the tracked knee; contralateral: leg of non-tracked

knee) were determined. The stride velocity was calculated as the stride length divided by the time between two consecutive heel strikes.

Kinematics

Four basic motion tasks were used to functionally determine the joint axes and centres [47]. Joint rotations were determined based on redundant marker clusters and a helical axis approach [71]. For clinically interpretable rotational components, the attitude vector was decomposed along the axes of the marker based joint coordinate system fixed in the proximal segments [47]. Only the sagittal plane rotations were compared between the different conditions. All kinematic data were normalized over a gait cycle [103].

The ranges of motion (ROMs) for the ankle a_ROM, knee k_ROM and hip h_ROM joints of both legs were defined as the maximal ranges occurring throughout the whole gait cycle. In addition, the first peak flexion in the stance phase k_max1 and the second peak flexion in the swing phase k_max3 of the ipsilateral knee and the minimal ipsilateral knee flexion in the late stance phase k_min2 were investigated.

Ground reaction forces

For the ground reaction force analysis, the first F_{z2} and second peaks F_{z4}, the minimal ground reaction force between the peaks F_{z3}, the loading rate b_n and unloading rate e_n of the vertical ground reaction forces (based on the definition of Stüssi and Debrunner [104] using the 80 % value of F_{z2} and F_{z4} to calculate the slope of the force after touchdown, respectively before take-off) were evaluated for level gait [105], whereas in stair descent only the first peak F_{z2} of the vertical ground reaction force was compared. Furthermore, the maximal posterior F_{ymax} and maximal anterior ground reaction forces F_{ymin} were examined.

Left-right asymmetry

To check for asymmetries between two consecutive steps of the ipsi- and the contralateral legs during level gait, the absolute symmetry index (ASI) (3.1) [105] was analysed for the ground reaction force parameters F_{z2}, F_{z3}, F_{z4}, as well as for the time distance parameters stride velocity, step length, and cadence. A critical level of 10 % was chosen to differentiate between a symmetric

and an asymmetric behaviour [106, 107].

$$ASI(\%) = \left(\frac{X_{ipsi} - X_{contra}}{(X_{ipsi} + X_{contra}) * 0.5} \right) * 100 \tag{3.1}$$

where X represents the parameter in question. All calculations were performed using MATLAB (Version R2014a, MathWorks, Natick, MA, USA).

3.3.4 Statistical analysis

A linear mixed factors ANOVA was used to evaluate whether the gait velocity differed between the conditions in both tasks. Two separate Pearson's bivariate correlation analyses, one each for kinematic and ground reaction force parameters, were undertaken to not only reduce the number of dependent variables in order to reduce the family-wise error rate, but also to avoid investigating essentially the same (or highly correlated) aspects of walking. To additionaly identify the kinematic and ground reaction force parameters that are velocity dependent, a further Pearson's bivariate correlation analysis was conducted. A linear mixed factors ANCOVA was then performed with walking velocity as a covariate for comparisons with the velocity dependent parameters k_max1, k_max3, h_ROM, k_ROM, a_ROM, F_{z2}, F_{z3}, F_{z4}, b_n, e_n, F_{ymin} and F_{ymax} in level gait, and h_ROM, k_ROM, F_{z2}, b_n, F_{ymin} and F_{ymax} in stair descent as the dependent variable. These parameters, which were within the ANCOVA adjusted for gait velocity (ANCOVA with velocity as a covariate), were compared between the conditions at the 25th, 50th and 75th percentiles of walking velocity, as well as the mean velocity. For the velocity independent parameters k_min2 in level gait and a_ROM, k_max1, k_min2 and k_max3 in stair descent, linear mixed factors ANOVAs were executed. In both the ANCOVA and the ANOVA models, the independent variables were age (with two levels young and old), condition (with 5 levels for each condition in level gait and 4 levels each condition in stair descent) and interaction age and condition. All p-values for fixed effects were adjusted for multiple comparisons using Holm-Bonferroni ranking correction.The *post hoc* comparisons were conducted using Least Significant Differences (LSDs). Since in level gait, all ground reaction force parameters correlated, only the parameter F_{z2} was tested for condition and age dependencies, whereas in stair descent, besides F_{z2} also F_{ymin} was included in the statistical condition and age analysis, because these parameters did not correlate. Similarly, since cadence and step length correlated with stride velocity, the condition and age analysis was only performed for the time distance parameter

stride velocity. Since no significant main effects of age, nor a significant interaction effect of age and condition were found for any parameters, except k_max1, the effect of condition was based on all 19 subjects (except for k_max1). For k_max1 the post hoc comparisons were performed for both age groups separately.

All statistical analyses were performed using IBM SPSS software version 23 (SPSS AG, Zurich, Switzerland) and the significance level was set at $p < 0.05$.

Furthermore, to depict the repeatability of waveforms within a test day for each execution form, the coefficient of multiple correlation (CMC) [108] was calculated over all trials of each subject for all kinematic as well as ground reaction force patterns.

3.4 Results

3.4.1 Time distance parameters

For level gait, the mean stride velocities in the FluMo conditions were significantly lower (28 %-32 %) than in the control conditions, but did not significantly differ compared to the slow control condition (Table 3.1). Similarly, during stair descent, gait velocity was significantly decreased in the FluMo conditions compared to the control conditions (19-22 % in young, 11-13 % in old age group) (Table 3.1).

In the FluMo conditions the contralateral step length (FluMo 0.61 ± 0.05m, FluMo int. 0.60 ± 0.05m) was slightly larger than the ipsilateral step length (FluMo 0.58 ± 0.04m, FluMo int. 0.57 ± 0.04m).

3.4.2 Kinematics

In level gait, all parameters besides the minimal knee angle in the late stance phase k_min2 were correlated with gait velocity. Regarding the influence of the condition, it was found that the first peak knee angle in the stance phase k_max1 (within ANCOVA adjusted for gait velocity), did not differ between the conditions (Table 3.1, Figure 3.1), except for the old group between the two FluMo and the slow control conditions. But the minimal knee angle in the late stance phase (k_min2), the maximal knee angle in the swing phase (k_max3), as well as h_ROM, k_ROM and a_ROM presented a significant effect of condition (Table 3.1, Figure 3.1, Figure

Table 3.1: Time distance and kinematic parameters. Mean and standard deviation of stride velocity, ankle ROM a_ROM, knee ROM k_ROM, hip ROM h_ROM, first peak knee angle in the stance phase k_max1, the minimal knee angle in the late stance phase k_min2 and the second peak knee angle in the swing phase k_max3 for the ipsilateral side in the young (y) and the old (o) age groups. Significant differences are presented in bold. Since stride velocity, step length and cadence were correlated, only stride velocity was tested for significance.

task	condition	group	*Stride velocity*[m/s]	*Step length*[m]	Cadence [$1/min$]	a_ROM [°]	k_ROM [°]	h_ROM [°]	k_max1 [°]	k_min2 [°]	k_max3 [°]
Level gait	Control 1	y	1.27 ± 0.10	0.70 ± 0.06	109.58 ± 2.52	32.4 ± 5.8	69.8 ± 1.9	44.4 ± 3.5	19.0 ± 5.9	3.0 ± 3.6	69.7 ± 4.5
		o	1.25 ± 0.15	0.70 ± 0.04	104.40 ± 9.26	32.3 ± 2.2	68.3 ± 5.9	47.4 ± 4.6	22.1 ± 5.5	2.9 ± 2.2	66.0 ± 6.0
	Control 2	y	1.18 ± 0.11	0.67 ± 0.05	106.06 ± 7.24	32.8 ± 5.9	67.7 ± 2.8	42.4 ± 2.2	17.4 ± 5.9	3.7 ± 3.8	68.3 ± 5.2
		o	1.10 ± 0.08	0.67 ± 0.05	99.39 ± 7.59	30.6 ± 2.7	67.0 ± 5.6	45.0 ± 4.1	20.2 ± 4.7	3.4 ± 2.2	64.8 ± 5.8
	FluMo	y	**0.92**^{a,b} **± 0.11**	0.58 ± 0.05	95.59 ± 6.99	**26.6**^{a,b,c} **± 3.8**	**62.3**^{a,b,c} **± 4.9**	**37.6**^{a,b,c} **± 1.9**	13.2 ± 6.4	**5.3**^{a,b,c} **± 4.3**	**63.6**^{a,b,c} **± 7.0**
		o	**0.89**^{a,b} **± 0.08**	0.58 ± 0.03	91.64 ± 9.71	**27.1**^{a,b,c} **± 1.7**	**61.5**^{a,b,c} **± 7.3**	**40.7**^{a,b,c} **± 2.8**	**18.6**^{c} **± 5.3**	**5.6**^{a,b,c} **± 3.2**	**61.3**^{a,b,c} **± 8.7**
	FluMo int.	y	**0.91**^{a,b} **± 0.11**	0.58 ± 0.05	94.47 ± 7.03	**26.3**^{a,b,c} **± 3.5**	**62.2**^{a,b,c} **± 5.3**	**38.2**^{a,b} **± 2.1**	13.1 ± 6.8	**4.9**^{a,b,c} **± 4.1**	**63.9**^{a,b} **± 7.1**
		o	**0.85**^{a,b} **± 0.09**	0.57 ± 0.05	89.41 ± 8.61	**27.2**^{a,b,c} **± 2.5**	**62.6**^{a,b,c} **± 5.7**	**40.1**^{a,b} **± 2.8**	**17.9**^{c} **± 4.9**	**5.4**^{a,b,c} **± 3.7**	**62.2**^{a,b} **± 6.9**
	Slow control	y	**0.91**^{a,b} **± 0.10**	0.59 ± 0.04	92.72 ± 7.69	31.0 ± 5.2	**65.7**^{a} **± 2.9**	**38.6**^{a} **± 1.9**	14.3 ± 5.5	3.8 ± 3.8	66.3 ± 4.9
		o	**0.84**^{a,b} **± 0.12**	0.60 ± 0.06	84.80 ± 10.25	27.9 ± 2.3	**64.1**^{a} **± 5.5**	**41.6**^{a} **± 4.1**	14.6 ± 4.8	3.3 ± 3.3	61.9 ± 6.2
Stair descent	Control 1	y	0.56 ± 0.05	0.32 ± 0.02	103.65 ± 9.40	55.8 ± 4.5	93.3 ± 3.8	23.4 ± 3.8	34.4 ± 5.3	29.1 ± 6.2	97.7 ± 3.9
		o	0.51 ± 0.03	0.32 ± 0.01	95.42 ± 6.53	57.3 ± 4.7	95.9 ± 4.7	24.0 ± 3.6	32.8 ± 5.4	26.8 ± 6.4	97.3 ± 6.5
	Control 2	y	0.54 ± 0.03	0.32 ± 0.02	102.88 ± 7.73	55.8 ± 4.0	94.1 ± 3.8	23.6 ± 3.7	34.6 ± 5.5	27.8 ± 5.8	98.6 ± 4.3
		o	0.51 ± 0.04	0.32 ± 0.02	95.65 ± 8.53	58.5 ± 3.4	96.6 ± 4.8	24.2 ± 3.4	32.7 ± 4.5	26.5 ± 4.4	97.5 ± 7.0
	FluMo	y	**0.47**^{a,b} **± 0.04**	0.32 ± 0.02	87.73 ± 5.86	56.9 ± 3.9	89.6 ± 4.2	21.8 ± 3.8	32.1 ± 5.6	26.2 ± 5.4	**95.6**^{a,b} **± 4.1**
		o	**0.45**^{a,b} **± 0.04**	0.32 ± 0.02	84.27 ± 7.11	58.0 ± 3.6	93.8 ± 3.0	23.0 ± 2.8	32.6 ± 4.5	25.9 ± 6.0	**96.7**^{a,b} **± 6.3**
	FluMo int.	y	**0.46**^{a,b} **± 0.04**	0.32 ± 0.02	86.5 ± 7.93	57.3 ± 3.6	89.8 ± 4.8	22.8 ± 3.9	31.6 ± 5.5	25.5 ± 5.5	**95.6**^{a,b} **± 4.6**
		o	**0.46**^{a,b} **± 0.04**	0.32 ± 0.01	86.53 ± 7.09	58.3 ± 3.1	93.4 ± 3.2	22.6 ± 2.9	33.6 ± 4.8	27.5 ± 5.4	**96.6**^{a,b} **± 6.6**

[a] significant difference from control condition 1 ($p < 0.05$).
[b] significant difference from control condition 2 ($p < 0.05$).
[c] significant difference from slow control condition ($p < 0.05$).

A.1, Figure A.2). A post-hoc analysis showed that a_ROM and k_ROM were significantly lower and k_min2 significantly higher during the FluMo conditions compared to the two control as well as to the slow control condition (Table 3.1). For h_ROM and k_max3, the FluMo condition showed a significantly lower ROM compared to the control as well as the slow control condition, whereas the FluMo intervention condition only differed significantly in comparison to the control 1 and 2 conditions, but not to the slow control condition, although both parameters were adjusted for velocity within the ANCOVA (Table 3.1).

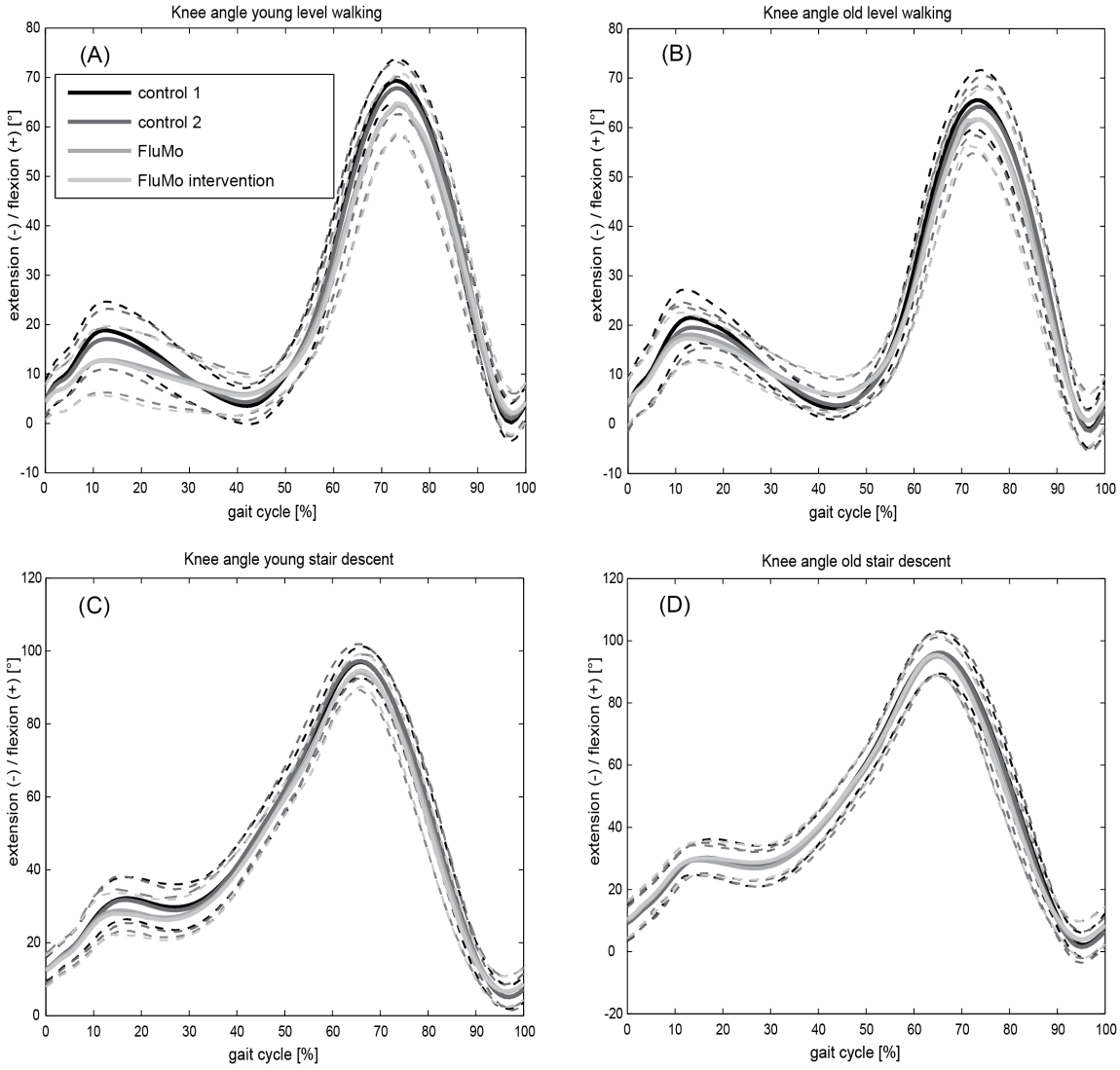

Figure 3.1: Knee flexion. Mean and standard deviations of knee flexion in level gait for young (A) and elderly (B) subjects, as well as in stair descent for young (C) and elderly (D) subjects, for the conditions control 1, control 2, FluMo and FluMo intervention.

In stair descent, only k_ROM and h_ROM were velocity dependent. k_ROM and h_ROM (adjusted for velocity within ANCOVA), a_ROM, the maximal knee flexion angle in the stance phase (k_max1) and the minimum knee flexion angle in the late stance phase (k_min2) did

not differ between any of the conditions (Table 3.1, Figures A.1, A.2). Furthermore, k_max3 was affected by the factor condition, revealing a significantly lower maximal flexion in the FluMo than in the control conditions during stair descent (Table 3.1).

3.4.3 Ground reaction forces

In level gait, as well as in stair descent all ground reaction force parameters correlated with gait velocity. Regarding condition comparison, neither for F_{z2}, which was within ANCOVA adjusted for velocity and tested in level gait, as well as stair descent, nor F_{ymin}, which was within ANCOVA adjusted for velocity and tested in stair descent only, exhibited any significant differences between the conditions (Table 3.2, Figures 3.2, A.3).

3.4.4 Absolute symmetry index and coefficient of multiple correlation

The ASI in step length cadence and stride velocity were smaller than 10 % except for the step length ASI's of the young group in the FluMo conditions (11.0 ± 4.6 % and 11.6 ± 4.9 %) and the stride velocity of the young group in the FluMo condition (10.1 ± 6.1 %) (Table 3.3). The ground reaction force parameters showed for all conditions averaged ASI below 4 % (Table 3.3). For all tasks and conditions the CMC were always higher than 98 %.

3.5 Discussion

The use of advanced technologies such as the moving fluoroscope for assessing the kinematics of skeletal structures under dynamic and loaded conditions presents an important step in understanding biomechanical interactions of the musculoskeletal system. Before such approaches can be accepted for wider clinical and research usage, however, it is critical to understand the potential role that the measurement technique itself plays on a subject's kinetic and kinematic patterns. In this study, level gait and stair descent were assessed both with and without accompaniment of the moving fluoroscope to assess whether the moving fluoroscope influences human gait. Moreover, an acoustic intervention was used to investigate whether exclusion of the noise of the motors could reduce any effects of the moving fluoroscope.

The freely chosen level gait stride velocities, the ipsilateral step lengths and the ipsilateral cadences of the control conditions were comparable to standard gait time distance parameters

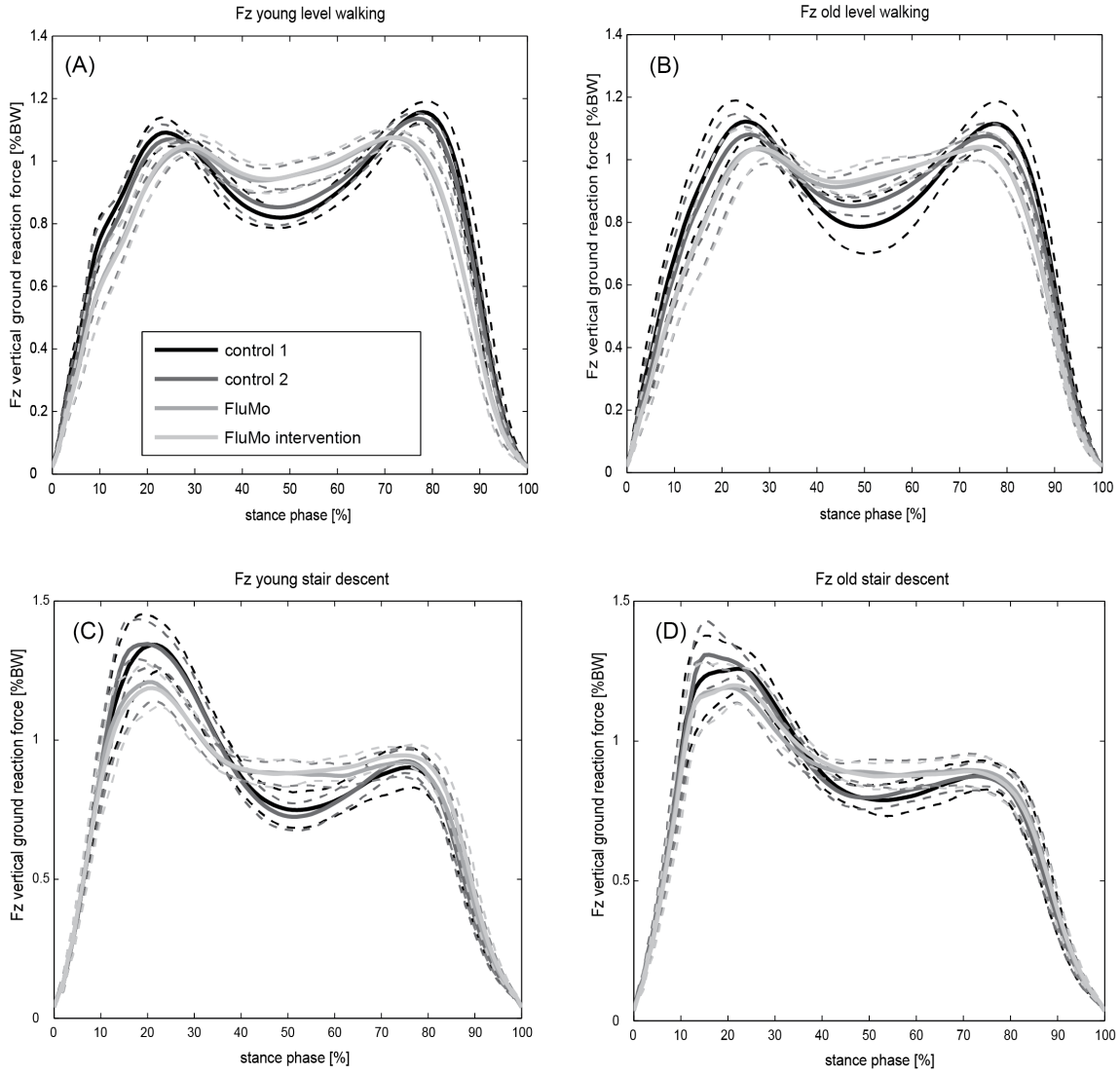

Figure 3.2: Vertical ground reaction forces. Mean and standard deviation of vertical ground reaction forces (F_z) in level gait for young (A) and elderly (B) subjects as well as in stair descent for young (C) and elderly (D) subjects for the conditions control 1, control 2, FluMo and FluMo intervention.

Table 3.2: Ground reaction force parameters. Mean and standard deviation of the first vertical peak ground reaction force F_{z2}, the minimal vertical ground reaction force between the peaks F_{z3}, the second vertical peak ground reaction force F_{z4}, the loading rate b_n, the unloading rate e_n, the maximal anterior ground reaction force F_{ymin} and the maximal posterior ground reaction force F_{ymax} for the ipsilateral side in the young (y) and the old (o) age groups. In level gait, only F_{z2} was statistically analysed because all other parameters correlated, whereas in stair descent, F_{z2} and F_{ymin} were statistically tested.

task	condition	group	F_{z2} [%BW]	F_{z3} [%BW]	F_{z4} [%BW]	b_n [%BW]	e_n [%BW]	F_{ymin} [%BW]	F_{ymax} [%BW]
Level gait	Control 1	y	1.10 ± 0.04	0.81 ± 0.03	1.17 ± 0.03	8.90 ± 0.68	-9.43 ± 1.08	-0.18 ± 0.02	0.20 ± 0.03
		o	1.14 ± 0.06	0.77 ± 0.08	1.12 ± 0.07	8.49 ± 1.69	-8.90 ± 1.47	-0.19 ± 0.04	0.21 ± 0.03
	Control 2	y	1.09 ± 0.04	0.84 ± 0.06	1.14 ± 0.01	8.01 ± 1.35	-8.43 ± 0.68	-0.16 ± 0.02	0.18 ± 0.02
		o	1.10 ± 0.05	0.84 ± 0.02	1.08 ± 0.04	7.35 ± 1.69	-7.58 ± 0.91	-0.17 ± 0.03	0.18 ± 0.02
	FluMo	y	1.06 ± 0.02	0.92 ± 0.04	1.08 ± 0.02	5.73 ± 0.80	-5.81 ± 1.00	-0.14 ± 0.02	0.12 ± 0.02
		o	1.06 ± 0.06	0.90 ± 0.03	1.05 ± 0.04	5.62 ± 1.34	-6.00 ± 1.15	-0.15 ± 0.04	0.13 ± 0.03
	FluMo int.	y	1.07 ± 0.02	0.93 ± 0.04	1.09 ± 0.02	5.63 ± 0.89	-5.88 ± 1.09	-0.14 ± 0.02	0.12 ± 0.03
		o	1.07 ± 0.06	0.91 ± 0.04	1.05 ± 0.04	5.42 ± 1.31	-5.87 ± 1.07	-0.15 ± 0.04	0.13 ± 0.03
	Slow control	y	1.07 ± 0.02	0.91 ± 0.05	1.09 ± 0.03	5.45 ± 1.22	-6.30 ± 1.18	-0.13 ± 0.02	0.14 ± 0.03
		o	1.07 ± 0.06	0.92 ± 0.03	1.04 ± 0.04	4.81 ± 1.55	-5.63 ± 1.18	-0.13 ± 0.03	0.14 ± 0.03
Stair descent	Control 1	y	1.43 ± 0.08			7.51 ± 1.98		-0.14 ± 0.02	0.15 ± 0.03
		o	1.42 ± 0.14			8.95 ± 2.68		-0.15 ± 0.02	0.15 ± 0.02
	Control 2	y	1.44 ± 0.17			8.83 ± 1.67		-0.14 ± 0.02	0.15 ± 0.03
		o	1.42 ± 0.16			9.23 ± 1.65		-0.15 ± 0.03	0.15 ± 0.02
	FluMo	y	1.28 ± 0.08			8.04 ± 1.84		-0.14 ± 0.03	0.13 ± 0.02
		o	1.30 ± 0.13			8.27 ± 1.68		-0.15 ± 0.02	0.14 ± 0.02
	FluMo int.	y	1.25 ± 0.12			7.65 ± 1.27		-0.14 ± 0.03	0.13 ± 0.03
		o	1.29 ± 0.12			7.86 ± 1.95		-0.15 ± 0.02	0.13 ± 0.02

Table 3.3: Absolute symmetry indexes (ASI). Mean and standard deviation of ASI for level gait in the young (y) and the elderly (o) age groups.

condition	group	ASI F_{z2} [%]	ASI F_{z3} [%]	ASI F_{z4} [%]	ASI *stride velocity* [%]	ASI *step length* [%]	ASI *cadence* [%]
Control 1	y	2.0 ± 1.6	2.1 ± 1.4	1.6 ± 1.4	3.4 ± 1.8	2.6 ± 2.7	1.8 ± 1.2
	o	3.5 ± 2.1	1.8 ± 1.7	3.0 ± 2.6	3.0 ± 2.0	8.9 ± 12.0	4.3 ± 4.9
Control 2	y	1.5 ± 1.0	1.1 ± 0.9	2.1 ± 1.9	4.9 ± 2.8	3.5 ± 3.2	2.4 ± 2.1
	o	2.7 ± 1.7	1.6 ± 0.8	2.0 ± 2.1	3.1 ± 2.1	3.1 ± 2.6	2.3 ± 1.3
FluMo	y	1.3 ± 0.9	1.3 ± 1.1	2.3 ± 1.5	10.1 ± 6.1	11.0 ± 4.6	5.6 ± 4.8
	o	3.1 ± 2.0	2.5 ± 1.6	2.0 ± 1.4	5.7 ± 3.1	7.5 ± 4.0	3.8 ± 2.4
FluMo int.	y	1.1 ± 1.2	1.1 ± 1.1	2.2 ± 1.7	9.7 ± 4.7	11.6 ± 4.9	4.0 ± 2.7
	o	3.2 ± 2.6	1.4 ± 1.3	2.1 ± 3.1	6.1 ± 4.7	9.4 ± 5.8	3.5 ± 2.6
Slow control	y	1.6 ± 0.9	1.2 ± 1.0	1.8 ± 1.1	4.6 ± 3.8	9.1 ± 15.7	7.3 ± 14
	o	2.7 ± 3.0	1.6 ± 1.0	2.0 ± 0.8	4.5 ± 3.2	4.6 ± 4.0	3.6 ± 2.7

of previous studies [108, 109]. In contrast, the gait velocity, step lengths and cadence of the conditions with the moving fluoroscope were lower than in the control conditions, indicating that the moving fluoroscope altered time distance parameters towards those of the slow walking condition. This is in contrast to the findings of [96], who found that on average people moved faster through the dynamic radiographic system while the robots were actively following their motion. This might be explained by the fact that in the latter study, subjects walked through the workspace of the robots, while the subjects in the present study walked within the moving fluoroscope. The slower gait velocity for the moving fluoroscope conditions can also partly be explained by the fact that some subjects had to be instructed to reduce the gait velocity to allow good tracking of the moving fluoroscope, due to the limited acceleration of the robot (ca. $8\mathrm{m}s^{-2}$). However, the stride velocities in the FluMo conditions were still in the range of the gait velocities measured in subjects with TKA [110], but slightly lower than the fastest TKA subjects reported within a meta-analysis of Abbasi-Faghi et al. [111]. Interestingly, the second control trials' velocities were significantly higher than in the FluMo conditions, but significantly lower than in the first control condition suggesting that the subjects were influenced by the previously slower trials of the FluMo conditions. In stair descent, the step length ($\sim$ 0.32m) was equal for all conditions due to the defined stair step length. Although the time distance parameters during level gait in general reflected a symmetric gait pattern (ASI $<$ 10 %), the contralateral step length was slightly larger ($>$ 10 % difference [106, 107]) than the ipsilateral step length in the FluMo conditions, suggesting that the step length of the ipsilateral leg might be influenced by the moving fluoroscope. This phenomenon might be partially explained by the somatic perception of the wire sensor that was attached to the ipsilateral leg and the divergent acceleration pattern of the moving fluoroscope during an ipsi- and a contralateral step.

All kinematic parameters of the ankle, knee and hip joints during the control conditions in level gait were similar to past research [103, 112, 113], whereas the FluMo conditions differed in some kinematic parameters from the control conditions. The moving fluoroscope influenced the maximal knee angle in the stance phase only for the old group in comparison to the slow control condition, but not the two control conditions. The maximal knee angle in the swing phase, the minimal knee angle in the late stance phase, as well as the ankle, knee and hip ROMs were significantly different when walking with the moving fluoroscope in comparison to walking without. Although within ANCOVA adjusted for walking velocity, the hip ROM as well as the maximal knee angle in the swing phase of the FluMo intervention condition only differed from the control condition with preferred gait speed but not from the slow gait

condition. Therefore, and especially also based on the significant difference between the slow control and the control 1 conditions for the hip and knee ROM, it must be assumed that velocity adjustment by including velocity as a covariate within the statistical analysis did not fully take effect. Comparing kinematic motion characteristics, it can be summarised that walking with the moving fluoroscope is very similar to walking at a slow gait speed (Figure 3.3).

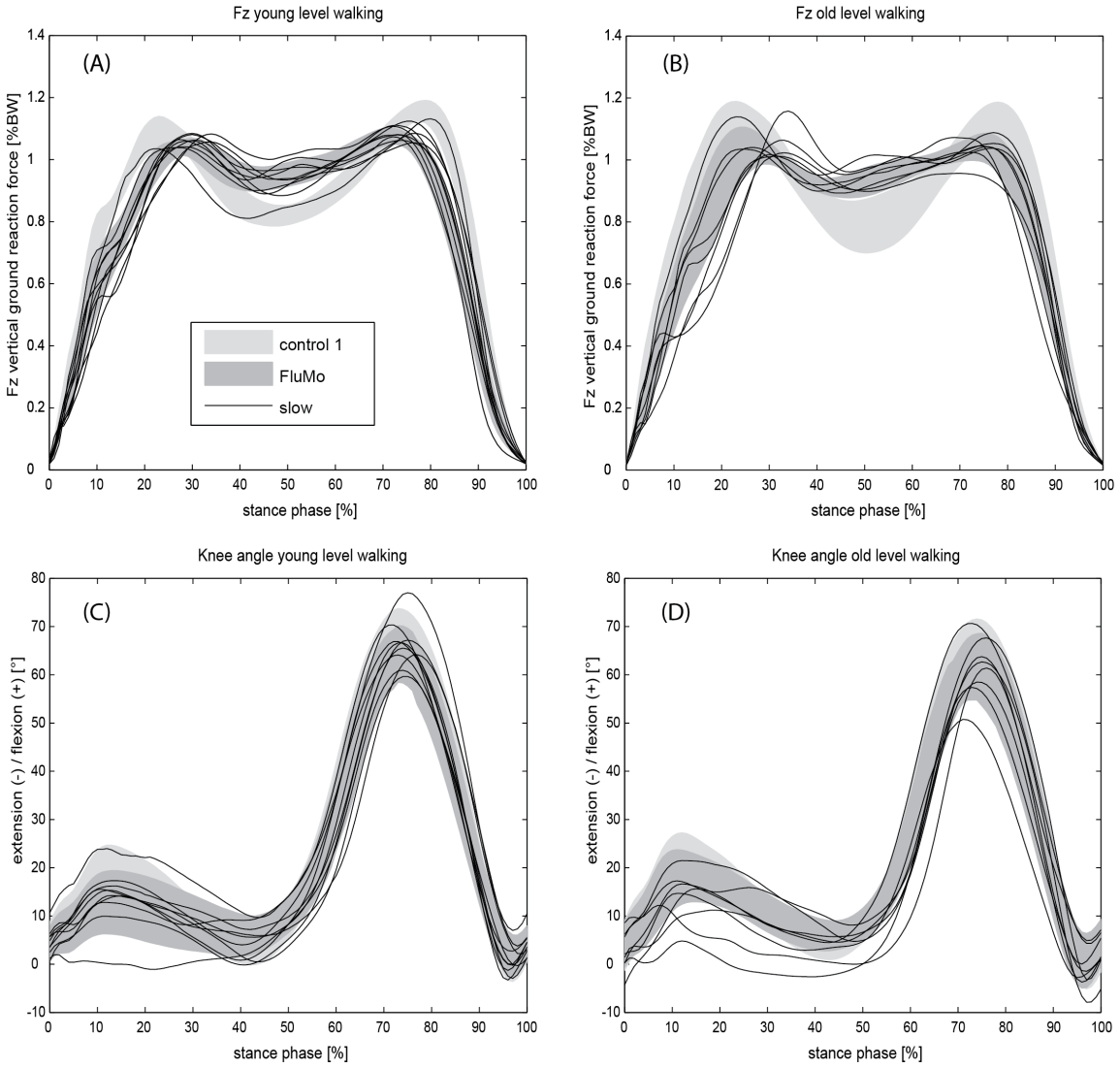

Figure 3.3: Knee flexion and vertical ground reaction force for the slow in comparison to the FluMo and the control 1 conditions. The grey areas represent the range between the mean plus/minus standard deviation of the vertical ground reaction forces (A, B) and knee flexion (C, D) for young (A, C) and elderly (B, D) subjects for the conditions control 1 and FluMo in level gait. The black lines represent the mean of the two slow gait trials for each subject.

Since it is well known that gait velocity has an influence on the kinematic parameters [114], velocity dependent parameters were within ANCOVA adjusted for walking speed to allow for condition comparisons. However, since velocity adjustment within the linear mixed factors ANCOVA is based on the assumption of a linear regression and not all parameters exhibit a linear

velocity dependency, a comparison of the kinematic parameters is somewhat limited in its validity. The efficacy of linear velocity adjustment especially seemed to fail for parameters that showed a significant difference between the FluMo conditions and the control 1 and 2 conditions, but not the slow control conditions, or between the slow control and the control 1 condition, although they were adjusted for velocity within the ANCOVA (e.g. k_max3, h_ROM). However, since a predefined gait velocity may have led to large adaptations in gait characteristics, the measurements of the control conditions with the self-selected gait speed still seem to be the preferential methodology. This study limitation needs to be kept in mind since it complicates the interpretation of the kinematic and kinetic parameters.

In stair descent, the ankle ROM was not influenced by the moving fluoroscope, but was slightly larger for all conditions than the values reported by Riener et al. [115]. The knee ROM as well as the first peak knee angle in the stance phase were comparable to the previous literature [115]. However, the moving fluoroscope did show a significant effect on the maximal flexion angle in the swing phase. While the maximal flexion angle in the swing phase was significantly different to both control conditions, it should be noted that e.g. the difference for the maximal knee flexion angle between the FluMo and the control 2 condition was for 9 subjects below 1°, for 3 subjects between 1° and 2°, for 5 subjects between 2° and 3° and for two subjects between 3° and 4°, while the inter-trial standard deviation of the individual subjects for the maximal flexion angle was up to 3.5° for the FluMo and 3.6° for the control 2 condition. Thus, although a significant influence in the latter parameter was found, the difference was in the range of the inter-trial variation of the individual subjects as well as the actual error that can be expected within skin marker measurements due to soft tissue artefacts [46, 116].

The vertical ground reaction forces in level gait exhibited a typical "m" shape with a first peak, an unloading phase and a second peak (Figure 3.2). All ground reaction force parameters were comparable to existing literature [105], except for the minimal vertical ground reaction force between the peaks, which was smaller in all conditions than the values presented by Stacoff and co-workers [105]. However, dependency of kinetic parameters on gait velocity, as observed in the larger first and second peaks of the vertical ground reaction forces and reduced unloading in between, when comparing the slow level gait and the FluMo conditions to the control conditions, is in agreement with previous studies [117]. The ground reaction force characteristics, as well as the gait velocity of the slow condition, were similar to the FluMo condition (Figure 3.3). Since the ground reaction force parameters, when adjusted for velocity within the ANCOVA, did not show any difference between walking with, compared to walking without the moving fluoroscope,

it can be concluded that ground reaction force characteristics when walking with the moving fluoroscope are similar to natural slow gait.

In this study, inter-limb symmetry was evaluated based on the vertical ground reaction forces. According to a previous study of Stacoff et al. [105], asymmetric gait patterns can be detected when ASI of the vertical ground reaction force parameters exceed 5 %. Since the ASI for the ground reaction force parameters of the present study were below 4 %, even when walking with the moving fluoroscope, it can be concluded that the subjects did not show unnatural gait patterns like limping when walking with the moving fluoroscope (Table 3.3).

Similarly, in stair descent, the first peak of the vertical ground reaction force, as well as the maximal anterior ground reaction force, both adjusted for gait velocity within the ANCOVA, did not show a significant impact of the condition (Table 3.2). Therefore, it can be concluded that the moving fluoroscope causes no change in the investigated kinetic parameters, when compared to walking at a similar gait speed.

Since no differences were found between the FluMo and the FluMo intervention condition in both tasks, it can be assumed that the sound of the moving fluoroscope did not influence the subjects during either level walking or stair descent. Since some kinematic parameters were indeed influenced when walking with the moving fluoroscope, other influences such as the appearance of the device, the wire sensor, and visual information such as the movement of the c-arm may have an influence on the subject's gait. Further improvement of the moving fluoroscope should therefore aim to replace the wire sensor with a tracking methodology that does not require direct contact with the subject.

3.6 Conclusion

To conclude, walking with the moving fluoroscope leads to a decrease in gait velocity compared to the control conditions, however gait with the moving fluoroscope did not differ from natural gait for all ground reaction force parameters when adjusted for differences in gait velocity. However, since some kinematic parameters were influenced, it cannot be completely excluded that at least some subjects were influenced by the moving fluoroscope, but statistical comparison in this respect was limited due to velocity differences between the conditions. Overall, gait characteristics in the natural gait condition were comparable to the conditions with the moving fluoroscope. However, walking with the moving fluoroscope is restricted to a limited gait speed, especially for

young subjects. For subjects with TKA showing slower gait velocities [110], the speed capability of the moving fluoroscope seems to be reasonable. To assess gait at standard gait velocities of healthy subjects, the moving fluoroscope would need to be optimized in order to allow higher accelerations to occur at higher gait velocities.

To conclude, the moving fluoroscope is suitable for comparisons between groups measured with the moving fluoroscope, such as e.g. comparisons between implant designs and healthy knees. However, care should be taken when comparing data to subjects walking at self-selected speed without the moving fluoroscope. Here, correction due to gait velocity differences should be treated with care, especially in relation to joint angles.

Chapter 4

Knee implant kinematics are task dependent

adapted from:

Pascal Schütz, Barbara Postolka, Hans Gerber, Stephen J. Ferguson, William R. Taylor, Renate List

Institute for Biomechanics, ETH Zürich, Switzerland

submitted

4.1 Abstract

Although total knee arthroplasty has become a standard surgical procedure for relieving pain, knowledge of the *in vivo* knee joint kinematics throughout common functional activities of daily living is still missing. The goal of this study was to analyse knee joint motion throughout complete cycles of daily activities in total knee arthroplasty subjects to establish whether a clinically important difference in joint kinematics occurs between different activities. Using advanced moving fluoroscopic techniques, we assessed tibio-femoral kinematics in six subjects throughout repetitions of complete cycles of walking, stair descent, sit-to-stand, and stand-to-sit tasks. The mean range of condylar anterior-posterior translation exhibited clear task dependency across all subjects, with mean ranges of motion for the medial condyle: 6.4 ± 1.2mm (level walking), 9.4 ± 2.6mm (stair descent), 7.0 ± 2.0mm (sit-to-stand), and 6.5 ± 1.4mm (stand-to-sit); and for the lateral condyle: 4.9 ± 0.9mm (level walking), 6.5 ± 1.7mm (stair descent), 4.7 ± 1.7mm (sit-to-stand), and 4.5 ± 0.9mm (stand-to-sit). A significantly larger anterior-posterior translation was observed during stair descent compared to level walking and stand-to-sit. Finally, local minima were observed at approximately 30° flexion for different tasks, which were more prominent during loaded than unloaded task phases. This characteristic is likely to correspond to the specific design of the PFC Sigma CR implant. From the data presented in this study, it is clear that flexion angle alone cannot fully explain tibio-femoral implant kinematics. As a result, it seems that the assessment of complete cycles of the most frequent functional activities of daily living is imperative when evaluating the behavior of a total knee arthroplasty design *in vivo*.

Keywords

Videofluoroscopy, total knee arthroplasty, activity dependency, A-P translation-flexion coupling, moving fluoroscope, single plane fluoroscopy, tibio-femoral kinematics, level walking, stair descent, gait analysis

4.2 Introduction

Total knee arthroplasty (TKA) has become a standard surgical procedure for relieving pain and restoring function in patients with degenerative joint diseases, mainly osteoarthritis. Although

most patients show little or no impairments after surgery, a large number of TKAs still fail in the longer term due to polyethylene wear, loosening, knee instability or infection [9]. In order to better understand the mechanisms leading to early failure or an unsatisfactory outcome in general, kinematic and kinetic measures during functional activities of daily living can provide a crucial understanding for further improving the longevity and functionality of TKAs. Through providing a baseline for developing and validating biomechanical models, such knowledge can allow the improvement of rehabilitation techniques, as well as the development of new concepts for knee implants.

Investigations into TKA function during complete gait cycles using skin marker based motion analysis have been successful in determining global segment kinematics, thereby allowing the estimation of external joint moments [32, 49, 50]. However, this approach is known to be strongly affected by soft tissue artefacts [46, 52], and does not allow an accurate quantification of tibio-femoral anterior-posterior (A-P) translation and internal/external rotation [46, 54, 118, 119]. In order to determine such inaccessible joint kinematics, imaging methods such as single plane fluoroscopy, [38, 39, 90] as well as dual orthogonal fluoroscopy [36, 93], with a subsequent 2D/3D registration, now allow an analysis of the relative movement of the implant components without soft tissue artefact. Since these static fluoroscopic systems possess a limited field of view, they are constrained to capturing only very restricted movements of the knee (e.g. during sitting/standing, deep knee bends) or allow only a small portion of the whole motion cycle to be tracked [5, 73, 87, 94, 95, 95, 120]. As a result, these techniques provide little or no access to functional measurement of activities that involve either loading and unloading, toe-off and heel strike impact, or muscle activation and deactivation, and especially not throughout multiple consecutive cycles. To overcome these limitations of a static image intensifier, dynamic single and dual plane systems have been introduced [36, 37, 39]. The moving fluoroscope developed at the Institute for Biomechanics, ETH Zürich, allows not only tracking of free level gait but also tracking of the knee joint during stair descent, which is considered to be a challenging daily activity for subjects with knee disorders [32, 105].

To allow a sufficient range of motion and avoid overloading of the passive structures [121, 122], the kinematic behavior of the natural tibio-femoral joint has been of high interest, and has therefore been investigated extensively in cadaveric studies [27], using bone-pins [54], as well as MRI [30, 123], RSA [65] and videofluoroscopy [29, 66, 67]. Similarly, the biomechanical outcomes after TKA have been extensively examined in order to understand the specific design characteristics of the replacement joint that allow healthy knee joint kinematics to be mimicked

[27], and thereby avoid overloading of the surrounding soft tissue structures. Despite the high level of interest, relative motion of the tibio-femoral joint remains controversially discussed, possibly due to the different techniques used to analyse the movement data, which are known to affect interpretation of the kinematics [74, 124]. As an example, both medial and lateral pivot motions in the transverse plane have been found during a similar change in flexion angle [27, 67]. However, despite these problems, it is still clear that a number of factors do play a role in modulating joint kinematics. Here, knee flexion angle [27], limb alignment [125], and different design of the implant [22, 126] are all known to play critical roles on the biomechanical outcome of the joint, but these have mainly been assessed either quasi-statically or during very restricted movements of the knee. Importantly, knowledge of changes in the motion between the tibia and femur during the most common functional activities of daily living i.e. walking and stair descent are still missing, but could be critical for understanding the dominant biomechanical influences on the joint. Specifically, no data is currently available examining the tibio-femoral kinematics during complete consecutive cycles of both free level gait and stair descent.

With the aim to establish whether a clinically important difference in joint kinematics occurs between functional tasks, tibio-femoral motion was analysed by videofluoroscopy during walking and stair descent, in comparison to sit-to-stand-to-sit, in subjects with a TKA, especially focussing on tibiofemoral internal/external rotation and A-P translation of the condyles.

4.3 Methods

4.3.1 Subjects

One female and five male subjects (average age of 72.8 $\pm$ 8.5 years; BMI 24.3 $\pm$ 2.2kgm^{-2}) with a unilateral PFC Sigma Curved cruciate retaining (CR) fixed-bearing TKA (DePuy Synthes, Johnson and Johnson), provided written, informed consent to participate in this study, which was approved by the local ethics committee (EK 2011-N-6). All subjects exhibited a good functional outcome (KOOS score 91.2 $\pm$ 5.7, no/very low pain with a VAS $<$ 2) and were measured in the gait lab at least one year postoperatively (4.2 $\pm$ 3.5 years).

4.3.2 Motion tasks

Level walking, stair descent, and sit-to-stand-to-sit were measured in this study. Prior to radiographic measurements, trials without imaging were performed until the subjects felt comfortable walking with the moving fluoroscope. For each motion task, five valid cycles were captured, in which the knee remained within the field of view of the image intensifier during the stance as well as the swing phase, and the force plates were hit correctly. The activity "level walking" required walking straight ahead on the floor; "stair descent" included walking down three 0.18m steps; "sit-to-stand-to-sit" was performed as a single task without support from the upper extremities.

4.3.3 Motion capture system and ground reaction forces

A 3D motion analysis system using 12 MX40 motion-capture cameras (Vicon MX system, Oxfords Metrics Group, UK) was employed to capture the movement of a marker attached to the sternum in order to establish the start and end events of the sit-to-stand-to-sit task, with a marker velocity of either $>$ or $<$ 0.02m/s used as the threshold criteria.

Ground reaction forces were measured using six force plates mounted in the floor and two mobile force plates mounted in the stair steps (Kistler, Instrumentation, Winterthur, Switzerland) to determine the heelstrike and toe-off events for level walking and stair descent, with a threshold of 25N. All force plates were decoupled from the surrounding floor in order to ensure that the force acquisition was not disturbed by the moving fluoroscope.

4.3.4 Moving fluoroscope

The moving fluoroscope [37–39] at the Institute for Biomechanics, ETH Zürich, was used to track the joint motion and image the tibio-femoral implants throughout several consecutive cycles of level walking and stair descent as well as during the sit-to-stand-to-sit task. The image capture was performed using a modified BV Pulsera videofluoroscopy system (Philips Medical Systems, Switzerland) with a field of view of 30.5cm, pulsed image acquisition rate of 25Hz, 8ms radiation pulse-width, 1ms image shutter time, and an image resolution of 1000 x 1000 pixels with a grayscale resolution of 12 bits. The system has previously been used to analyze joint kinematics in patients after total knee and ankle arthroplasty *in vivo* [38, 39, 41, 127–129].

4.3.5 Data processing

Distortion correction of the videofluoroscopic images was performed using an optimisation algorithm to correct for local distortions based on images of a reference grid [38, 41]. The projection parameters of the videofluoroscopic system (focal distance, and location of the principle point in the image plane) were determined by least-squares optimization using five images of a calibration tube [38, 41]. 3D CAD models of the implant components were then fitted to the 2D fluoroscopic images (Figure 4.1) using a registration algorithm based on the approach presented by Burckhardt and co-workers [40]. Root mean square registration errors using this process have been reported to be $\leq 0.25°$ for all rotations, 0.3mm for in-plane, and 1.0mm for out-of-plane translations [37].

4.3.6 Tibio-femoral kinematics

Relative tibio-femoral rotations were determined using the joint coordinate system presented by Grood and Suntay [70], based on the local femoral and tibial implant coordinate systems (Figure 4.2, left). Translations of the femoral condyles relative to the tibial component were described using the weighted mean of the ten nearest points of each femoral condyle to the upper plane of the tibial component. The positions of these nearest points were presented in the coordinate system of the tibial component, thus representing the motion of the femur relative to the tibia (Figure 4.2, right). To interpret joint kinematics, internal tibial rotation would therefore result in anterior translation of the medial, and/or posterior translation of the lateral, nearest femoral point(s) on the tibia. All kinematic trials were then normalized to one gait cycle.

4.3.7 Statistics

A total of eight linear mixed-model analysis of variances (ANOVAs), with subject as a random effect, were conducted to comprehensively analyse tibio-femoral kinematics. Specifically, five mixed-model ANOVAs were performed to test the effects of the task on ranges of tibio-femoral rotations and A-P translations of the condyles. Here, task-dependency was investigated with rotational (flexion/extension, internal/external, ab/adduction) and translational (medial A-P, lateral A-P) ranges of motion (ROMs) as dependent variables and task as the independent variable with four different levels (level walking, stair stair descent, sit-to-stand, stand-to-sit) for each of those kinematic parameters. Two mixed-model ANOVA were performed to test the effects

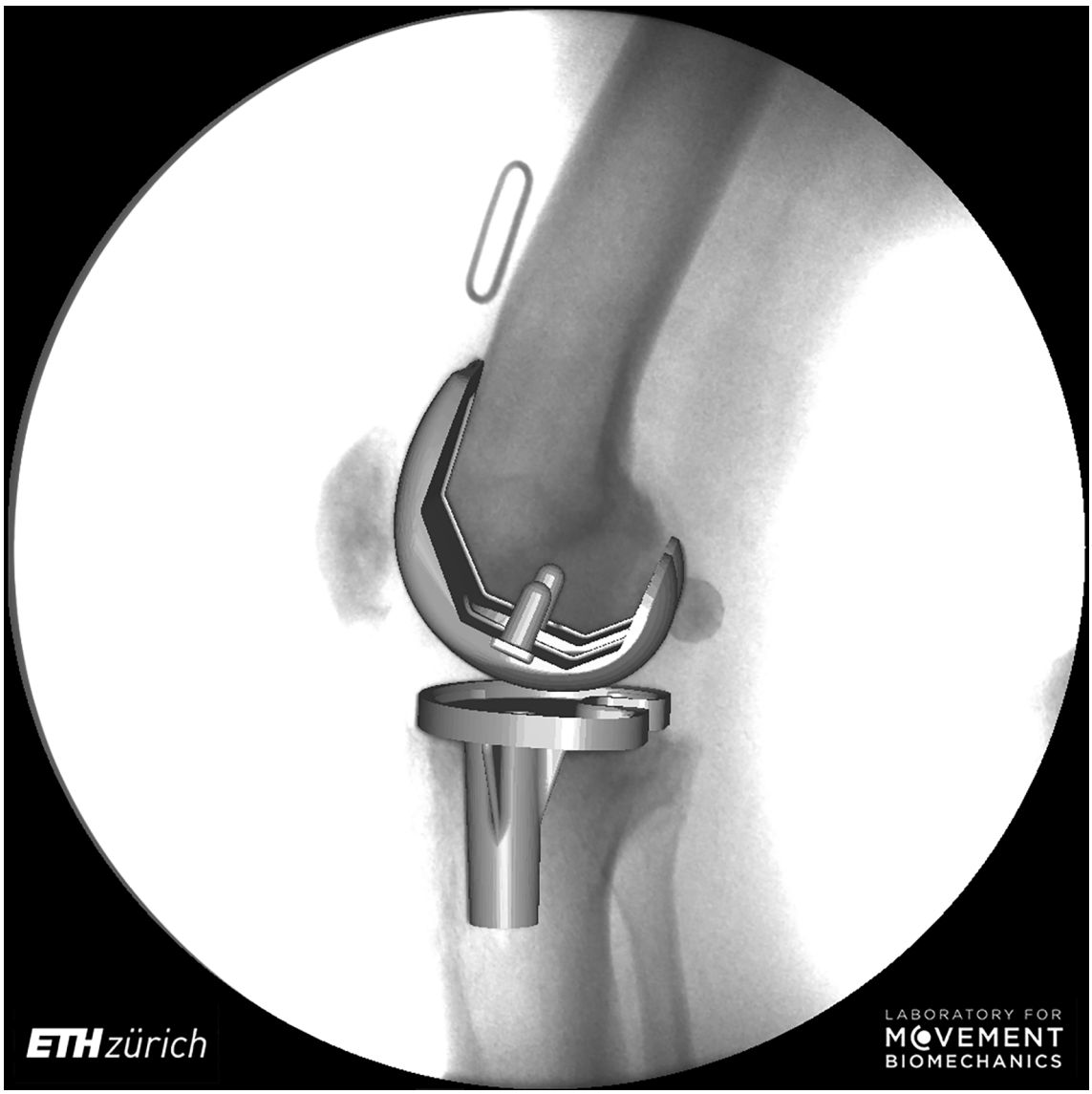

Figure 4.1: Exemplary instant of 3D tibial and femoral components registered to the 2D fluoroscopic image. The 2D/3D registration of all images allows the internal joint kinematics to be determined over the complete cycles of functional activities.

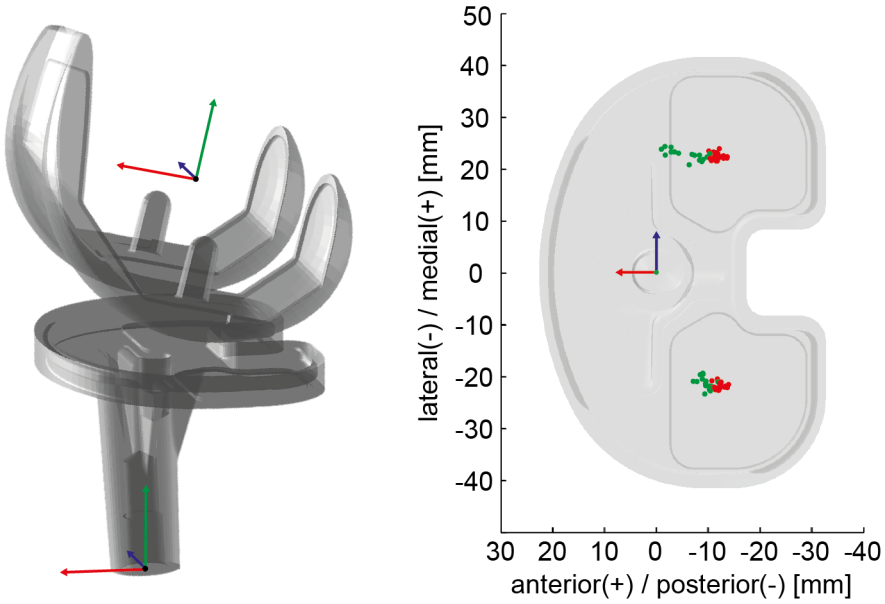

Figure 4.2: Implant coordinate systems for the femoral and tibial components (left) and nearest points for stance (red) and swing (green) phase for an exemplary trial of stair descent presented in the coordinate system of the tibial component (right).

of phases of task (e.g. loaded or unloaded phases) on range of A-P translation of the medial and lateral condyles. In order to analyse phase-dependency, range of A-P translation of the condyle was the dependent variable, while task with four levels (level walking, stair descent, sit-to-stand, stand-to-sit) and phases of task with two levels (stance and swing phases) were the independent variables. One mixed-model ANOVA was conducted to test the effects of loading sites (e.g. medial or lateral condyles) on range of A-P translation. The dependency on loading sites was tested with translation range in A-P as the dependent variable and task with four levels (level walking, stair stair descent, sit-to-stand, stand-to-sit) and loading sites with two levels (medial or lateral condyles) as the independent variables. Post-hoc comparisons were conducted using Least Significant Differences (LSD) approach and significance levels were adjusted for multiple comparisons using Bonferroni correction. All ANOVAs were conducted in SPSS (SPSS 23, IBM, United States).

In order to analyse the effects of task dependency on AP-translation at specific flexion angles one-dimensional statistical parametric mapping (SPM) approach was used [130]. One-way ANOVA was performed using the open-source toolbox SPM-1D (Todd Pataky 2017, version M.0.4.5), with region of interest defined as the full ranges of flexion-angles that are involved in each activity. Here, as loading conditions were totally different between the two phases (stance versus swing) of the gait activities, the two phases were treated as separate tasks. Thus within the SPM approach One-way ANOVA was performed with A-P translation as dependent variable and task

with six levels (level walking stance, level walking swing, stair descent stance, stair descent swing, sit-to-stand and stand-to-sit) as independent variables. Post-hoc comparisons were conducted using two-sample t-tests and significance levels were adjusted for multiple comparisons using Bonferroni correction.

4.4 Results

The mean ranges of joint flexion over all subjects were similar for stair descent (83.9 ± 6.3°), sit-to-stand (83.3 ± 5.6°), and stand-to-sit (84.8 ± 5.0°) (Table 4.1; Figure 4.3), but significantly lower for level walking (58.4 ± 4.1°). No differences between the tasks could be found in mean range of internal/external rotation or ab/adduction (Table 4.1; Figure 4.4). Mean toe-offs were observed at 62.1 ± 1.7 % of the level walking cycle and at 64.1 ± 3.2 % of the stair descent cycle.

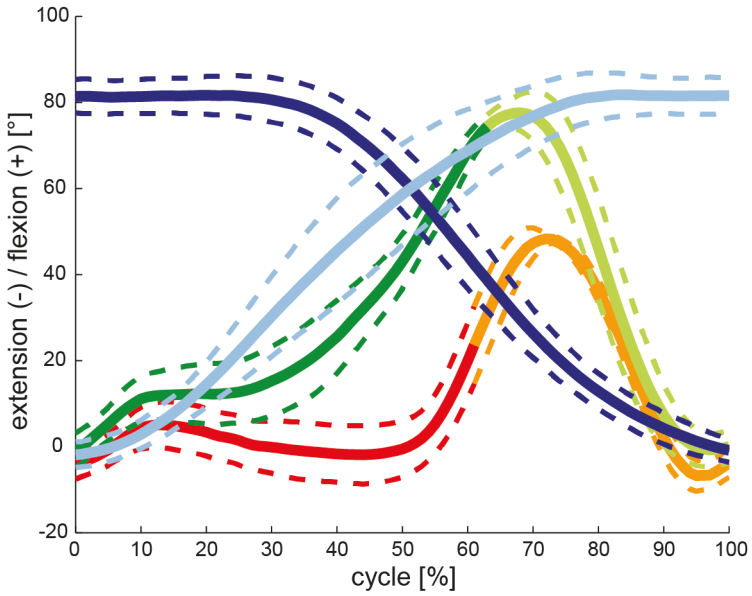

Figure 4.3: Tibio-femoral flexion is presented for all tasks, including mean and SD over all subjects. Loaded and unloaded activity phases are shown respectively for level walking (red/orange), stair descent (green/light green), sit-to-stand (dark blue), and stand-to-sit (light blue).

In general, when tibio-femoral translations and rotations were examined (Figure 4.4), mean and standard deviations of the individual subjects exhibited repeatable individual motion characteristics, indicating small variability between the trials within each single subject, but large inter-subject variations were observed. For example, one subject exhibited a clearly distinct pattern of ab/adduction during swing phase of level gait compared to the group.

The mean range (difference between minimal and maximal value) of medial condylar A-P trans-

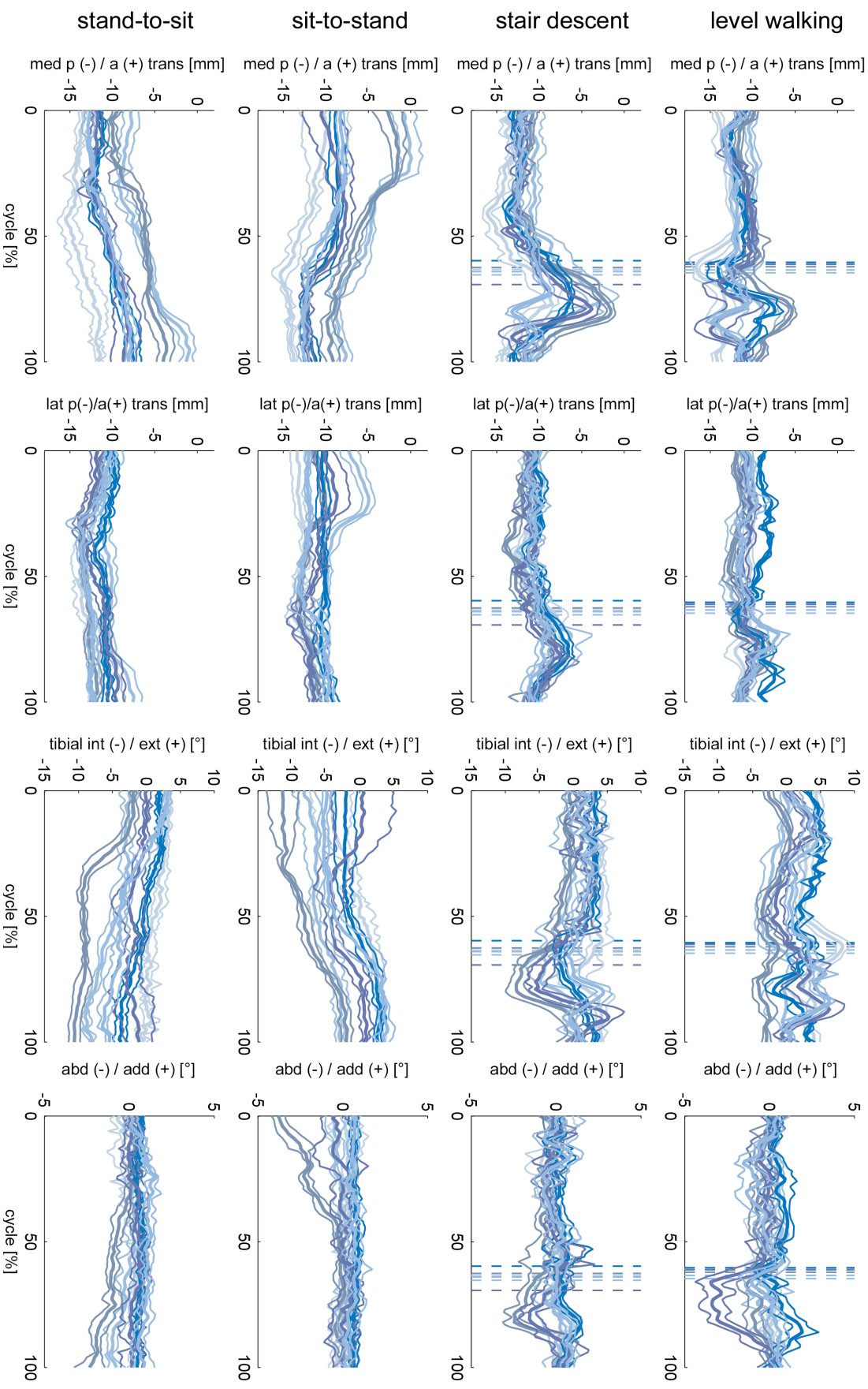

Figure 4.4: Tibio-femoral kinematics are shown for the activities of level walking, stair descent, sit-to-stand, and stand-to-sit for each single subject, represented by the different colors, including the mean and SD over all repetitions. The columns are presented in % cycle, and show the A-P translation of the medial and lateral condyles, as well as the tibial internal/external rotation, and joint ab/adduction. For level walking and stair descent the dashed lines indicates the mean timepoint of toe-off for each subject.

lation exhibited a clear task dependency across all subjects (Table 4.1). The mean ranges of A-P translation for the medial condyle were: 6.4 ± 1.2mm (level walking), 9.4 ± 2.6mm (stair descent), 7.0 ± 2.0mm (sit-to-stand), and 6.5 ± 1.4mm (stand-to-sit); and for the lateral condyle: 4.9 ± 0.9mm (level walking), 6.5 ± 1.7mm (stair descent), 4.7 ± 1.7mm (sit-to-stand), and 4.5 ± 0.9mm (stand-to-sit). Here, a significantly larger mean range of A-P translation was observed on the medial condyle during stair descent compared to level walking and stand-to-sit. No significant differences between the tasks could be found for the mean range of A-P translation on the lateral condyle. The ranges of A-P translation observed over the full cycles across all subjects were significantly larger for the medial than for the lateral condyle. When activity phases were considered, the mean range of A-P translation for the unloaded swing phases of level walking and stair descent was significantly larger than for the loaded stance phases (Table 4.1). The single greatest posterior and anterior translations of the medial femoral condyle relative to the tibia were -17.9mm at 60 % during a cycle of level walking and 1.6mm at 18 % of a sit-to-stand cycle (in different subjects). The corresponding greatest translations of the lateral femoral condyle were -15.5mm at 40 % during stand-to-sit and -2.6mm at 73 % during stair descent.

In order to establish whether the observed kinematic differences between tasks were simply a function of flexion angle, the flexion dependent A-P translations and internal/external rotations for the different tasks were examined. On average, the lateral A-P translations during the swing phase of stair descent differed significantly from the loaded stance phase (for 24° to 36° flexion), as well as from the sit-to-stand (for 17° to 46° flexion) and stand-to-sit (for 10° to 54° flexion) tasks (Figure 4.5). In addition, the swing phase of level walking showed significant differences to the stand-to-sit task for a certain range of flexion (29° to 36°). Looking at the mean tibial rotation with increasing flexion, a linear increase in internal tibial rotation was observed for the loaded stance phase of stair descent, as well as during the two sitting tasks. During the unloaded swing phase of stair descent, tibial internal rotation also increased with increasing flexion, but not in a linear manner. However, no increase in internal rotation was observed with increasing flexion in either phase of level walking.

Due to the large variation between subject kinematics (Figure 4.4), especially for the medial condyle, task dependency was also investigated on an intra-subject basis over the flexion series (Figure 4.6). Significant task dependency of the loaded phases was found for all subjects between gait activities and the two sitting tasks. When the loaded stance and the unloaded swing phases were compared, all subjects exhibited significant differences when performing stair descent, and two out of six during level gait. Furthermore, four out of six subjects showed a significant

Table 4.1: Tibio femoral rotations and A-P translation range for all tasks. For level gait and stair descent the stance and swingphase were presented separately. Mean and standard deviation over all subjects. Flex/ex: flexion/extension, abd/add: abduction/adduction, int/ext: internal/external tibial rotation, st: stance phase, sw: swing phase, med: medial, lat: lateral, A-P: anterio-posterior.

rotation [°]	***flex/ex***	***abd/add***	***int/ext***	***flex/ex (st)***	***abd/add (st)***	***int/ext (st)***	***flex/ex (sw)***	***abd/add (sw)***	***int/ext (sw)***
level walking t1	58.4 ± 4.1 *t2,t3,t4	3.1 ± 0.9	8.2 ± 1.6	29.5 ± 4.2	2.0 ± 0.5	5.9 ± 1.1	57.6 ± 3.6	2.8 ± 0.9	6.8 ± 1.4
stair descent t2	83.9 ± 6.3 *t1	3.4 ± 0.7	9.2 ± 2.0	75.1 ± 6.4	2.8 ± 0.3	5.9 ± 1.7	82.8 ± 5.9	2.5 ± 0.9	8.4 ± 2.4
sit-to-stand t3	83.3 ± 5.6 *t1	2.3 ± 1.1	8.7 ± 1.7						
stand-to-sit t4	84.8 ± 5.0 *t1	2.2 ± 0.7	7.7 ± 2.0						

translation [mm]	***med A-P***	***lat A-P***	***med A-P (st)***	***lat A-P (st)***	***med A-P (sw)***	***lat A-P (sw)***
level walking t1	6.4 ± 1.2 *t2	4.9 ± 0.9	3.6 ± 0.9 *p	3.0 ± 0.6 *p	6.1 ± 1.3 *p	4.4 ± 1.0 *p
stair descent t2	9.4 ± 2.6 *t1,t4,c	6.5 ± 1.7 *c	5.0 ± 1.0 *p	3.7 ± 0.7	8.4 ± 2.3 *p	4.9 ± 1.2
sit-to-stand t3	7.0 ± 2.0 *c	4.7 ± 1.7 *c				
stand-to-sit t4	6.5 ± 1.4 *t2	4.5 ± 0.9				

**t#: significantly different from task t#, based on the adjusted level of significance of $\alpha = 0.008$ (example: *t2 means significantly different to stair descent)*
**p: significant difference between stance and swing phase, based on the adjusted level of significance of $\alpha = 0.025$*
**c: significant difference between the medial and lateral condyle, based on the adjusted level of significance of $\alpha = 0.013$*

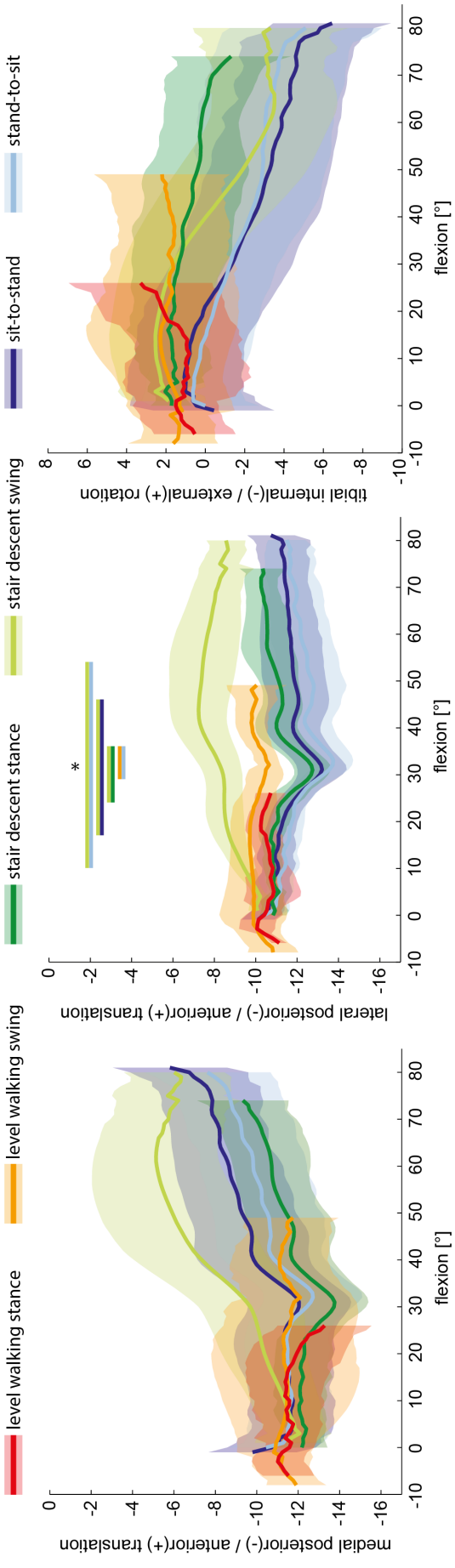

Figure 4.5: A-P translation for the medial (left) and lateral (centre) condyles, as well as tibial rotation (right) are shown as a function of the flexion angle. The tasks level walking, stair descent, sit-to-stand, and stand-to-sit are presented as the mean of all six subjects, with the group SD shown as transparent. Note that an anterior translation of the nearest point on the medial condyle and/or posterior translation on the lateral condyle represents an internal rotation of the tibial component. *: Significant differences, found between the tasks for certain ranges of flexion, were indicated with bars in the colors of the respective tasks with an adjusted level of significance of $\alpha = 0.003$.

difference in A-P translation at the same flexion angles between the movement directions in the two sitting tasks.

Finally, local minima were observed at approximately 30° flexion in most of the A-P translation-flexion curves for different tasks (Figure 4.5), which were more prominent during loaded task phases.

4.5 Discussion

To improve functionality and quality of life, as well as support independent living, joint replacement with a TKA aims to relieve pain and restore function of the knee joint throughout daily living. While numerous studies have investigated joint movement, a fundamental understanding of tibio-femoral kinematics during dynamic and continuous functional activities of daily living remains lacking, mainly due to the limitations of static imaging modalities [120, 131] or the soft tissue artefacts associated with skin-marker based techniques [52]. As a result, the subtle kinematic differences caused by different activities, including different flexion angles, muscular activity, dynamic loading conditions (e.g. impact at heel-strike and toe-off), remain generally unknown. The aim of this study was therefore to determine whether knee joint kinematic behavior after total joint replacement is dependent upon the investigated task and loading conditions. Using dynamic videofluoroscopy [37], we observed that tibio-femoral kinematics were not simply flexion dependent, but rather varied between level walking, stair descent, sit-to-stand, and stand-to-sit.

For the first time, the kinematics of the PFC Sigma Curved CR fixed-bearing TKA (DePuy Synthes, Johnson and Johnson) have been evaluated for several consecutive cycles of functional activities, including loaded stance and unloaded swing phases. Here, a comparison of stair descent and the two sitting tasks at the same flexion angles but with different moving directions (Figure 4.5), has clearly demonstrated that an activity dependent A-P translation-flexion coupling exists. In this respect, it seems that loading and unloading of the implant, together with the movement dynamics and muscular activation patterns, play crucial roles in governing the relative motion within the joint. Additionally, differences in implant movement characteristics, even between the phases of similar gait activities (e.g. level walking and stair descent) at the same joint flexion angles (Figure 4.5), further highlight the importance of analyzing whole gait cycles. Here, a complete understanding of the combination of loading/unloading together with

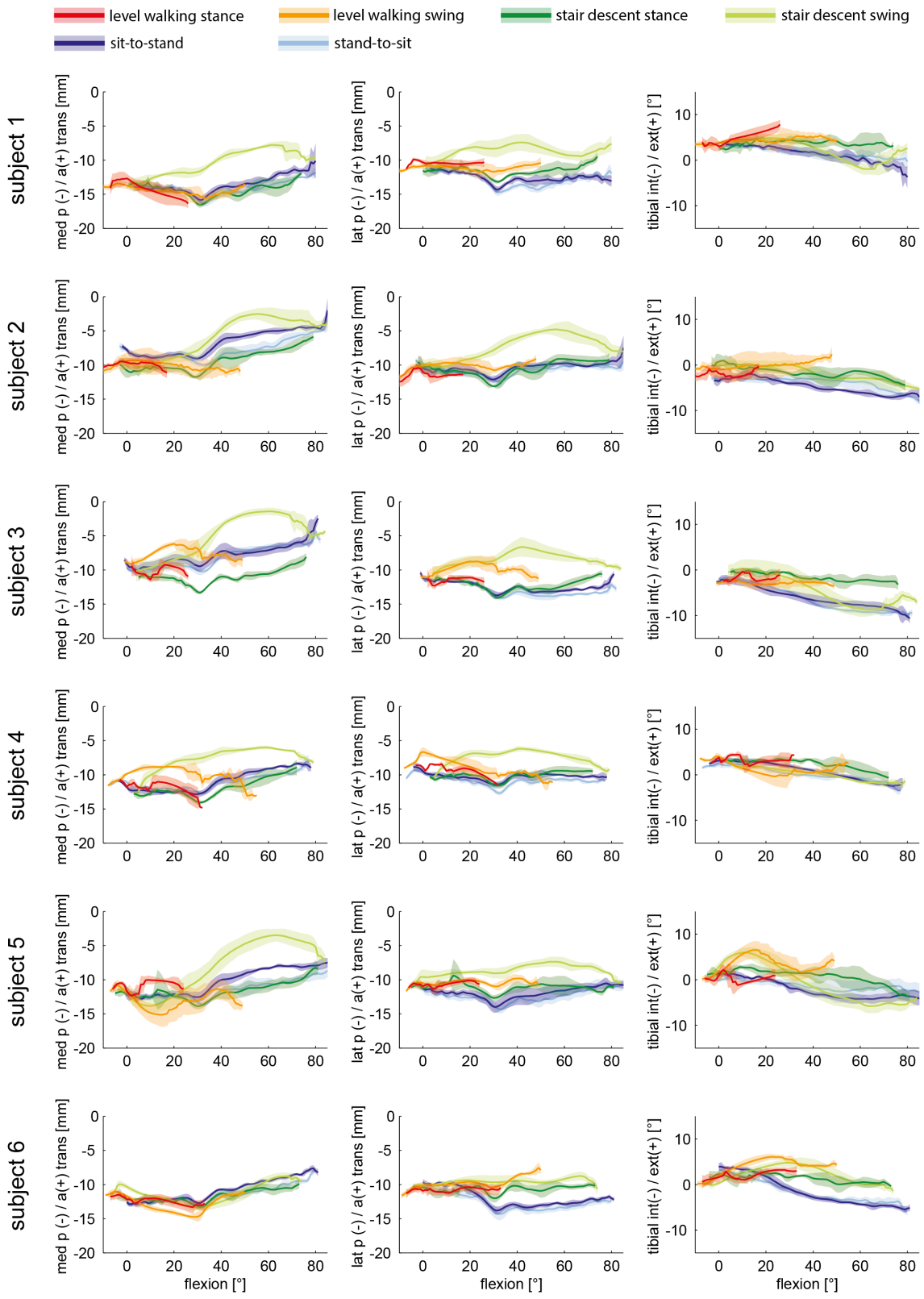

Figure 4.6: A-P translation for the medial (left) and lateral (centre) condyles, as well as tibial rotation (right) are shown as a function of the flexion angle. The tasks level walking, stair descent, sit-to-stand, and stand-to-sit are presented for each of the six subjects as the mean of all repetitions, with the subject SD shown as transparent.

the changes in movement directions, might, therefore, be critical for implant design in order to successfully avoid soft tissue overloading[11], but also provide sufficient joint stability for enhanced patient satisfaction [6, 10]. In our study, it was interesting to observe a clear perturbation in the kinematic behavior during the loaded activity phases, characterised by a local minimum in the A-P translation at 30° flexion (Figure 4.5). This characteristic is in agreement with observations of other studies [16, 85, 132] and plausibly corresponds with the change in femoral radius of the PFC Sigma CR implant, and this specific feature could therefore be modulated, controlled or even removed with a different implant design. Interestingly, this feature was much less prominent in the unloaded phases, where the geometry seems to have less impact on kinematic guidance.

The small range of joint flexion involved in level walking has to be considered in the interpretation of the results. The typical local minimum in joint flexion during the stance phase of level walking was not observed during stair descent (Figure 4.3), which is in agreement with the findings of former skin marker studies on healthy knees [115, 133]. Moreover, the range of axial rotation occurring during the stance phase of level gait was comparable to the study of Banks and Hodge [73], as well as the study of Schmidt and co-workers [87]. However, the additional access to the motion during the swing phase in our study has resulted in an overall larger range of axial rotation. Banks and Hodge [73] found a significant difference in axial rotation between treadmill walking and a step-up exercise, whereas the results of our study indicate that only flexion/extension ranges of motion exhibited a task dependency, while transverse and frontal plane ranges of motion did not differ. Specifically for the PFC Sigma CR implant, Schmidt et al. [87] reported a smaller A-P translation range of the medial condyle (-5.4mm at heel strike to -6.7mm at 33 % stance phase) but slightly larger translation on the lateral side (-3.8mm at heel strike to -7.8mm at toe off) for discrete timepoints during the stance phase of walking, compared to our study. For the sitting tasks, larger values especially for the medial and lateral condyle were found compared to deep knee bend up to 90° flexion performed in other studies with a PFC Sigma CR implant [19]. It therefore seems that the additional freedom offered by the moving fluoroscope, which includes not only the loaded stance phase, as in other studies, but also the swing phases of movement and the associated changes in accelerations, movement direction, muscle activity, ground impact etc., is necessary before an encompassing understanding of the joint motion can be achieved.

In order to compare the results of knee kinematic studies in an objective manner, as well as ensure correct clinical interpretation, the method for kinematic data analysis must be considered with care. Here, the use of a femur fixed geometric axis approach instead of an instantaneous

nearest point approach is known to change interpretation of the A-P characteristics [74, 124, 134]. Such sensitivities could be especially important when considering the PFC Sigma CR implant investgated in our study, which has two different femoral radii and could therefore lead to crosstalk between flexion and A-P translation. However, the larger A-P translation found for the medial condyle compared to the lateral condyle for all tasks (when using the nearest point technique) indicates that the centre of rotation in the transverse plane in this implant is relatively stable and might be located on the lateral side of the joint, at least for some phases of the activity. The results of this study revealed a number of interesting aspects relating to the kinematics of this PFC Sigma CR implant. We clearly observed subject-specific movement patterns across the different activities, which were considerably larger than any of the intra-subject differences measured between repetitions. Such differences between subjects indicate that individual anatomical and surgical characteristics, including soft tissue tension [135], component implantation [136], and limb alignment [125] among others, may all play an important role in governing the subject-specific movement patterns. One such characteristic of clinical interest is the possible occurrence of femoral lift-off. Our analyses of ab/adduction suggest that low-level lift-off did indeed occur in 1-2 subjects at specific instances within the functional activities. Whether such kinematic anomalies are indicative of a clinical problem remains to be elucidated, but the ability to detect such small kinematic differences between subjects could suggest that the detailed assessment of internal joint movement (using e.g. moving fluoroscopic techniques) might be able to support clinical assessments of joint function. Similar to other studies investigating joint kinematics, the wide-spread extrapolation of our results to e.g. healthy joints or other implants is restricted by a number of limitations. In particular, the small number of subjects included in our study limits its statistical power for the non-significant differences to represent the more general outcome in a larger population. Furthermore, while the use of a single-plane moving fluoroscope offers considerable advantages in the accurate capture of functional joint kinematics without restrictions due to soft tissue artefacts, the registration of 3D models to 2D images is known to be subject to relatively large out-of-plane errors [37, 38]. Such inaccuracies exclude the interpretation of any relative medial-lateral movement of the components. In addition, the extreme accelerations that occur in the human knee joint limit the ability of the moving fluoroscope to track walking activities at speeds beyond that of slow-gait [137]. Finally, this study included only TKA subjects with a good clinical outcome. It remains to be investigated whether these results can be extrapolated for understanding joint kinematics in other implants, including TKAs with bad outcome, or also healthy knees.

In summary, comparisons between the different tasks and phases within the six subjects investigated in our study showed a clear task dependency but the impact of the task on the underlying kinematics seems to be subject-specific. Differences in dynamics, limb alignment, range of motion, muscle activation, or balancing of the ligaments, might well be able to explain these subject-specific characteristics. However, from the data presented within this study, it is clear that flexion angle alone cannot fully explain tibio-femoral implant kinematics. As a result, it seems that the assessment of complete cycles of the most frequent functional activities of daily living seems to be imperative when evaluating the behavior of a TKA design *in vivo*.

4.6 Acknowledgements

The study was financially supported by a research grant from DePuy Synthes (Johnson and Johnson). The authors would like to thank all the subjects who took part in this study, Dr. med. Reto Grünig (Leuggern Hospital, Switzerland) for recruiting the subjects, Prof. Dr. Edgar Stüssi, Dr. Monika Zihlmann, Dr. Mauro Foresti, Jacqueline Stucki, Marco Hitz and Peter Schwilch for their contribution to the developpement of the moving fluoroscope and all the students who helped with the measurements and postprocessing.

Chapter 5

GMK Sphere implant exhibits medial stability during gait activities *in vivo*: A dynamic videofluoroscopy study

adapted from:

Pascal Schütz[1], **William R. Taylor**[1], **Barbara Postolka**[1], **Sandro F. Fucentese**[2], **Peter P. Koch**[3], **Michael A.R. Freeman**[4], **Vera Pinskerova**[5], **Renate List**[1]

[1]Institute for Biomechanics, ETH Zürich, Switzerland

[2]Balgrist University Hospital, Zürich, Switzerland

[3]Winterthur Cantonal Hospital, Zürich, Switzerland

[4]Royal London Hospital, London, UK

[5]Medical faculty, Charles University, Prague

in preparation

5.1 Abstract

Joint stability is a primary concern in total knee joint replacement. The GMK Sphere prosthesis was specifically designed to provide medial stability, while permitting rotational freedom of the joint through a flat lateral tibial surface. The objective of this study was to establish whether the GMK Sphere prosthesis provides greater *in vivo* medial stability during gait activities than conventional posterior-stabilized (PS) fixed-bearing and ultra-congruent (UC) mobile-bearing designs.

The anterior-posterior (A-P) translation and internal/external rotation of three cohorts, each with 10 good outcome subjects (2.9 ± 1.6y postop), with a GMK Sphere, GMK PS or GMK UC implant were analysed throughout complete cycles of gait activities using dynamic videofluoroscopy. The GMK Sphere showed the smallest range of medial A-P translation for level walking, downhill walking, and stair descent (3.7 ± 0.9mm, 3.2 ± 0.8mm, 4.0 ± 1.4mm), followed by the GMK UC (5.9 ± 1.0mm, 8.2 ± 1.8mm, 9.0 ± 1.9mm) and the GMK PS (10.6 ± 2.3mm, 10.4 ± 2.7mm, 12.0 ± 1.6mm) designs. The GMK Sphere exhibited the largest range of lateral A-P translation (12.5 ± 2.2mm), as well as the largest range of tibial internal/external rotation (13.2 ± 2.2mm), both during stair descent.

This study has shown that the GMK Sphere provides medial A-P stability during gait activities and still allows rotational freedom. The additional comparison against the conventional GMK PS and UC designs, not only demonstrates that implant design is a key factor in governing tibio-femoral kinematics, but also that the design itself probably plays a more dominant role for joint movement than the type of activity being undertaken.

Keywords

Medial stability, total knee arthroplasty, moving fluoroscope, single plane fluoroscopy, design dependency, gait activities

5.2 Introduction

To maintain sufficient range of motion after a total knee replacement, but also not overload the surrounding soft tissue structures, mimicking tibio-femoral kinematics of the healthy knee

is thought to be beneficial in the development of total knee arthroplasty (TKA) designs. In posterior cruciate retaining as well as in cruciate-substituting designs with little conformity between the femoral and tibial articular surface, paradoxical anterior motion has been observed during flexion [13]. This could lead to overloading of the surrounding tissues or a feeling of joint instability [6, 10, 138]. A highly constrained design is able to provide anterio-posterior (A-P) stability, but could restrict the functional range of motion and raise the required constraining forces, thus promoting implant loosening [10].

To provide both A-P stability and a large pain-free range of axial rotation throughout daily activities, medial pivot designs have recently been introduced. One such design, the GMK Sphere prosthesis (Medacta International, Lugano, Switzerland), was specifically designed to constrain the medial condyle through geometrical conformity, while the flat unconstrained lateral tibial surface allows A-P translation of the lateral condyle in order to permit rotational freedom of the joint. In this respect, the implant is thought to closely mimic the kinematics of the natural knee [27]. Until now, the *in vivo* kinematics of this novel implant design have only been investigated during kneeling, lunging, dynamic step-up/down and pivoting movements [24]. Here, little or no translation of the medial femoral condyle was observed, while the lateral condyle translated posteriorly with increasing flexion, resulting in a tibial internal rotation. However, until now, no investigation into the joint kinematics has been undertaken during dynamic gait activities that include functional loading and unloading of the joint, impact at heel-strike, and changing muscle activation patterns. Since such gait activities belong to the most frequently performed daily tasks, but also challenge subjects with knee disorders [32, 34, 105], their inclusion in a complete evaluation of the functionality of a TKA design therefore seems critical.

In addition to a multitude of examinations using skin marker-based optical techniques that suffer from errors due to soft tissue artefact [43, 52, 118], the assessment of joint kinematics has been extensively investigated using imaging techniques such as MRI [30, 31, 123], RSA [65, 139] and fluoroscopy [12, 29, 66, 90], but also in studies using bone-pins [42, 54, 140] or in cadaveric specimens [27], in order to provide higher levels of accuracy. Imaging studies have allowed a detailed analysis of the *in vivo* internal tibio-femoral kinematics throughout knee flexion, but are generally limited in the examination field of view, and therefore do not allow tracking of the knee joint during full cycles of dynamic gait activities, or are restricted to imaging only a portion of the whole motion. To overcome the constraints of such static imaging approaches, dynamic systems have been developed [36, 37] that now allow investigation into tibio-femoral kinematics throughout complete cycles of level walking, downhill walking and stair descent. The

use of such a system has, for the first time, recently shown that tibio-femoral kinematics depend on the activity performed and that clear differences between the loaded stance and the unloaded swing phases of gait activities exist [141]. Furthermore, it is now known that treadmill walking alters joint kinematics compared to free level walking [36].

Whether the intended kinematic behavior of the GMK Sphere design principle, that has been presented during lunge and step-up activities, is also present for dynamic gait activities remains unknown. Therefore, the objective of this study was to compare the *in vivo* kinematics of the GMK Sphere prosthesis to the conventional GMK Primary posterior stabilized (PS) fixed-bearing and the GMK Primary ultra-congruent (UC) mobile-bearing TKA for level walking, downhill walking and stair descent.

5.3 Methods

5.3.1 Subjects

In total, 30 subjects with a unilateral TKA and good clinical outcome (WOMAC between 0 to 28) provided informed written consent to participate in this study, which was approved by the local ethics committee (KEK-ZH-Nr.2015-0140). Three cohorts, each with 10 subjects, possessing either a GMK Sphere (2 male / 8 female, aged 68.8 ± 9.9, 1.7 ± 0.7 years postop, BMI 25.4 ± 3.7), a GMK Primary PS (5m/5f, aged 69.0 ± 6.5, 3.1 ± 1.6 years postop, BMI 27.6 ± 3.5) or a GMK Primary UC (3m/7f, aged 75.0 ± 5.1, 3.9 ± 1.5 years postop, BMI 25.9 ± 3.2) implant were measured in the Laboratory for Movement Biomechanics, ETH Zürich, while performing various activities of daily living.

5.3.2 Motion tasks

The kinematics and kinetics of 3 functional gait activities: level walking (straight ahead on the floor), downhill walking (10° inclined slope) and stair descent (three 0.18m steps), were captured according to the set-up described by List and co-workers [37]. Familiarization trials with the moving fluoroscope (see below) were performed for each activity prior to acquiring at least five repetitions that included the radiographic assessment.

5.3.3 Ground reaction forces and motion capture system

Eight force plates (Kistler AG, Winterthur, Switzerland), which were fully decoupled from the surrounding floor, provided undisturbed ground reaction forces (GRFs) during all measured gait activities [37]. A GRF threshold of 25 N was used to determine the gait events. The trajectories of a heel marker, captured using an optoelectronic system consisting of 22 infrared cameras (Vicon MX system, Oxfords Metrics Group, UK), were used to define the second heel strike event of downhill walking, which was not instrumented with a force plate.

5.3.4 Moving fluoroscope

To image complete, consecutive cycles of the knee joint during level walking, downhill walking and stair descent, the moving fluoroscope was employed to capture the relative movements of the femoral and tibial components with a measurement frequency of 25Hz during the investigated gait activities [37, 127, 141]. Detailed information about the videofluoroscopic image capture are provided in the literature [37–39, 41, 127, 128, 141].

5.3.5 Data processing

2D/3D registration

The acquired digital images were corrected for distortion using a local correction algorithm based on a reference grid [38, 41]. The optical projection parameters of the fluoroscopic system, namely focal distance and principal point, were determined from five images of a calibration tube [38]. The three dimensional orientation of the implant components was determined using a 2D/3D registration algorithm based on the approach developed by Burckhardt and co-workers [40]. This process has reported registration errors of $\leq$ 0.25° for all rotations, 0.3mm for in-plane, and 1.0mm for out-of-plane translations for a similar TKA [38, 41].

Tibio-femoral Kinematics

The joint coordinate system approach reported by Grood and Suntay [70], based on the femoral and the tibial implant coordinate systems (Figure 5.1), has been used in this study to describe the tibio-femoral rotations. A-P translations of the medial and lateral femoral condyles relative

to the top plane of the tibial baseplate were defined using the weighted mean of the ten nearest points on each condyle. In order to reduce bias due to different implant sizes in the three groups, the locations of the medial and lateral nearest points, presented in the tibial coordinate system, were normalized to a medium femur size with a notch distance of 44mm (normalization factor=44mm/notch distance). All implant kinematic data were interpolated linearly to allow 101 data points for interpretation over complete activity cycles.

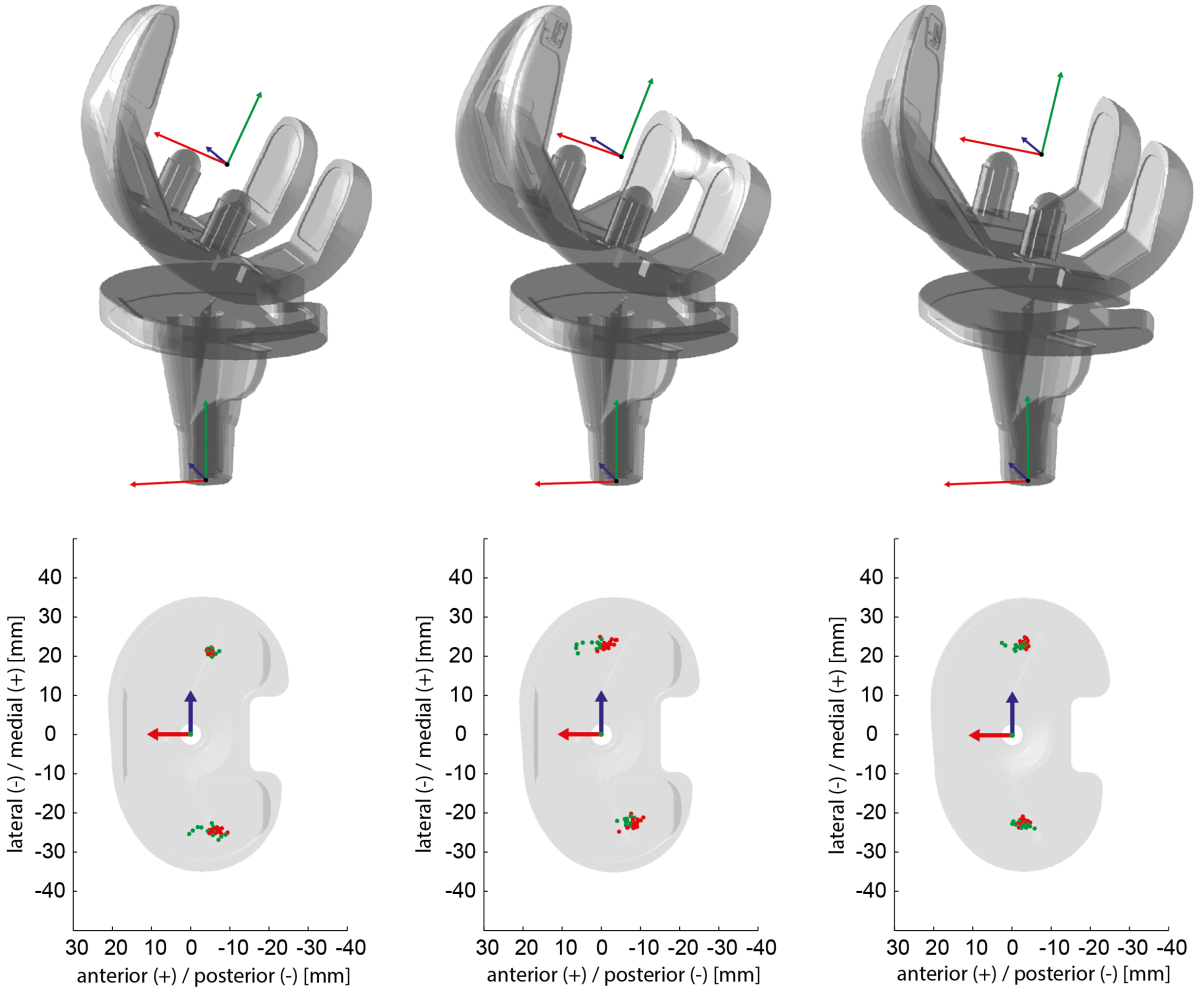

Figure 5.1: Implant coordinate systems for the femoral and tibial components of the GMK Sphere (left), GMK PS (centre) and GMK UC (right), including the and nearest points for stance (red) and swing (green) phases for exemplary trials of level walking presented in the associated coordinate system of the tibial component. for the GMK Sphere (left), GMK PS (centre) and GMK UC.

5.3.6 Statistics

The null hypothesis was defined as no difference in kinematics between the different designs. To test this hypothesis for the three tibio-femoral rotations, as well as for the medial and lateral

A-P translation of the condyles, 5 mixed-model ANOVAs with subject as a random effect were performed. Here, the influence of the design was investigated with rotational (flexion/extension, internal/external, ab/adduction) and translational (medial A-P, lateral A-P) ranges of motion (ROMs) as dependent variables, and design with three levels (GMK Sphere, GMK PS, GMK UC) and task with three levels (level walking, downhill walking and stair descent) as the independent variables. Post-hoc comparisons were conducted using a Least Significant Differences (LSD) approach and significance levels were adjusted for multiple comparisons using Bonferroni correction. All ANOVAs were conducted in SPSS (SPSS v23, IBM, United States).

5.4 Results

In general, the implant design influenced the kinematic patterns to a greater degree than the different activities (Figures 5.2, 5.3, 5.4). While a high level of inter-subject conformity was observed on the medial condyle of the GMK Sphere, the greatest variability in tibio-femoral kinematics was observed on its lateral side.

5.4.1 Rotations

All three implants exhibited equal ranges of joint flexion during downhill walking and stair descent, but the GMK Primary UC showed significantly reduced flexion during level walking compared to the GMK PS (Table 5.1). The GMK Sphere exhibited a significantly larger range of tibial internal/external rotation compared to the GMK UC for all tasks and compared to the GMK PS for stair descent. No differences were found between the implant design kinematics for ab/adduction.

The tibial components of the GMK PS and UC designs remained, on average, internally rotated throughout the full range of flexion of all activities, including loaded stance and unloaded swing phases (Figure 5.5). In contrast, the GMK Sphere exhibited a different kinematic coupling between flexion and tibial rotation especially for the loaded stance phase of level walking and the unloaded swing phases of all activities. Here, the GMK Sphere showed an increase in external rotation, which was followed by an internal rotation, but the orientation of the tibia relative to the femoral component generally remained externally rotated. No clear differences in tibial rotation could be seen for the loaded stance phases of stair descent and downhill walking compared to the conventional designs.

Table 5.1: Range of motions for all three tibio-femoral rotations for the GMK Sphere, GMK PS and GMK UC during level walking, downhill walking and stair descent. Mean and SDsd for all groups are reported for:. Flex/ex: Flexion/extension (Flex/ex), int/ext: tibial internal/external rotation (int/ext), and ab/add: abduction/adduction (ab/add).

	full gait cycle										**loaded stance phase**									**unloaded swing phase**								
	flex/ex [°]				**int/ext [°]**				**ab/add [°]**			**flex/ex [°]**			**int/ext [°]**			**ab/add [°]**			**flex/ex [°]**			**int/ext [°]**			**ab/add [°]**		
level walking																													
GMK Sphere	62.7	±	4.9		**11.9**	±	**4.2**	***b**	2.8	±	0.8	34.2	±	6.2	7.3	±	2.8	1.8	±	0.4	61.9	±	5.4	9.2	±	3.2	2.5	±	0.7
GMK PS	**63.5**	±	**4.7**	***a**	10.5	±	1.9		2.9	±	0.8	33.0	±	7.2	7.9	±	1.3	2.2	±	0.6	61.8	±	5.7	8.3	±	1.5	2.3	±	0.7
GMK UC	**57.2**	±	**4.8**	***a**	**8.1**	±	**2.5**	***b**	2.3	±	0.6	30.2	±	4.2	6.2	±	2.8	1.6	±	0.3	56.4	±	5.5	5.9	±	1.6	2.0	±	0.7
downhill																													
GMK Sphere	70.0	±	4.5		**11.5**	±	**2.7**	***c**	2.6	±	1.0	51.5	±	6.0	6.3	±	1.7	1.5	±	0.2	69.9	±	4.6	10.1	±	2.5	2.3	±	0.9
GMK PS	69.9	±	5.3		8.9	±	2.1		2.6	±	0.7	50.1	±	8.3	6.3	±	2.0	2.1	±	0.7	68.7	±	6.3	7.3	±	1.8	2.0	±	0.6
GMK UC	66.1	±	3.4		**7.9**	±	**2.3**	***c**	2.2	±	0.7	47.3	±	4.8	5.6	±	1.9	1.5	±	0.2	65.6	±	3.8	6.1	±	1.9	1.9	±	0.7
stair descent																													
GMK Sphere	89.5	±	5.5		**13.2**	±	**2.2**	***d,e**	3.0	±	1.2	77.5	±	6.4	6.6	±	2.4	2.1	±	0.8	89.1	±	5.3	12.8	±	2.4	2.3	±	1.0
GMK PS	90.2	±	5.5		**9.0**	±	**2.5**	***d**	2.9	±	0.7	78.8	±	9.2	6.6	±	3.1	2.5	±	0.7	89.9	±	5.6	7.6	±	1.9	2.0	±	0.6
GMK UC	87.5	±	4.4		**8.4**	±	**3.3**	***e**	2.3	±	0.7	76.6	±	5.6	6.0	±	2.5	2.0	±	0.5	87.3	±	4.5	7.3	±	3.3	1.7	±	0.5

**: Significantly different, based on the adjusted level of significance of* $\alpha = 0.005$

5.4.2 A-P translation

The motion patterns of the mean A-P translations of each subject (Figures 5.2, 5.3, 5.4) for the GMK Sphere showed very constrained medial condylar motion with almost no inter-subject variation throughout full cycles of level walking (mean SD 0.6mm), downhill walking (mean SD 0.5mm) and stair descent (mean SD 0.6 mm), whereas the lateral condyle was found to allow subject-specific motion patterns, resulting in high inter-subject variability (mean SD level walking 4.8 mm, downhill 3.9 mm, stair descent 3.7mm). In contrast, the two conventional designs exhibited similar inter-subject variability for both condyles with slightly larger variation for the GMK PS (mean SD med 2.2-2.4mm, lat 1.9-2.2mm), than for the GMK UC design (mean SD medial 1.7-1.8mm, lateral 1.8-1.9mm). Of importance was that intra-subject variability was extremely low (maximal mean SD for a single subject was 1.5mm, observed during stair descent).

The medial range of A-P translation differed significantly between all three investigated designs (Table 5.2). Here, GMK Sphere showed the smallest A-P translation for the medial condyle for level walking, downhill walking and stair descent, followed by the GMK UC and the GMK PS. For the lateral condyle, the GMK UC showed a significantly smaller range of A-P translation for all activities compared to the GMK Sphere and for downhill walking and stair descent compared to the GMK PS. For all designs, the ranges of A-P translation for both condyles were smaller during the loaded stance phases compared to the unloaded swing phases (Figures 5.2, 5.3, 5.4, Table 5.2), with minimal mean ranges found during stance for the medial condyle of the GMK Sphere of 2.0 $\pm$ 0.2mm for level walking, downhill walking 1.8 $\pm$ 0.3mm, and stair descent 2.5 $\pm$ 0.9mm. The largest and smallest range of A-P translation found throughout full cycles of the activities in a single trial were observed in a medial (1.6mm during downhill walking) and lateral (21.3mm during level walking) condyle of two subjects with a GMK Sphere implant.

The conventional designs exhibited similar kinematic coupling characteristics (relationship between joint flexion, A-P translation, and internal/external rotation) for the medial and lateral condyles, but with considerable differences between the loaded stance and unloaded swing phases (Figure 5.5). The medial condyle of the GMK Sphere exhibited almost no translation over the full range of joint flexion for all activities and even for the unloaded phases. The lateral condyle, however, exhibited a kinematic coupling comparable to the conventional designs but with a large variation between subjects. Posterior translation with increasing flexion was found for the lateral condyle of the GMK Sphere during the loaded stance phase of stair descent. However, different patterns of tibio-femoral movement with joint flexion were found for the conventional PS

and UC designs as well as the lateral condyle of the GMK Sphere for the stance phase of level walking and downhill walking. Here, little or only anterior translation was observed for flexion angles $> 15 - 20°$. In general (apart from the medial condyle of the GMK Sphere) all condyles then exhibited a greater range of motion, moving anteriorly with a different kinematic coupling pattern, for all unloaded swing phases.

The conventional designs exhibited similar kinematic coupling characteristics (relationship between joint flexion, A-P translation, and internal/external rotation) for the medial and lateral condyles, but with considerable differences between the loaded stance and unloaded swing phases (Figure 5.5). The medial condyle of the GMK Sphere exhibited almost no translation over the full range of joint flexion for all activities and even for the unloaded phases. The lateral condyle, however, exhibited a kinematic coupling comparable to the conventional designs but with a large variation between subjects. Posterior translation with increasing flexion was found for the lateral condyle of the GMK Sphere during the loaded stance phase of stair descent. However, different patterns of tibio-femoral movement with joint flexion were found for the conventional PS and UC designs as well as the lateral condyle of the GMK Sphere for the stance phase of level walking and downhill walking. Here, little or only anterior translation was observed for flexion angles $>$15-20°. In general (apart from the medial condyle of the GMK Sphere) all condyles then exhibited a greater range of motion, moving anteriorly with a hysteresis pattern, for all unloaded swing phases.

5.5 Discussion

The sphere-in-sphere articulation on the medial side of the GMK Sphere implant is a design characteristic that was included to provide A-P stability of the replacement joint. The flat lateral condyle was then intended to allow rotational freedom, with the ultimate goal of mimicking the kinematics of the healthy knee joint [27]. While a preliminary understanding of the effectiveness of this design has been provided in subjects undertaking step-up/down [24], for the first time, the *in vivo* kinematics of the GMK Sphere prosthesis have now been analysed during level walking, downhill walking and stair descent. These measurements have been enabled by the unique ability of the moving fluoroscope [37] that has allowed the assessment of 3D tibio-femoral kinematics throughout complete cycles of different gait activities without errors being introduced due to soft tissue artefact [52, 54]. The additional comparison against conventional GMK PS and UC designs using the same methodology, not only importantly demonstrates that implant design is

Table 5.2: Range of A-P translation for the medial (med) and lateral (lat) condyles for the GMK Sphere, GMK PS and GMK UC during level walking, downhill walking and stair descent. Full gait cycles as well as loaded stance and swing phase are presented.

	full gait cycle							**loaded stance phase**						**unloaded swing phase**					
	med A-P				**lat A-P**			**med A-P**			**lat A-P**			**med A-P**			**lat A-P**		
level walking																			
GMK Sphere	**3.7**	±	**0.9**	***a,b**	**10.9**	±	**4.5**	***d**	2.0	±	0.2	6.3	±	2.9	3.4	±	1.1	8.8	±	2.4
GMK PS	**10.6**	±	**2.3**	***a,c**	8.6	±	1.7		5.9	±	1.1	5.1	±	1.1	9.8	±	2.5	7.1	±	2.1
GMK UC	**5.9**	±	**1.0**	***b,c**	**5.7**	±	**1.4**	***d**	3.4	±	1.2	3.5	±	1.2	5.1	±	0.8	4.9	±	1.1
downhill																			
GMK Sphere	**3.2**	±	**0.8**	***e,f**	**10.2**	±	**3.1**	***h**	1.8	±	0.3	5.3	±	1.3	3.0	±	1.0	9.0	±	2.5
GMK PS	**10.4**	±	**2.7**	*e,g	**9.4**	±	**2.3**	***i**	5.4	±	1.6	5.0	±	1.1	8.5	±	2.9	6.6	±	1.9
GMK UC	**8.2**	±	**1.8**	***f,g**	**5.9**	±	**1.1**	***h,i**	3.9	±	0.9	3.1	±	1.0	6.8	±	1.3	4.9	±	1.2
stair descent																			
GMK Sphere	**4.0**	±	**1.4**	***j,k**	**12.5**	±	**2.2**	***m**	2.5	±	0.9	5.8	±	2.3	3.5	±	1.6	12.2	±	2.3
GMK PS	**12.0**	±	**1.6**	***j,l**	**11.0**	±	**2.7**	***n**	4.7	±	1.2	5.2	±	1.2	10.5	±	1.6	10.0	±	2.7
GMK UC	**9.0**	±	**1.9**	***k,l**	**7.1**	±	**1.6**	***m,n**	4.3	±	1.1	3.7	±	1.0	7.9	±	1.9	5.8	±	1.4

**: Significantly different, based on the adjusted level of significance of* $\alpha = 0.005$

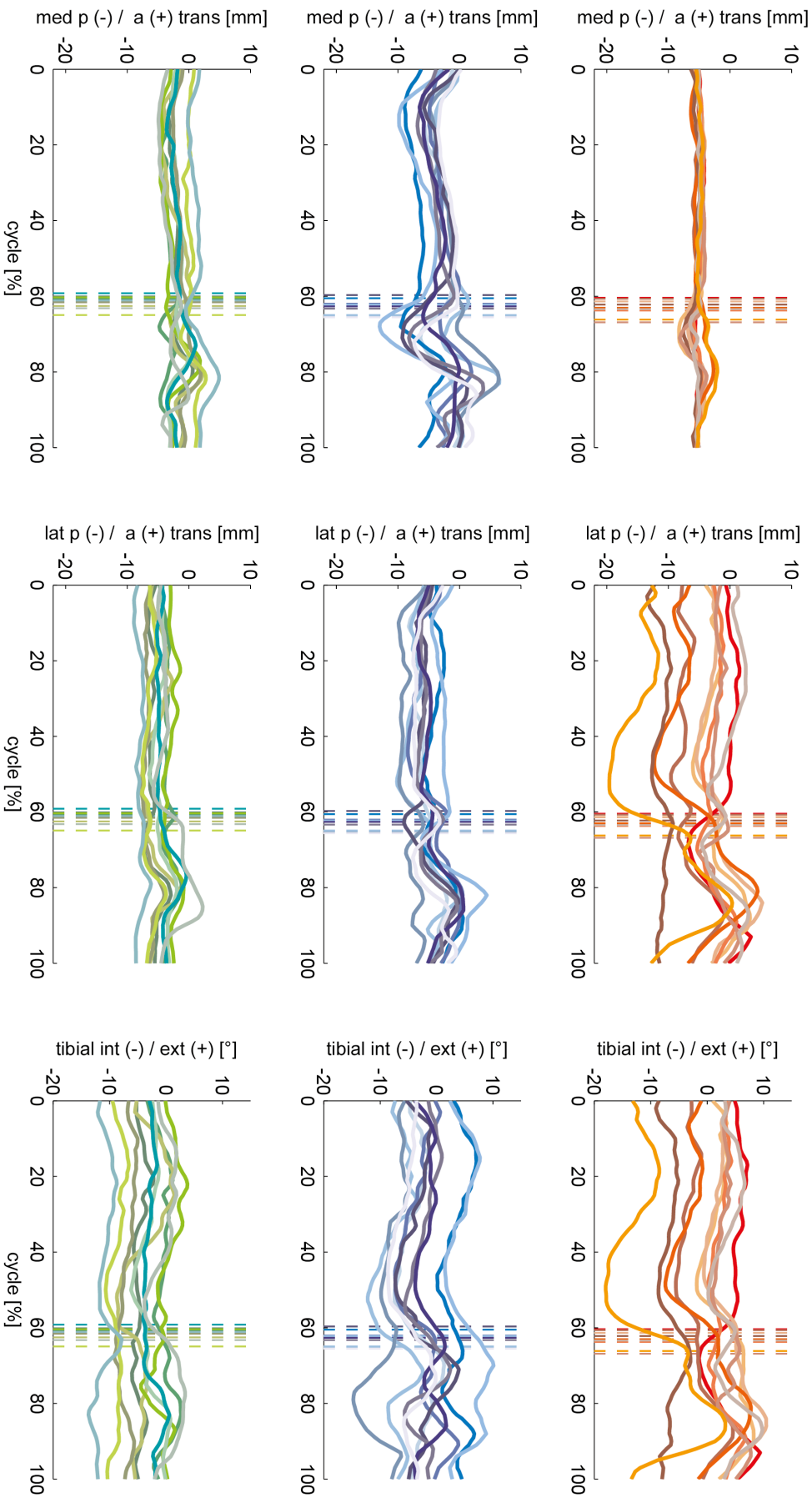

Figure 5.2: Subject means of A-P translation for the GMK Sphere (red tones), GMK PS (blue tones) and GMK UC (green tones) throughout full cycles of level walking. The average instance of toe-off of each subject is shown as a vertical line.

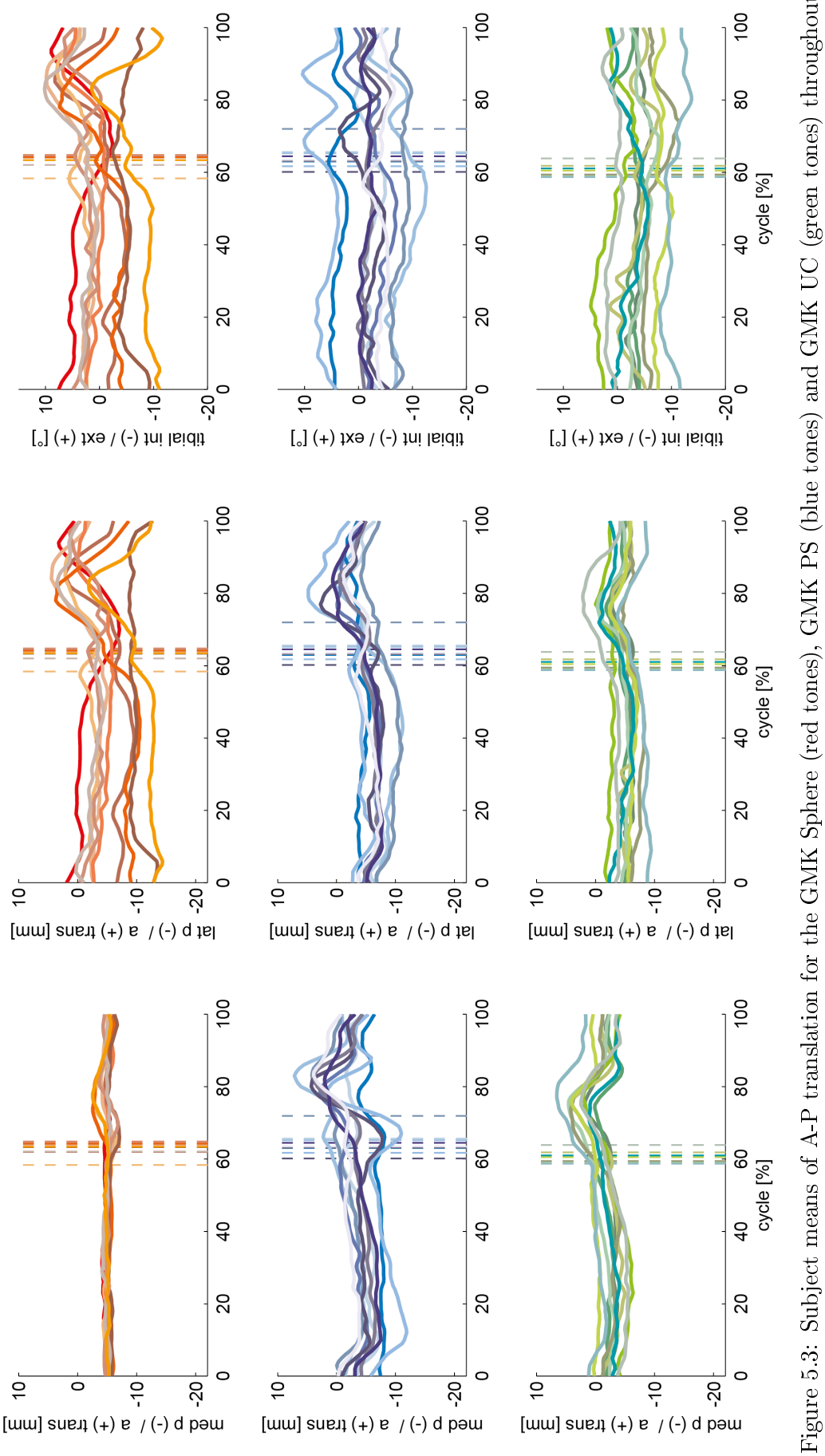

Figure 5.3: Subject means of A-P translation for the GMK Sphere (red tones), GMK PS (blue tones) and GMK UC (green tones) throughout full cycles of downhill walking. The average instance of toe-off for each subject is shown as a vertical line.

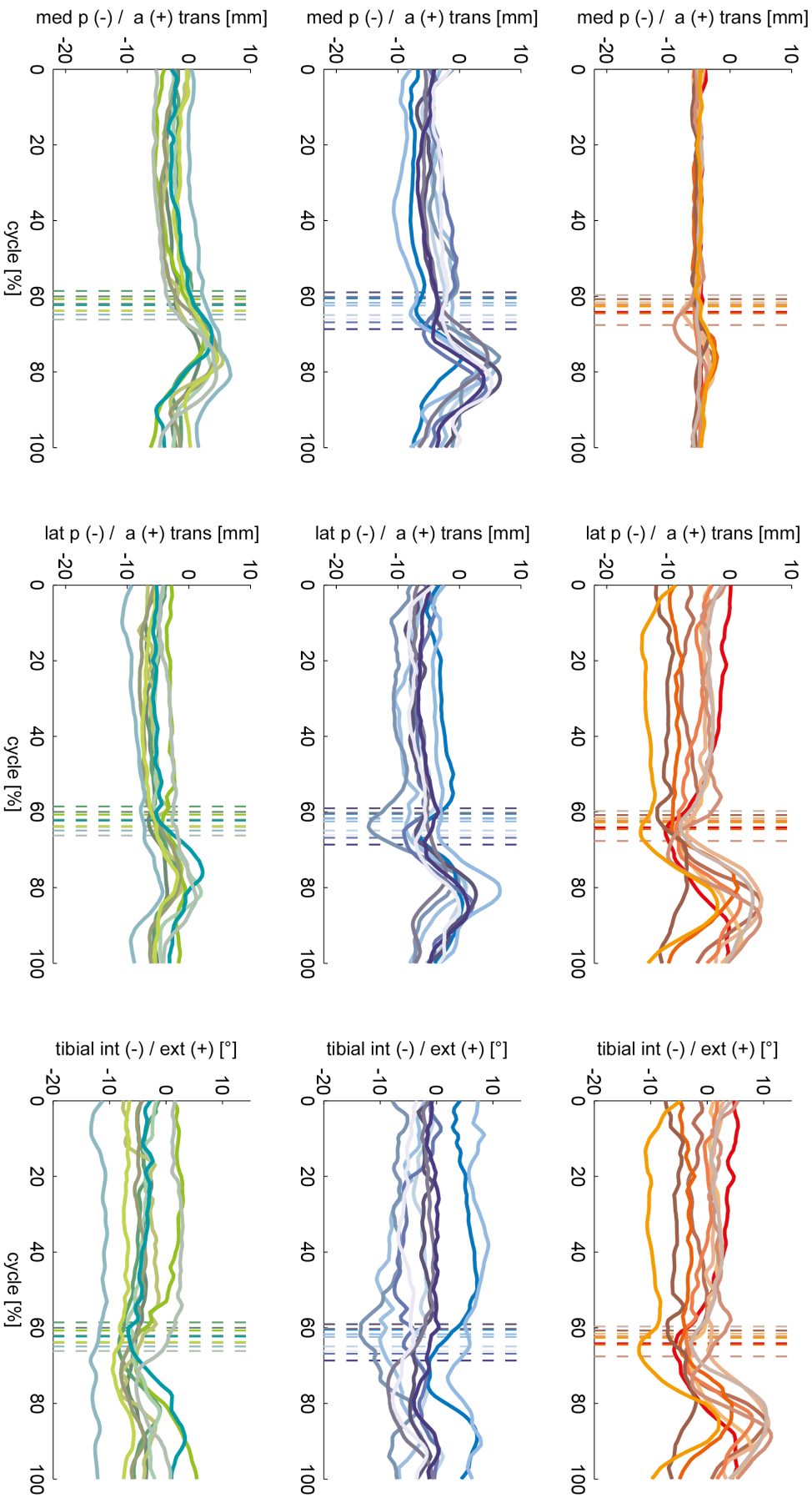

Figure 5.4: Subject means of A-P translation for the GMK Sphere (red tones), GMK PS (blue tones) and GMK UC (green tones) throughout full cycles of stair descent. The average instance of toe-off for each subject is shown as a vertical line.

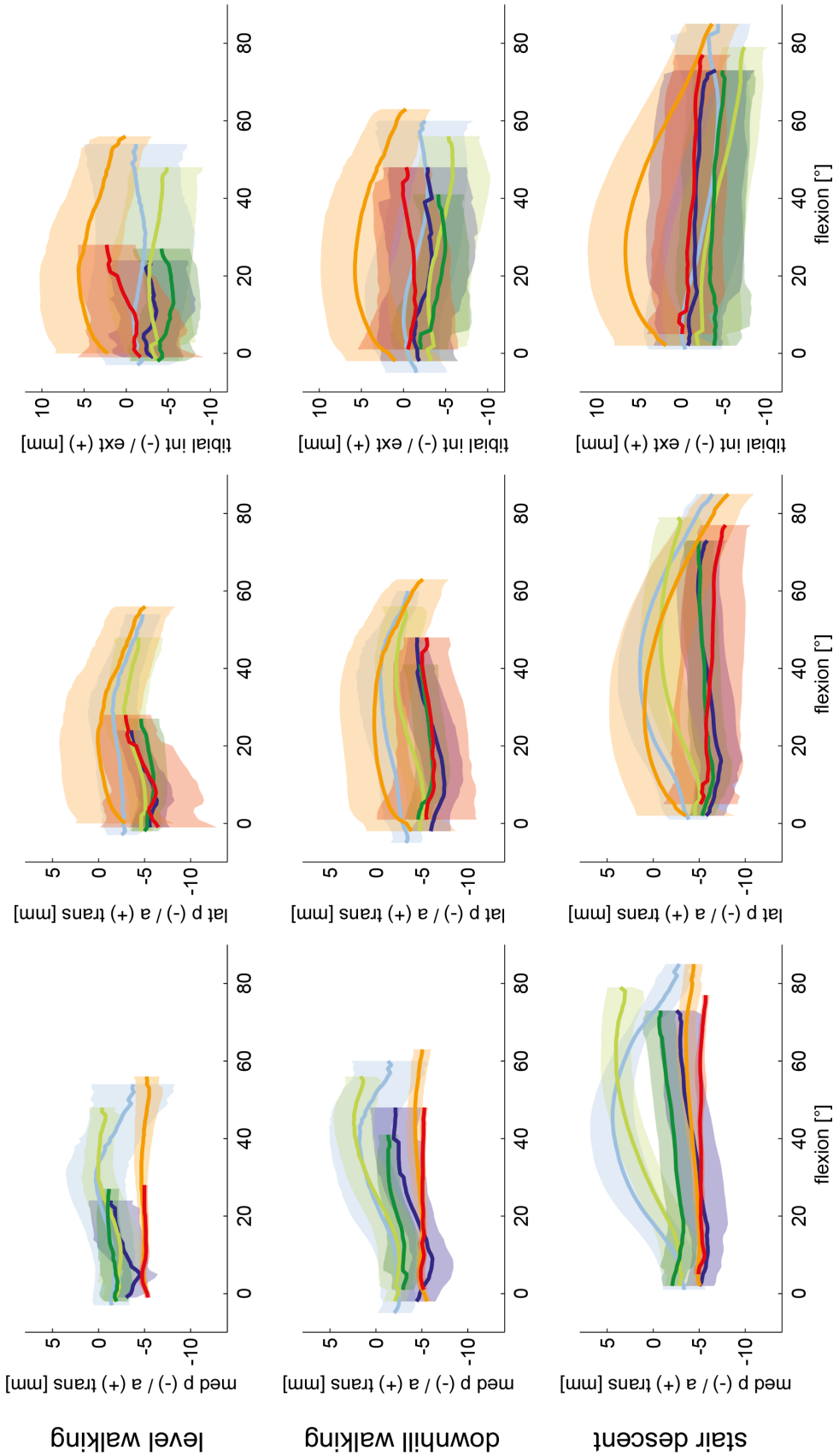

Figure 5.5: A-P translation of the medial (left) and lateral (centre) condyle as well as tibial rotations (right) for specific flexion angles. Mean and SDs over the subject groups were are presented for the GMK Sphere (red/orange), GMK Primary PS (blue/light blue) and GMK Primary UC (green/light green) for the loaded stance (dark) and unloaded swing (light) phases of level walking, downhill walking and stair descent.

a key factor in driving tibio-femoral kinematics, but also that the design itself can play a more dominant role for joint movement than the type of activity being undertaken.

The mean ranges of tibio-femoral rotation (Table 5.1) of the GMK Sphere over the complete gait cycles were equal or even larger than the PS and UC designs in all three planes and for all activities, suggesting that little or no additional restrictions in rotational freedom occur due to the medially constrained compartment design. The lower range of rotation in the UC design, however, indicates that the implant design may restrict the joint rotational freedom. Here, the UC design shows comparable values to those reported for level walking and stair descent with a cruciate retaining implant design [141]. The ranges of tibial rotation determined during the loaded stance phase of level walking (GMK Sphere: 7.3 ± 2.8°, GMK PS: 7.9 ± 1.3°, GMK UC: 6.2 ± 2.8°) and stair descent (GMK Sphere: 6.6 ± 2.4°, GMK PS: 6.6 ± 3.1°, GMK UC: 6.0 ± 2.5°) were comparable to studies investigating the healthy knee *in vivo* during the stance phase of normal gait and stair descent [42, 54, 66]. The largest range of tibial rotation, however, was clearly observed during the unloaded swing phase of gait, which is consistent with the study of natural knee kinematics by Lafortune and co-workers [42].

The results of our study demonstrate that a distinct kinematic coupling exists between the average tibial-rotation and the joint flexion angle for the GMK Sphere for the unloaded swing phases of all activities (also the stance phase of level walking). The observed externally rotated tibia indicates that the specific design of the GMK Sphere leads to more external rotation (depending on the loading and the activity) than the more conventional designs. When comparing the joint kinematics during the loaded stance phase of stair descent against the results of a dynamic step-up/down activity investigated by Scott and co-workers [24], who found a general increase in internal tibial-rotation with increasing flexion, the small increase in internal rotation with increasing flexion angle observed in our study (Figure 5.5), does indeed suggest that a kinematic coupling occurs. For the additional activities investigated in our study, e.g. the stance phase of level walking, however, a contrary coupling was observed, with increasing tibial external rotation with flexion, indicating that tibial rotation has a relationship with flexion angle that also varies with implant design and activity [42, 141]. In both cases, it should be noted that large inter-subject variations were observed, and interpretation of the "average" kinematic coupling needs to be interpreted carefully.

The high repeatability in A-P translation between the five intra-subject trials allows subject specific motion characteristics to be distinguished (Figures 5.2, 5.3, 5.4), indicating that less

constraints imposed by the implant design results in highly individual motion characteristics. The highly constrained medial side of the GMK Sphere exhibited the lowest inter-subject variation (average SD 0.5-0.6mm), and the subject specific motion characteristics therefore appear to be almost exclusively expressed on the minimally constrained lateral side of the implant (average SD 3.7-4.8mm). The slightly larger variation found for the PS implant for both condyles (average SD 1.9-2.4mm) compared to the UC design (average SD 1.7-1.9mm) confirms the influence of the component design constraints. The individual motion characteristics found within the implant groups might additionally be explained by other factors including anatomy, component alignment, ligament tension, muscle activation, or individual spatial/temporal gait characteristics, but the relative influence of these factors on joint kinematics remains to be investigated in further studies.

Interestingly, for all activities, subject specific A-P translation in the highly constrained medial sphere-in-sphere articulation of the GMK Sphere implant occurs only at the beginning of swing phase (Figures 5.2, 5.3, 5.4). This increase in A-P translation seems to have been made possible by the spherical condyle lifting-off out of the socket after unloading the joint and before the contraction of the surrounding muscles of the knee preparing for the on-coming heel-strike. An increase in proximo-distal distance between the femoral and tibial component was also observed at the same time and in the same subjects. Whether this kinematic phenomenon results from the femoral component rolling or sliding up the inlay, or whether it is associated with either joint abduction or a collateral ligament laxity induced (uni- or bi-lateral) lift-off remains to be investigated. However, this finding seems to underline the importance of ligament balancing on the *in vivo* kinematics of the GMK Sphere during unloaded phases of gait activities.

The significantly smaller ranges of A-P translation found for the medial condyle of the GMK Sphere (stance: 1.8-2.5mm, swing: 3.0-3.5mm) during the loaded stance phase of the three gait activities, as compared to the conventional designs, indicates a high level of A-P stability for the medial condyle. The ranges of A-P translation of the lateral condyle (stance: 5.3-6.3mm, swing: 8.8-12.2mm) did not differ from the ranges found for the PS design, and were larger than those exhibited by the UC design. Similar to the values determined for joint rotation, these values suggest that the stable medial condyle of the GMK Sphere does not limit the freedom of the lateral condyle. These ROMs for the medial and lateral condyles of the GMK Sphere were comparable to the A-P translations found for the healthy knee during loaded stance phases of level walking and stair descent [66, 142], but smaller in magnitude for the lateral condyle compared to deep knee bend or squatting activities that include larger flexion angles [28, 30]. A comparison of

these kinematic results against A-P translations for natural knees during gait activities remains extremely difficult, primarily because healthy knee kinematics themselves remain controversially discussed [66, 67].

Posterior translation of the lateral condyle with increasing flexion, as described by Iwaki and co-workers [27] for cadaveric knees and found for the GMK Sphere during lunge and step-up/down activities by Scott and co-workers [24], was for the loaded stance phases only seen during stair descent of the GMK Sphere (Figure 5.5, centre). The so-called "paradoxical" movement reported in the literature [13], describes anterior translation of the femoral condyle(s), despite increasing joint flexion. In our study, the loaded stance phases of the conventional PS and UC implants for both condyles during all activities, showed tendencies towards anterior translation (at flexion angles >15-20°), thus confirming the presence of this paradoxical type motion. It is interesting to note that this type of movement was also observed in the lateral condyle of the GMK Sphere during level walking – the first occurrence of this observation in this implant. The distinct kinematic behavior of the three gait activities and loaded and unloaded phases highlights the importance of including different gait activities for an improved evaluation of implant design.

It must be noted that a number of factors limit the extrapolation of the findings of this study for a general understanding of joint biomechanics in larger populations. Here, the low number of subjects examined, combined with an unequal gender distribution, could bias the observed kinematic outcomes, and thereby restrict a comprehensive understanding of the differences in motion characteristics between implants. While additional subjects could elucidate the extreme ranges of motion, the differences in subject-specific kinematics are already clear even in the low number of subjects examined in this study, and already highlight the condylar range of motion freedom and activity dependency within the design specific constraints. The low gait speeds of the subjects walking with the moving fluoroscope has been addressed previously [137], in which it is already known that the kinematics resemble those during slow walking. From an analysis perspective, the out of plane error of the single plane fluoroscope [37] only allows a limited evaluation of the medio-lateral translation of the implant components, which have therefore not been reported in this study. However, the use of this technology has clearly allowed a new understanding of implant kinematics throughout complete cycles of functional gait activities, including the effects of muscle contraction and relaxation, as well as loaded and unloaded activity phases.

The results of this study confirm that the design principle of the GMK Sphere, in providing A-P

stability through a medial sphere-in-sphere articulation and allowing rotational freedom through a flat lateral compartment, is successful in terms of the *in vivo* kinematics produced throughout the performed gait activities. From a clinical perspective, whether patients prefer the medial stabilized implant over conventional designs, was not the focus of this study, and remains to be assessed elsewhere [138]. An improved knowledge of healthy tibio-femoral kinematics during similar complete cycles of dynamic functional gait activities, as well as their modulating factors, remains critically required before implant designs are better able to mimic healthy joint motion. In this study, however, we have been able to show that innovative TKA designs such as the GMK Sphere are able to provide medial A-P stability and still allow rotational freedom, but that the motion of the lateral condyle is still highly subject specific and activity dependent.

5.6 Acknowledgement

The study was financially supported by Medacta International and the Comission for Technology and Innovation (CTI) Switzerland. The authors would like to thank all the subjects who participated in this study, as well as Nathalie Kühne and Michel Schläppi who supported recruitment of the subjects, Prof. Dr. Edgar Stüssi, Prof. Dr. Stephen Ferguson, Dr. Hans Gerber, Dr. Monika Zihlmann, Dr. Mauro Foresti, Jaqueline Stucki, Marco Hitz and Peter Schwilch for their contribution to the development of the moving fluoroscope, and Michael Angst and all the students who helped with the measurements and post-processing.

Chapter 6

A comprehensive assessment of the musculoskeletal system: The CAMS-Knee data set

adapted from:

William R. Taylor[1], Pascal Schütz[1], Georg Bergmann[2], Renate List[1], Barbara Postolka[1], Marco Hitz[1], Jörn Dymke[2], Philipp Damm[2], Georg Duda[2], Hans Gerber[1], Verena Schwachmeyer[2], Seyyed Hamed Hosseini Nasab[1], Adam Trepczynski[2], Ines Kutzner[2]

[1]Institute for Biomechanics, ETH Zürich, Switzerland

[2]Julius Wolff Institute, Charité – Universitätsmedizin Berlin, Germany

Journal of Biomechanics, vol.65, pp. 32-39, 2017

DOI: 10.1016/j.jbiomech.2017.09.022

open access

6.1 Abstract

Combined knowledge of the functional kinematics and kinetics of the human body is critical for understanding a wide range of biomechanical processes including musculoskeletal adaptation, injury mechanics, and orthopaedic treatment outcome, but also for validation of musculoskeletal models. Until now, however, no datasets that include internal loading conditions (kinetics), synchronized with advanced kinematic analyses in multiple subjects have been available. Our goal was to provide such datasets and thereby foster a new understanding of how *in vivo* knee joint movement and contact forces are interlinked – and thereby impact biomechanical interpretation of any new knee replacement design. In this collaborative study, we have created unique kinematic and kinetic datasets of the lower limb musculoskeletal system for worldwide dissemination by assessing a unique cohort of 6 subjects with instrumented knee implants (Charité – Universitätsmedizin Berlin) synchronized with a moving fluoroscope (ETH Zürich) and other measurement techniques (including whole body kinematics, ground reaction forces, video data, and electromyography data) for multiple complete cycles of 5 activities of daily living. Maximal tibio-femoral joint contact forces during walking (mean peak 2.74BW), sit-to-stand (2.73BW), stand-to-sit (2.57BW), squats (2.64BW), stair descent (3.38BW), and ramp descent (3.39BW) were observed. Internal rotation of the tibia ranged from 3° external to 9.3° internal. The greatest range of anterio-posterior translation was measured during stair descent (medial 9.3 ± 1.0mm, lateral 7.5 ± 1.6mm), and the lowest during stand-to-sit (medial 4.5 ± 1.1mm, lateral 3.7 ± 1.4mm). The complete and comprehensive datasets will soon be made available online for public use in biomechanical and orthopaedic research and development.

Keywords

Internal loading conditions, *in vivo* kinematics, moving fluoroscope, EMG, ground reaction forces, telemetry, tibio-femoral joint contact forces

6.2 Indroduction

Accurate knowledge of the internal loading conditions in the human musculoskeletal system forms the basis for understanding a wide range of biomechanical processes including musculoskeletal

adaptation [143, 144], orthopaedic treatment outcome [145], wear and failure mechanisms [146], overloading and injury mechanics [147], as well as for optimising implant designs, and validating musculoskeletal models [148]. However, many aspects of modelling and understanding biomechanical interactions in the human musculoskeletal system, are limited by the lack of availability of complete and synchronous kinematic and kinetic datasets. In their "Grand-Challenge", Fregly and co-workers annually released musculoskeletal datasets based on data collected from a single subject implanted with a force-measuring knee replacement [149, 150]. The distribution of these datasets signified a landmark in the ability of the entire musculoskeletal modelling community worldwide to use this data and validate their own lower limb models. However, the limited number of subjects and datasets available has limited any population or activity based modelling. Furthermore, kinematics of the limbs were primarily extracted from optical motion capture (only walking on a treadmill was measured fluoroscopically), which is subject to soft tissue artefact [52], and the accuracy of the kinematic assessment therefore clearly limited the ability to understand the role of tibio-femoral motion on the internal joint contact forces.

Videofluoroscopy allows the accurate reconstruction of objects with a known geometry in 3D space, and has thus become a well-accepted imaging technique to acquire kinematic information of artificial joints during simple functional movement tasks such as squatting or rising from a chair. However, measurements during functional activities of daily living such as walking and stair descent have remained extremely limited: the heavy physical structure of the imaging technology has generally restricted the development of mobile devices. As such, only a handful of mobile units exist that enable the tracking of moving joints. The Laboratory for Movement Biomechanics, ETH Zürich, has developed a single plane moving fluoroscope that is capable of tracking human joints throughout complete cycles of activities of daily living [39] (Figure 6.3). By determining the projection parameters and subsequent 2D/3D registration, it is possible to accurately reconstruct the 3D kinematics of e.g. the knee joint [90, 92, 151], without inaccuracies associated with soft tissue artefact.

The development of telemetric implants at the Charité – Universitätsmedizin Berlin, Germany, has allowed improved understanding of the internal loading conditions that occur in subjects with artificial joints. Using strain gauges fixed within the shaft of the tibial component, this technology allows the tibio-femoral forces and moments that act within the implant to be captured during dynamic activities in the knee joints of human subjects *in vivo* [152]. Comprehensive information about the loading of orthopaedic implants is already provided in the Orthoload database (www.orthoload.com). However, until now, this data has mainly been limited to joint

kinetics. In this respect, expansive data for multiple subjects that includes accurate information of both joint kinetics and kinematics remains elusive. In a unique collaborative effort, the "Comprehensive Assessment of the Musculoskeletal System" (CAMS-Knee) project aimed to unite these technologies and capture synchronous datasets of kinematics and kinetics of the human knee. With the goal to make these datasets widely available, it was our aim to support the field of musculoskeletal biomechanics and provide researchers and industry a reliable and highly accurate resource for model validation and research into the movement and loading of the human knee, particularly in subjects with total knee replacements.

6.3 Materials and methods

6.3.1 Subjects

Six subjects (5m, 1f, aged 68 ± 5 years, mass 88 ± 12kg, height 173 ± 4cm) each with an instrumented TKA [152] were measured 5-7 years post-operatively while performing multiple repetitions of different activities of daily living. All testing of subjects involved within this project were performed in accordance with the Declaration of Helsinki. The study was approved by the local ethics committees of the Charité (EA4/069/06) and ETH Zürich (EK 2013-N-90) and all subjects provided written informed consent prior to participation.

6.3.2 Telemetry

Each subject possessed an INNEX knee implant (Zimmer, Switzerland; type FIXUC), in which the tibial component was modified and instrumented with a 9-channel telemetry transmitter (90-100 Hz), allowing six-component load measurements of the 3 contact forces and 3 joint moments acting on the tibial component to be recorded with a mean measurement error below 2 % [152]. The construction consisted of two trays with hollow stems made from titanium alloy bar stock, which were separated by a small gap. The inner stem was connected to the upper plate and fitted, slightly undersized, into the outer stem of the lower plate. Both stems are welded together at their distal ends. Surgical implantation involved cementation of the lower plate onto the resected tibia as usual, hence allowing the inner stem to deform elastically when the upper plate is loaded. The load-dependent deformations of its stem were then measured using 6 semi-conductor strain gauges. All signals were sensed and transmitted using a custom-

made, inductively powered telemetry circuit [153]. During measurements, the subjects wore an external coil and antenna around the shank, which were connected to a custom-made receiver and amplifier. The signals were recorded together with the patient video on a digital video tape and prepared for post-processing evaluation. One of the audio tracks recorded the demodulated pulse trains of the telemetry signals and the other the synchronization signal. Finally, all forces and moments were determined and presented in the tibial coordinate system (detailed in Figure 6.1).

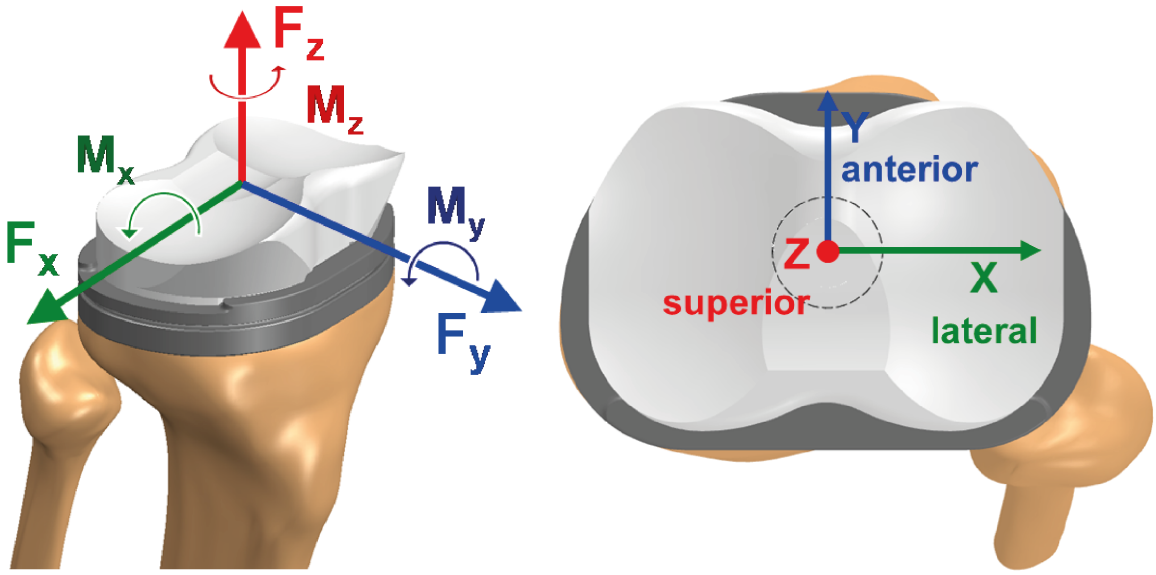

Figure 6.1: Coordinate system of the instrumented tibial tray. Figure adapted from (Kutzner et al., 2010) [154] and reprinted with permission.

6.3.3 Fluoroscopy

To overcome the limitations of marker-based kinematic measurements, which are affected by soft tissue artefacts [52, 155], tracking fluoroscopic techniques for dynamically imaging internal skeletal structures and metallic implant components have been developed [38, 39, 98]. The videofluoroscope C-arm unit was mounted on an automated trolley (maximum acceleration horizontal 9ms^{-2}, maximum velocity horizontal 5ms^{-1}) that allows dynamic tracking of the joint in question. The additional ability of the C-arm to track the joint at up to 1.33ms^{-1} vertically (maximum vertical acceleration 4ms^{-2}), thus enabling the joint to be tracked throughout several gait cycles of free level and downhill walking as well as stair descent [37].

The videofluoroscopic image capture was performed using a modified BV Pulsera videofluoroscopy system (Philips Medical Systems, Switzerland) with a field of view of 30.5cm, pulsed

image acquisition rate of 25Hz, 8ms radiation time, 1ms shutter time of the CCD-sensor and an image resolution of 1000 x 1000 pixels with a grayscale resolution of 12 bits [38, 39, 41, 98, 129].

Image distortion of the videofluoroscopic images was eliminated by a local correction algorithm [38, 41, 129] using a reference grid containing approximately 1300 beads. Since the position of the beads relative to one another was known, the projection of the reference grid was restored by means of a polynomial approximation. The projection parameters of the videofluoroscopic system (focal distance and location of the principle point in the image plane) were determined using a least-squares optimization, which was based on five images of a calibration tube (300mm long with two Plexiglas®plates). At well defined positions (accuracy: $\pm$ 0.03mm), each plate was filled with either 12 or 13 metal pellets, providing a total of 25 correspondence points.

Once the projection parameters of the fluoroscope were determined, its orientation and location relative to the video-photogrammetric system were determined [37, 38]. Here, the grid used for the image distortion correction was also equipped with six reflective markers screwed at predefined positions. The grid was rotated and displaced into multiple poses, with radiographs of the grid's beads and simultaneous assessment of the marker positions allowing the relationship between their local coordinate systems to be determined. In order to determine the projection matrix, a least squares optimization was used to find the orientation and position of the fluoroscopy system relative to the origin of the video-photogrammetric set-up. Optical markers were additionally fixed to the C-arm of the moving fluoroscope to allow the position of the moving fluoroscope to be continually determined and referenced to the global lab coordinate system. 2D/3D registration of the 2D fluoroscopic images was performed by fitting CAD models of the implant components. The registration algorithm was based on the approach developed by [40], in which the pose of the 3D implant CAD models was determined through fitting a synthetic image of the CAD model to the fluoroscopic image by minimizing the difference in gradient magnitudes as well as pixel grey values within the region of interest defined by a slightly enlarged outline contour, to create the optimal matching scenario for each time point. Registration errors, assessed for a similar TKA, were $<$ 1 degree for all rotations, $<$ 1mm for in-plane and $<$ 3mm for out-of-plane translations [38]. The output is the 3D pose of the tibial and femoral components relative to the lab or image intensifier coordinate systems according to [70].

6.3.4 Whole body kinematics

To analyse the full body kinematics, a 3D motion capture system (Vicon, Oxfords Metrics Group, UK) consisting of twenty-six MX40 and T160 motion-capture cameras recorded the motion of 75 skin markers attached to the skin at a sampling frequency of 100 Hz. The markers were attached mainly to the lower extremities (Figure 6.2; Table 6.1), and specifically encompassed all marker positions required for the IfB marker set [47], the OSSCA bone landmark and cluster marker sets [134, 155–159], as well as the lower-limb Plug-in-Gait marker locations (Vicon Peak®, Oxford, UK).

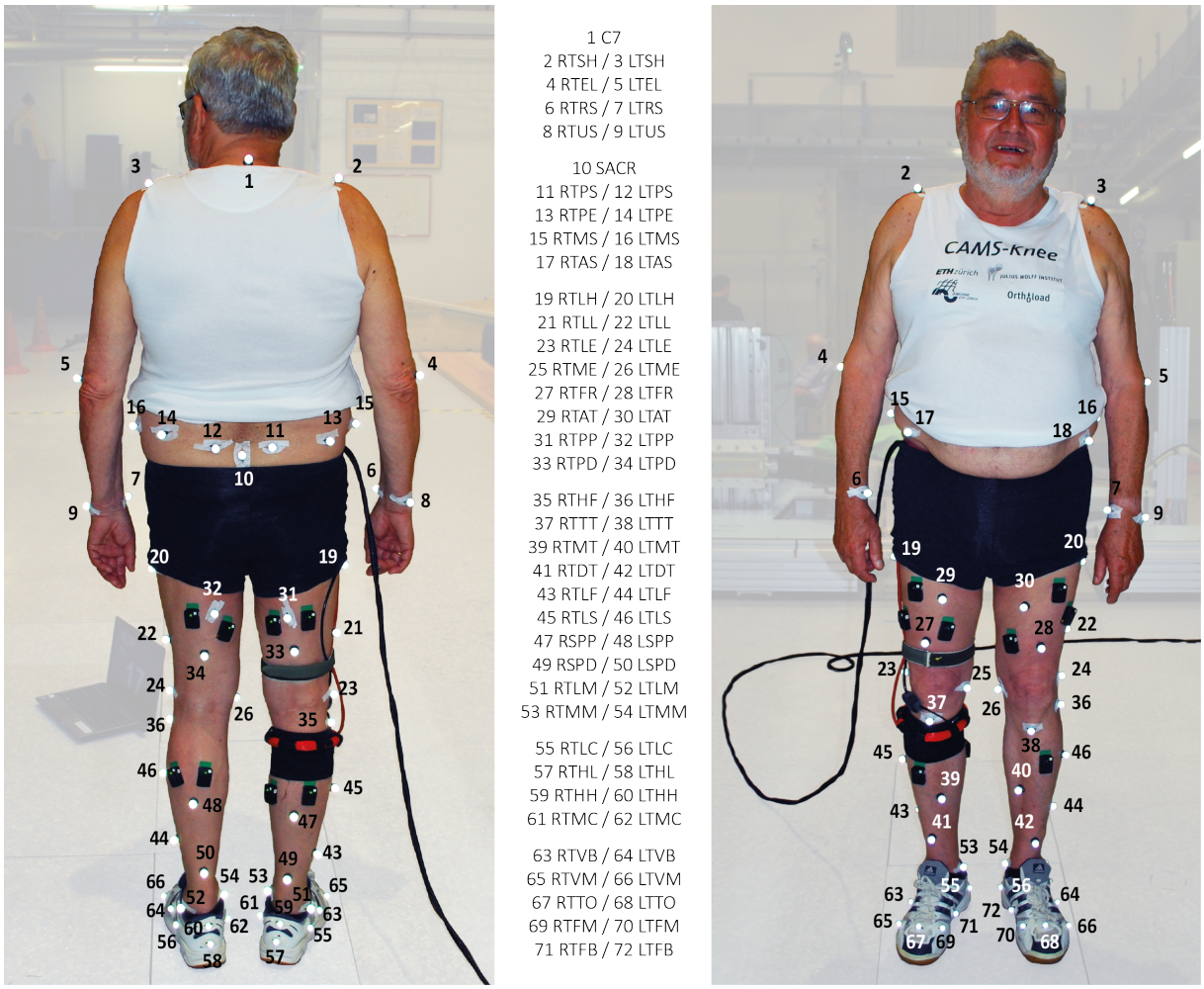

Figure 6.2: Positions of the reflective markers. The naming convention relates to the description of the placement in Table 6.1.

Table 6.1: Description of the skin marker placement.

Segment	**Marker Position**	**Marker Name**
Trunk / Arm	Seventh cervical vertebra	C7
	Highest point of the acromion	RTSH / LTSH
	Epicondyle radial	RTEL / LTEL
	Styloid process of radius	RTRS / LTRS
	Ulnar styloid process	RTUS / LTUS
Pelvis	Sacrum	SACR
	Posterior superior iliac spine	RTPS / LTPS
	Crista iliaca, dorsal	RTPE / LTPE
	Mid superior iliac spine	RTMS / LTMS
	Anterior superior iliac spine	RTAS / LTAS
Thigh	Lateral thigh on 50% thigh length	RTLH / LTLH
	Lateral thigh on 20% thigh length	RTLL / LTLL
	Lateral epicondyle	RTLE / LTLE
	Medial epicondyle	RTME / LTME
	Front thigh, one hand above knee	RTFR/ LTFR
	Ventral thigh on 50% of the length	RTAT / LTAT
	Upper 1/3 of the dorsal thigh	RTPP / LTPP
	Lower 1/3 of the dorsal thigh	RTPD / LTPD
Shank	Head of fibula	RTHF / LTHF
	Tibial tuberosity	RTTT / LTTT
	Mid tibia on 50% shank length	RTMT / LTMT
	Lower 1/3 of the ventral shank	RTDT / LTDT
	Lateral fibula on 30% shank length	RTLF / LTLF
	Upper 1/3 of the lateral shank	RTLS / LTLS
	Upper 1/3 of the dorsal shank	RSPP / LSPP
	Lower 1/3 of the dorsal shank	RSPD / LSPD
	Lateral malleolus	RTLM / LTLM
	Medial malleolus	RTMM / LTMM
Rear foot	Calcaneus lateral below lateral malleolus	RTLC / LTLC
	Calcaneus posterior inferior	RTHL / LTHL
	Calcaneus posterior superior	RTHH / LTHH
	Calcaneus lateral below medial malleolus	RTMC / LTMC
Forefoot	Base of fifth metatarsal	RTVB / LTVB
	Head of fifth metatarsal	RTVM / LTVM
	Head of second metatarsal	RTTO / LTTO
	Head of first metatarsal	RTFM / LTFM
	Base of first metatarsal	RTFB / LTFB

6.3.5 Ground reaction forces

Six force plates (B1 and B2, type 9281B, 400×600 mm, B3 and B4, type 9285, 400×600 mm, B5, type 9281C, 400×600 mm and A1, type 9287B, 600×900 mm, 2000 Hz; Kistler, Winterthur, Switzerland) aligned with the walkway, were used to measure the ground reaction forces (GRFs). These force plates were decoupled from the surrounding floor through their installation on an isolated concrete foundation (mounted directly on the ground floor below) to eliminate signal noise caused by ground vibration due to movement of the fluoroscope. The staircase and the ramp used for downhill walking were equipped with two mobile force plates (C1 and C2, type 9286AA, 400×600mm, 2000Hz; Kistler, Winterthur, Switzerland). To obtain the exact location of the origin, as well as the orientation of the mobile force plates, the position of calibration markers plugged into the force plates were captured.

All force plates were additionally calibrated to improve the estimation of the centre of pressure (CoP) with an in-situ point of force application calibration method [160]. As a result of the procedure, the mean error of the determined CoP was thereby reduced from 0.8 to 19.8mm before correction to within a range of 0.04 to 2.2mm.

6.3.6 EMG

The muscular activities and their coordinated responses were detected using a 16-channel wireless EMG system (Trigno, Delsys, USA), which was checked prior to subject measurements to ensure there was no interference from the implant telemetry data transfer. The EMG dual surface electrodes are placed on the preselected muscles to detect the myoelectric signals throughout the motion tasks. The recorded data was telemetrically sent to the workstation and synchronized with the kinematic measurements.

The electrodes were attached to the skin at eight predominant muscle sites on each lower limb (Figure 6.3). At the beginning of the test session, the EMG signals during maximal voluntary contractions (MVC) of each muscle were recorded. For this purpose, the following four motion tasks were performed for both legs:

Triceps surae: One legged standing together with lifting the heel to stand on tiptoe.
Quadriceps: With the subject sitting on a bench, with their lower legs hanging down, extension of the knee joint was performed against a load by means of a strap around the lower leg, just

above the ankle.

Hamstrings: With the subject sitting on a bench, with their lower legs hanging down, flexion of the knee joint was performed against a load by means of a strap around the lower leg, just above the ankle.

Tibialis anterior: With the subject standing, dorsiflexion of the ankle was performed against a manual resistant force provided by the investigator.

6.3.7 Video

Videos of each measurement were recorded using a digital camera (Panasonic NV-GS400) together with a digital video recorder (GV-D1000) for event documentation. The synchronization to the audio track, on which the telemetry data was stored, was performed by an LED light (delay $\leq$ 1 video frame).

6.3.8 Synchronisation

All measurement systems recorded simultaneously and were temporally synchronised. While the GRFs and EMG data were read directly into Vicon Nexus, fluoroscopic images were synchronized using a TTL trigger signal input into Vicon to temporally register each frame. In addition, Vicon was synchronized with the internal force measurement telemetry by sending a TTL trigger signal to the telemetry system.

6.3.9 Activities

Calibration tasks

Before the fluoroscopic measurements were performed, each subject performed basic motion tasks according to [47], in order to allow functional determination of the joint centres at the hips, as well as axes of rotation for the knee and ankle joints.

Prior to the measurement with the moving videofluoroscopic system, practice trials without imaging were performed until the subjects felt comfortable with the measurement systems and protocols. Free level gait, downhill walking, stair descent, sit-to-stand and stand-to-sit, as well as squatting activities, were then performed while all measurement systems were active. For each

Table 6.2: EMG electrode placement for both the left (channels 1-9) and right (channels 10-16) limbs.

Channel	**Muscle**	**Description of EMG electrode placement**
1/9	RectFem	50% from the anterior spina iliaca superior to the superior aspect of the patella [161]
2/10	VastusMed	4 fingers superior of the superior part of the patella [161]. If necessary, the electrode was placed a little more superiorly on the muscle belly, such that it did not interfere with the strap of the wire sensor
3/11	VastusLat	One hand-width superior of the superior aspect of the patella [161]
4/12	TibAnt	1/3 from the tip of the fibula to the tip of the medial malleolus
5/13	HamMed	50% between the medial epicondyle of the femur and the ischial tuberosity (Semitendinosus) [161]
6/14	HamLat	50% between the fibula head and the ischial tuberosity (Biceps femoris long head) [161]
7/15	GastroMed	One hand-width below the hollow of the knee on the medial muscle belly [161]
8/16	GastroLat	One hand-width below the hollow of the knee on the lateral muscle belly [161]

motion task, a minimum of five valid trials were acquired. For a valid trial, the knee had to be in the field of view of the image intensifier during the stance as well as the swing phase, and the force plates had to be hit correctly.

Level walking

Level walking included walking straight ahead over 5 force plates embedded in the floor (Figure 6.3).

Downhill walking

A ramp, consisting of a walkway with a 10° inclined slope (18 %) and two included embedded force plates (registered to the global coordinate system), was developed to perform downhill walking. Each subject started walking and the fluoroscope tracked to measure the final complete gait cycle of the downhill walking.

Stair descent

Walking downstairs consisted of descending a staircase of three steps, each 18cm in height. Force plates were mounted within the stairs, each registered to the global coordinate system.

Sitting and rising from a chair

Sit-to-stand and stand-to-sit were both measured in one motion sequence. The subject started in a sitting position, rose to an upright standing position and sat down again. Subjects were seated at an angle to the fluoroscope to avoid interference from the second knee.

Squat

For the squat activity, subjects stood with stationary feet, approximately shoulder width apart, and hands stretched forwards. Knee joint flexion was then performed as far as possible before returning to the standing position.

6.3.10 Processing of the data

Tibio-femoral A-P translations and proximo-distal (p-d) distances were described using the distance-weighted means of the 10 nearest points on each of the medial and lateral femoral condyles (surface element edge length approx. 2.8mm) relative to the tibial baseplate, which were re-calculated for each time point of the recorded kinematics to account for relative motion and rotation of the implant components. These nearest contact points on the medial and lateral condyles therefore effectively describe the motion of the femur with respect to the tibial compo-

Table 6.3: Description of the activities performed.

Activity	**Description**
Level walking	Walking straight ahead over 5 force plates embedded in the floor
Downhill walking	Walking down a walkway with a 10° inclined slope (18%), which included two force plates
Stair descent	Walking down an instrumented stair with three steps, each 18cm in height
Sitting and rising from a chair	The two tasks stand-to-sit and sit-to-stand were measured as a single sequence. The subject started in a sitting position, rose to an upright standing position and sat down again.
Squat	Standing with stationary feet, approximately shoulder width apart with hands stretched forwards Knee joint flexion as far as individually possible before returning to the standing position

nent, rather than the motion of the tibial component itself. As a result, anterior translation of the medial contact point would denote internal tibial rotation.

For all gait activities, all kinematic and kinetic parameters were temporally normalized to a complete gait cycle. The gait cycle was defined from heel-strike to heel-strike. Heel-strikes and toe-offs were defined using a ground reaction force threshold of 25N. Mean and standard deviation of the parameters were extracted from at least five valid cycles of each activity and presented as a function of time normalised the activity cycle.

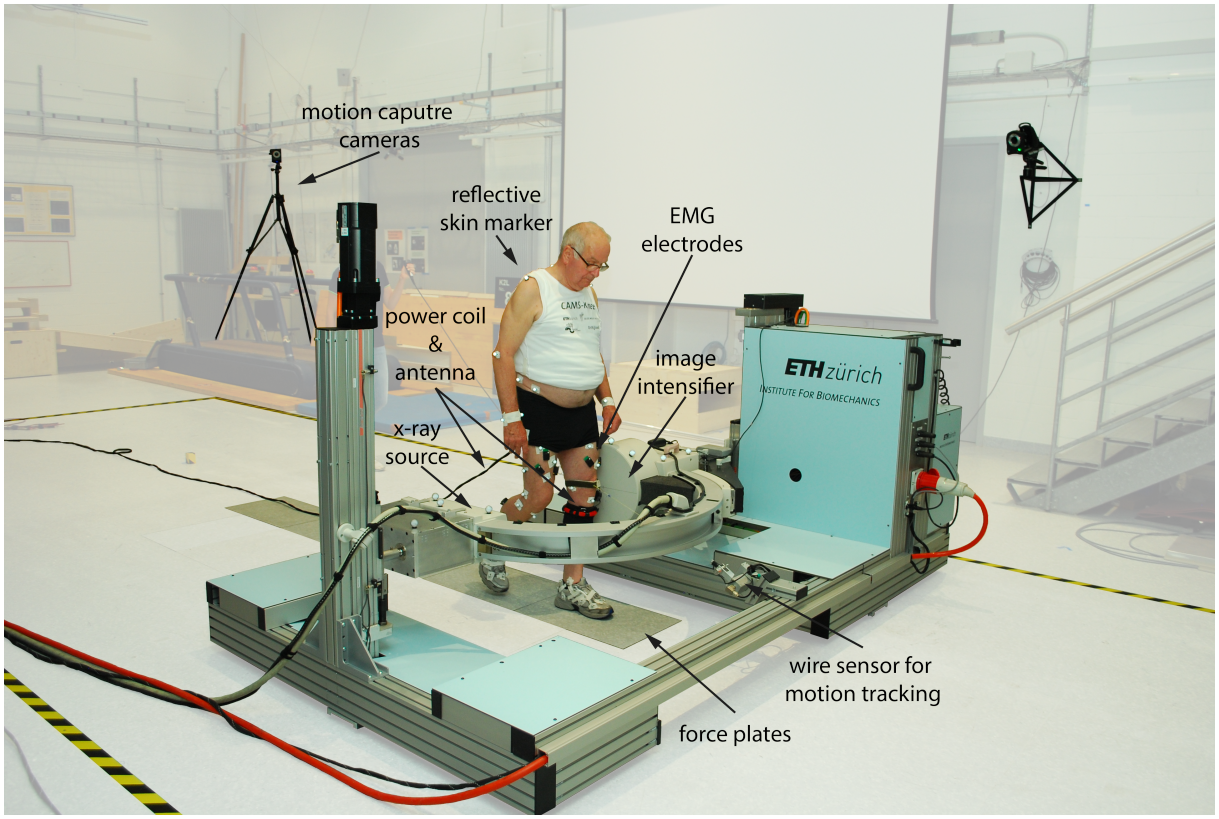

Figure 6.3: Example of the data capture set-up for one subject during level walking. The moving fluoroscope was developed at the Institute for Biomechanics, ETH Zürich, consisting of a C-arm mounted on a moving trolley. The system is capable of real-time tracking of the knee throughout complete cycles of level walking, stair descent and ramp descent activities.

6.4 Results

In general, all subjects were able to successfully undertake all activities. Considerable variations in both kinematic and kinetic parameters were observed between subjects, but also between trials in individuals. Exemplary results of the kinematic and kinetic parameters obtained by moving videofluoroscopy and the instrumented knee implant during different activities are presented for

one of the measured subjects (Figure 6.4). However, it is our intention that complete datasets for all subjects, all activities, all trials and all measurement modalities will be made freely available for non-commercial usage. Consequently, the following results are all presented as mean values over all subjects in order to provide a greater overview of the population kinematics and kinetics:

Knee flexion angles during level walking, downhill walking and stair decent exhibited a biphasic pattern for all subjects. The mean knee flexion ROM across all subjects for level walking was 56.0 ± 6.4°, 65.2 ± 3.0° for downhill walking, and 87.1 ± 4.4 for stair descent. The sit-to-stand and stand-to-sit activities resulted in a knee flexion to a mean of 76.0 ± 6.8°, and extended to a mean of -3.9 ± 11.2°. In a similar manner, the knee flexion reached a mean of 73.1 ± 9.4° during the squat activity.

The mean ad-abduction of the knee remained nearly constant throughout all activities and did not exceed 2 degrees. External rotation of the tibia was rarely observed. Internal rotation of the tibia increased with increasing knee flexion for almost all activities, resulting in a relatively large RoM, ranging from 3° external (occurring during gait) to 9.3° internal (during squats) rotation. A-P translation of the nearest medial and lateral articular points (as described above) demonstrated different patterns during different activities, but with similar RoMs. The greatest RoM was measured during stair descent (medial 9.3 ± 1.0mm, lateral 7.5 ± 1.6mm), while the lowest RoM was observed during the stand-to-sit activity (medial 4.5 ± 1.1mm, lateral 3.7 ± 1.4mm). The minimum p-d distance between the tibial and femoral components remained relatively constant, but some variations were visible during the walking task in this subject. The mean range of p-d distance was 1.4 ± 0.3mm, 1.7 ± 0.6mm, 2.0 ± 0.5mm, 1.1 ± 0.2mm, 1.3 ± 0.3mm, 1.5 ± 0.5mm for level walking, ramp walking, stair descent, stand-to-sit, sit-to-stand, and squat respectively.

The tibio-femoral joint contact forces reached a mean peak of 2.74BW during walking (highest single peak value of 3.73BW was found in the database: Figure 6.4), 2.73BW during sit-to-stand, 2.57BW during stand-to-sit, and 2.64BW during the squat exercises. However, considerably higher forces of approximately 3.38BW and 3.39BW were observed during stair descent and ramp descent respectively. In general, the compressive forces followed different patterns during different activities; however, these patterns had nearly consistent shapes between subjects. As can be seen from the maximum and minimum values across all subjects and all trials (shown as "*" and "o" respectively for walking only; Figure 4), considerable variability was observable between subjects. Of note was that the highest joint contact forces did not necessarily relate to

the joint kinematics.

6.5 Discussion

Accurate knowledge of the relationship between joint kinematics and kinetics *in vivo* forms the foundation of understanding and improving many clinical and rehabilitation treatments in the fields of orthopaedics and sports medicine. To date, however, access to such datasets remains astonishingly restricted. In this CAMS-Knee project, we have directly addressed this deficit by providing accurate kinematic and kinetic data in a small population during a range of functional activities. After their public release in 2018, these unique datasets will lay the foundations for understanding the complex interactions between the hard and soft tissue structures in the human knee and can thus be used towards e.g. verifying and improving novel surgical implants and techniques, developing novel injury prevention or rehabilitation strategies, and analysing the biomechanics of joint degeneration, but will also importantly provide a gold standard for the validation of biomechanical computational models.

To date, the most extensive datasets that include accurate measurements of the internal tibio-femoral joint contact forces have been made available on www.orthoload.com or published as part of the grand challenge [149, 150]; but this data is limited in several ways, including number of subjects, accuracy of the kinematic measurements, extensiveness of the datasets (repetitions, number of activities etc.), and limited range of measurement for moving activities. The data measured within the CAMS-Knee project are the first datasets to be made publicly available that include comprehensive data on multiple subjects, multiple activities, multiple repetitions and multiple synchronised measurement technologies.

The data measured within the CAMS-Knee project are aligned with previous reports on internal tibio-femoral loads [149, 150, 154], in which forces of 2.5-3BW for normal walking were presented. The observed higher forces during stair decent and ramp descent were not unexpected due to the increase in muscle activity required to induce the movement and for joint stabilisation in these more challenging exercises, and are also consistent with previous measurements in these subjects (www.orthoload.com). In terms of kinematics, it is clear that this highly constrained prosthesis limits the motion of the knee, even during walking, producing similar A-P translation and internal-external rotation to other implants [88, 162], but slightly less rotation compared to the natural knee [42], where internal-external rotation of up to 10° was observed. The collected

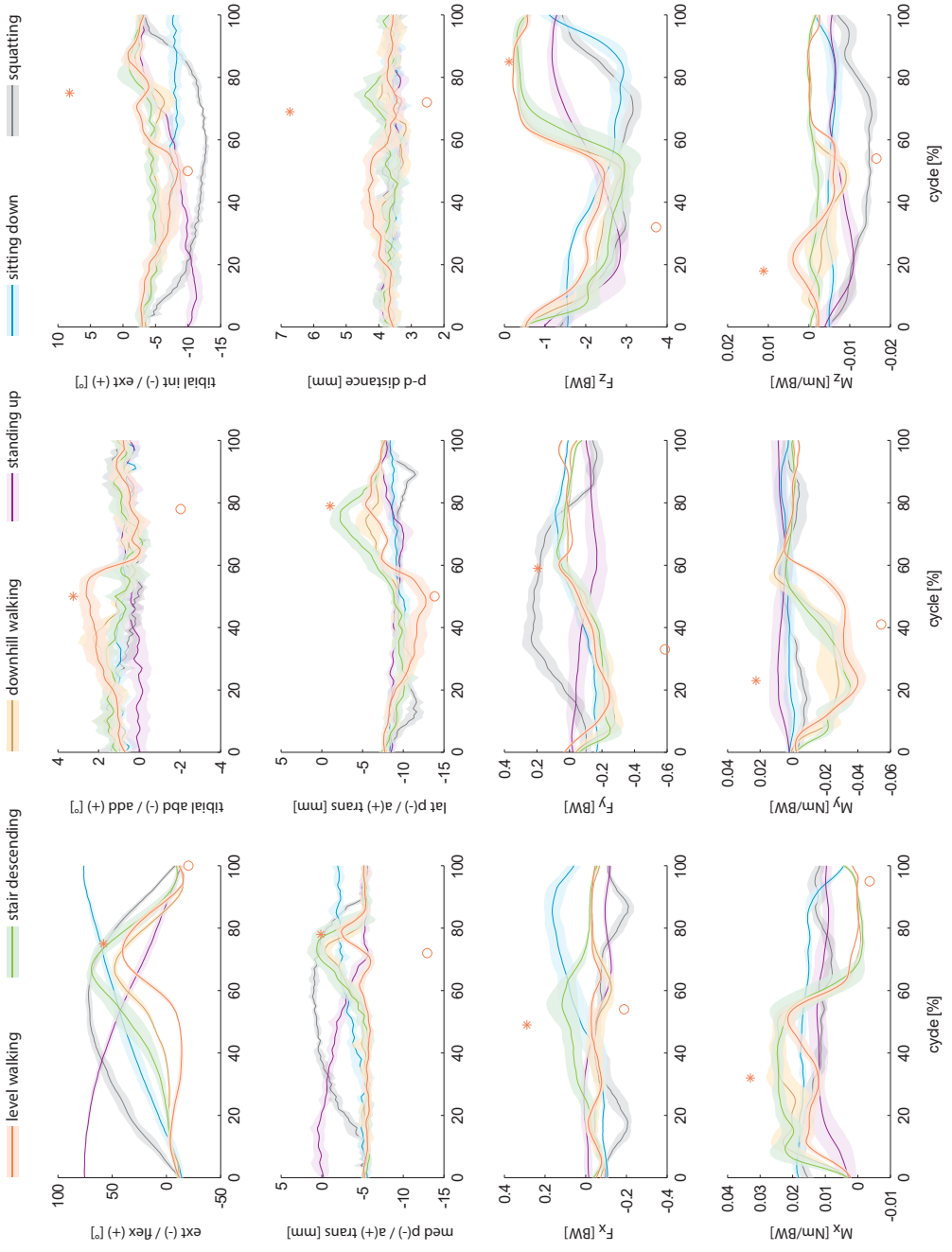

Figure 6.4: Exemplary outcomes of some of the primary kinematic and loading datasets are shown for a single subject throughout different activities of daily living. The thick lines represent the average of all repetitions for this one subject, while the associated standard deviations are shown as a shaded area. The single maximum (*) and minimum (o) values from all subjects and all trials of normal walking are shown to provide an impression of the range and timing of the most extreme values observed across the datasets of the entire study population.

data were not all obvious however, and open a number of questions for further investigation. As an example, p-d motion between the implant components was observed in the presented level walking data (Figure 6.4), posing the question as to whether lift-off of the femoral component occurs. In this case, we are of the opinion that no lift-off occurs, but rather that the simultaneous posterior translation of the lateral condyle pushes the components apart due to the highly congruous shape of the inlay, but that contact with the inlay still remains; a theory that could be supported by the smooth proximal movement of the femoral component over an extended duration of the cycle, but also that this period coincides with the phase of highest tibial internal rotation. However, it is entirely possible that the loading and unloading of the implant, which has hardly been measured throughout complete cycles in real world (non-treadmill) walking scenarios previously, could partially explain this anomaly. The fact that the observed peak p-d motion ranges from ca. 3-7mm in other subjects and trials, however, possibly indicates the requirement for improved 2D/3D component registration to remove outliers, or indeed possible lift-off of the femoral component. Further investigation into such aspects is clearly warranted, and will hopefully be undertaken in future collaborative research projects.

Despite extreme care taken in the planning and execution of this study, there were still a number of limitations to the quality of the data collected. First and foremost, only a single plane fluoroscope was used for the analysis of internal kinematics, and 2D-3D fitting accuracy in the out-of-plane axis is known to be lower than for in-plane registration [38]. Consequently, the assessment of e.g. femoral component to inlay contact may be limited. In addition, the quality of the images, and therefore the accuracy of 2D-3D registration, is clearly limited when the second leg crosses through the imaging plane. This problem was exacerbated in this study since four out of the six subjects assessed possessed bi-lateral TKAs. As a result, a small number of images were obscured by the contralateral implant and could not be reconstructed. In addition, the subjects assessed in this study averaged 68 years old and possessed at least one TKA. The interpretation and extrapolation of any musculoskeletal assessments to younger or healthy subjects may be limited, especially in light of the highly congruent INNEX knee implant that is known to considerably constrain tibio-femoral translation and rotation. Unfortunately, no detailed analysis of the pre-operative kinematics and kinetics was performed, therefore also restricting a deeper understanding of any correlation with e.g. pre-operative limb alignment. As a final point to consider, it is known that the moving fluoroscope inflicts an encumbrance on free walking through unusual noise and visual impediment, and results in a kinematic equivalent of slow walking [137]. However, despite these limitations, the ETH Zürich moving fluoroscope

is one of the only systems available worldwide that is able to track the knee during complete cycles of activities of daily living, and thereby still offers a unique insight into joint kinematics in combination with ground reaction force measurements, throughout loaded and unloaded phases of gait.

After a proprietary period for data analysis, the comprehensive CAMS-Knee datasets will become freely available for non-commercial usage at www.cams-knee.orthoload.com. In order to download the full datasets, recipients will be required to sign a licence agreement, provide full name, position, and contact details, but also specify their intended usage of the data. With this information, we anticipate building a community of users, who will be able to interact, support each other, and even provide e.g. open source models based on the datasets. As a result, we expect the CAMS-Knee data to positively impact on current scientific and clinical approaches for the assessment and management of joint disease and injury, with tremendous potential for becoming reference datasets in medical innovation world-wide.

6.6 Acknowledgements

The authors would like to thank the RMS Foundation for their generous support that has allowed this data to be collected and made available to the scientific community. We also sincerely appreciate the support from ZimmerBiomet for making the CAD models of the INNEX femoral component and inlay available to us within the CAMS-Knee project.

6.7 Conflict of interest statement

There are no conflicts of interest.

Chapter 7

Synthesis

Patient satisfaction after TKA is highly related to the ability to perform activities of daily living successfully and without pain [7]. While patient satisfaction is highly subjective and driven by expectations of the patient [7], TKA kinematics can provide objective measures, to evaluate the *in vivo* function of TKA during activities of daily living and improve implant designs to better replicate the healthy knee motion. With the unique moving fluoroscope, it was for the first time possible to include level walking, downhill walking and stair descent in studies with patients to evaluate different implant designs.

Therefore, the overall objective of this PhD thesis was to provide an improved understanding of factors driving the *in vivo* TKA kinematics in different functional activities. In addition to extensively investigated knee bending exercises with continuous flexion, the impact of the implant design during functional gait activities was investigated. The results of this thesis showed the importance of analysing gait activities in addition to knee bending activities and showed the ability of design features to constrain and guide condylar motion. Highly constrained compartments resulted in less range of motion and smaller variations between subjects, whereas unconstrained compartments led to larger ranges of motion and larger variation between the subjects, reflected in individual motion patterns.

The **influence of the moving fluoroscope** [37–39] **on gait patterns** was investigated in a study including young and elderly subjects walking with and without the moving fluoroscope (chapter 3). An acoustic masking intervention (ear protectors) was included in an additional condition to investigate the influence of the motor sound on gait characteristics. Time distance, kinematic (skin marker analysis) and kinetic (ground reaction forces) parameters were analysed.

The results showed neither differences between the young and elderly group nor an effect of the acoustic masking intervention. Importantly, a decreased gait speed (28-30 %) has been determined when walking with the moving fluoroscope compared to normal overground walking. Changes in gait speed are known to alter the gait characteristics [114, 117] and were observed by Yamokoski and Banks [96] when using a dynamic radiographic system. When walking with the moving fluoroscope, small alterations in kinematic parameters were observed, even when corrected for gait speed. Therefore, the occurrence of alterations due to the moving fluoroscope cannot be completely excluded but the alterations were small, especially in relation to the accuracy of skin marker measurements [116]. However, the absence of differences in kinetic parameters, when corrected for gait velocity, as well as the comparable kinematic gait characteristics to the slow control condition demonstrated that slow walking with the moving fluoroscope is comparable to slow gait. The observed gait speeds in the current thesis were comparable to the reduced gait speed reported for TKA subjects [110]. Therefore, for an evaluation in subjects with TKA, the set-up with the moving fluoroscope is capable to track gait activities at gait speeds in the range of the self selected gait speed without altering the natural gait characteristics.

To investigate the **relation of the activity and TKA kinematics**, six good outcome subjects with a unilateral cruciate-retaining fixed-bearing implant design were analysed during two sitting tasks with continuous flexion or extension as well as during level walking and stair descent. For the first time tibio-femoral implant kinematics of complete cycles of level walking and stair descent, including loaded stance and unloaded swing phases, were presented for this implant. The potential to clearly distinguish between subject specific motion patterns of the implant components was demonstrated and a clear task dependency was observed across all subjects in mean range of condylar A-P translation. In addition, larger ranges of condylar A-P translation were observed for the unloaded swing phase compared to the loaded stance phase for level gait and stair descent.
Despite large variations between subjects, differences in average kinematic coupling of A-P translation and flexion were found between the unloaded swing phases compared to loaded phases, pointing out the importance of analysing complete gait cycles. The results presented in this study showed that flexion angle alone, as in knee bending activities, cannot fully explain tibio-femoral TKA kinematics during gait activities. Therefore, beside activities with continuous flexion, gait activities should be included in a complete evaluation of an implant design.

The activity was identified as an important driving factor of TKA kinematics. Especially for gait activities, including dynamic loading and unloading of the knee joint in combination with flexion

and extension, the kinematic behaviour of the femoral and tibial component cannot be explained by the flexion angle alone. Changes in A-P translation mainly occur when there is a change in loading, movement direction (flexion/extension) or muscle activation. This finding is in line with the A-P translations found by Guan and co-workers [36] investigating a posterior-stabilized implant design during complete cycles of overground and treadmill walking.
The stance phase of stair descent with continuous flexion until toe-off showed the same kinematic coupling of A-P translation and flexion as for the sitting activities and therefore seems to be comparable to knee bending exercises most frequently used for evaluation of *in vivo* TKA kinematics [5, 13–26]. This finding was confirmed when comparing the stance phase of stair descent of the medial pivot design to the results of Scott and co-workers [24] during a step-up/down exercise [24]. During the unloaded swing phase, stair descent shows a completely different kinematic coupling than during stance phase, with more anterior translation during extension before a posterior translation occurs prior to the next heel strike. This behaviour cannot be fully explained by the extension movement alone, as a different pattern was observed during the loaded sit-to-stand activity, covering the same range of extension. Therefore, it needs to be a combination of loading/unloading, flexion/extension and muscle activation, which drive the TKA kinematics during gait activities.

The sensitivity of condylar A-P translation to the loading condition or execution of the activity has been shown in studies investigating loaded and unloaded knee bending [16, 19, 28, 30] or knee bending with different initial rotations [28, 31]. This implies that a different execution of an activity can alter the condylar motion. This could also be the case when comparing different gait speeds [114, 117], or when the gait pattern is altered by environmental factors or when walking on a treadmill [36]. Due to the sensitivity of condylar motion to the activity, for a direct kinematic comparison between implant designs or for comparison against the healthy knee, the activities should be ideally performed in the same activity set-up and with the same instructions.

It has been shown that tibio-femoral kinematics and especially condylar motion are very sensitive to their definition [28, 74]. The use of different conventions can lead to different interpretation of the data. In the current thesis, condylar motion was described using a nearest point approach, describing the points on each condyle with the smallest distance to the top plane of the tibial tray. This method is widely used in the analysis of knee implants. The additional description of condylar motion using a geometric center axis (GCA) approach has emphasized the sensitivity of the condylar motion to its definition, also described in the literature [28, 67, 74, 124]. For the implant design with two radii, the effect of different definitions to describe condylar motion can

be seen exemplarily (Figure A.4). While the nearest point approach showed larger medial A-P translation, suggesting a centre of rotation on the lateral condyle, the GCA approach showed opposite results with larger translations on the lateral condyle resulting in a more medial centre of rotation. These results could be explained by cross-talk between flexion angle and A-P translation using a GCA approach.
Differences between nearest point approaches, contact point approaches or flexion axis based approaches should be taken into account when comparing the results of different studies. When comparing implant kinematics to healthy kinematics, the individual anatomies make comparison even more difficult. Therefore, processing of the kinematics using different definitions as done in this thesis is crucial to compare values across the literature and for clinical interpretation of the results.

To understand the **effect of implant design** on the more complex kinematic behaviour during gait activities, an innovative implant design providing medial stability was investigated compared to a conventional ultracongruent mobile-bearing and a posterior-stabilized fixed-bearing design (chapter 5). In addition to level walking and stair descent in the previous study (chapter 4), downhill walking, as another challenging task with larger A-P forces, was included [34]. Ten good outcome subjects in each implant group were analysed. The capability of implant designs to constrain *in vivo* TKA kinematics during gait activities was demonstrated but the large subject specific differences in A-P translation patterns when freedom was provided by the design showed that guiding of the motion remains difficult. The occurrence of subject specific differences indicates that other factors like anatomical differences [163], surgical alignment [164], soft tissue tension [135] and muscle activation pattern [147, 165] could be responsible for the individual variations.

In total, five different types of implant designs were investigated in this thesis using the same methodology to establish the effect of the design on the TKA kinematics during daily activities: A cruciate retaining-fixed bearing implant (chapter 4), a medial pivot design (chapter 5), a posterior-stabilized fixed-bearing design (chapter 5) as well as two ultra-congruent designs with mobile- (chapter 5) and fixed-bearings (chapter 6).

In general, the design of the implant was found to have a larger impact on the TKA kinematics than the different gait activities, namely level walking, downhill walking and stair descent. For all implant designs, level walking and stair descent was included in the evaluation. The ranges of flexion/extension and internal/external rotation throughout complete cycles of level walking

and stair descent showed larger values for the posterior-stabilized and the medial pivot design compared to the cruciate-retaining design and the ultra-congruent mobile-bearing design, but all comparable to the values found for the natural knee in a bone pin study [42]. The medial pivot design showed clearly larger ranges of tibial rotation compared to the other designs for stair descent suggesting more rotational freedom for deep flexion activities compared to the other designs. As all of these values are very well within the range of corresponding values for the natural knee, no definite statement about better/worse can be inferred from that. For each of the implant designs, the ranges of ab/adduction during complete cycles of level walking were similar but all smaller than the values found for the healthy knee [42]. Whereas this is associated with functional restrictions or a consequence of the alignment during surgery needs to be further investigated.

Higher conformity between the femoral component and the inlay was clearly associated to a smaller condylar translation in A-P direction. The medial pivot design with a sphere-in-sphere articulation on the medial side and a flat lateral compartment exhibited smallest range of A-P translation for the medial condyle (level gait: 3.7±0.9mm, stair descent: 4.0±1.4mm) and largest range for the lateral condyle (level gait: 10.9±4.5mm, stair descent: 12.5±2.2mm) found across all implant designs. The ultra-congruent design with more constraints by the geometry of the inlay led to smaller ranges of A-P translation for both condyles compared to the posterior-stabilized design with less conformity between the femoral condyle and the inlay.

The fact that conformity is directly related to the A-P translation during gait activities is especially impactful for the cruciate retaining design, in which the radius of curvature changes at a specific flexion angle thus leading to a corresponding change in conformity reflected in A-P translation. This characteristic can be clearly seen in the kinematic coupling of A-P translation and flexion as a local minimum followed by anterior translation described as “paradoxical” anterior motion [13–19, 68, 85]. The engagement of post and cam in the posterior-stabilized design could be the reason for the increased posterior translation prior to toe-off in some subjects during stair descent with angles in the region where engagement could occur. For the flexion range of level walking, however, posterior-stabilized designs showed relatively unconstrained condylar motion allowing individual motion patterns for both condyles including small amounts of "paradoxical" anterior translation with increasing flexion. Van Duren and co-workers [25] also concluded that an investigated posterior-stabilized design failed to fully restrain "paradoxical" anterior movement during a step-up and a deep knee bend activity.

The medial pivot design exhibited a larger A-P translation for the lateral condyle compared to the medial condyle, resulting in a medial centre of rotation during all gait activities and phases. All other designs with comparable constraints for both condyles, except the posterior-stabilized design during the loaded stance phase of stair descent (possible interaction of the cam-post feature), showed smaller differences between medial and lateral ranges of A-P translation between the condyles with a tendency to a lateral centre of rotation. Whether a medial or a lateral pivot movement of the condyle better replicates healthy kinematics during gait activities needs further investigation of the healthy tibio-femoral kinematics during dynamic gait activities including condylar motion.

While there is very limited information about implant kinematics during complete cycles of gait activities, our results of the posterior-stabilized design as well as for the cruciate-retaining design during level walking agreed well with values and motion characteristics found in another study that also investigated full cycles of overground walking in a posterior-stabilized design [88]. The medial pivot design in our study showed also comparable characteristics to the latter study but with larger magnitudes in A-P translation for the lateral condyle and larger differences between the subjects.
In contrast, the medial condyle of the medial pivot design as well as both condyles of the two ultra-congruent designs showed almost no A-P translation during the loaded stance phase and only small magnitudes of A-P translations during the unloaded swing phase. It remains speculative whether constraints in A-P direction improve the feeling of stability or limit the functionality of the knee and also if they could lead to high constraining forces. It might be highly dependent on the specific needs of a subject. For subjects with muscular deficits to stabilize the joint, a more constrained design in A-P direction can possibly improve stability, while for a subject with good muscular stabilization, a more unconstrained design could be beneficial to replicate healthy kinematics.

There is little known about healthy knee kinematics during gait activities. The existing literature reports controversial results for condylar motion of healthy knees during gait activities, with large variation between the individual subjects [66, 67]. Therefore, for a direct comparison of our results to healthy kinematics, ideally, the healthy knee joint should be investigated with the same methodology used for the TKA to avoid bias due to different execution of the activities (e.g. gait speed, instructions, set-up), environmental factors like the moving fluoroscope and definitions of axes and tracked condylar points.

Although the design was clearly able to guide the implant kinematics in constrained compartments during gait activities, **individual differences between the individual subjects** have been observed in unconstrained compartments. As the investigated subjects showed all good clinical outcome, the results in this thesis represent the range of successful kinematics with regard to clinical scores. The individual motion characteristics of different subjects indicated that condylar motion cannot be explained completely by the activity and the implant design, suggesting other subject specific factors to be important in guiding the TKA kinematics. Here, surgical alignment [164] of the implant, observed as initial A-P translation at heel strike in this thesis, and balancing of the collateral ligaments [135], resulting in different condylar lift-off patterns found during the unloaded swing phases in the current thesis, were identified to influence the kinematics.

Another potential factor for driving TKA kinematics is muscle activation [165]. Activation of the quadriceps and hamstring muscles having insertion points at the tibia could lead to different A-P magnitudes. Benedetti and co-workers [165] found a prolonged muscular co-contraction in TKA subjects and Boeth and co-workers [147] showed reduced A-P translation in anterior cruciate ligament deficient patients compared to healthy controls, possibly also due to co-contractions. Different muscle activation could therefore explain the occurrence of completely different magnitudes in A-P translation in subjects with a similar initial alignment at heel strike observed for the unconstrained lateral compartment of the medial pivot design in this thesis. Limb alignment could also play a role [163], but more pronounced in healthy knee kinematics than in TKA, where leg alignment is commonly corrected during surgery with alignment of the implant components (mechanical alignment [166]).

The large individual variation in kinematics, observed for unconstrained compartments in our study, limits the meaning of average A-P translations or rotations when describing TKA kinematics. Therefore, presenting the graphs and values for the individual subjects is crucial to provide more information and allow better interpretations than presenting average absolute positions or rotations at discrete time points only. It needs to be further investigated whether such individual differences are also common for healthy subjects during gait activities. If this subject specific kinematic behaviour is also observed in healthy subjects on one hand, the choice of the implant design should address the subject specific needs. On the other hand, if this variation between subjects is absent for healthy knees, implant design needs to be improved to better guide the kinematics towards the found patterns in healthy knees.

The results of this thesis show the potential of design features to constrain and guide condylar

motion. Highly constrained compartments resulted in less range of motion and smaller variations between subjects whereas unconstrained compartments led to larger ranges of motion and larger variation between the subjects, reflected in individual motion patterns. Here, numerical simulation of musculoskeletal models might provide an avenue to elucidate the possible contribution of soft tissue structures and how they influence the kinematic behavior of an implant in unconstrained compartments.

The collected datasets in the current thesis can be used as **input data** for such **modelling** [148, 167] to further understand the role of subject specific factors, such as muscle activity and ligament tension, in governing the individual kinematics when freedom is provided by the implant design.

The implant kinematics presented in chapter 4 and 5 were assessed in combination with motion capture and force plates and can therefore be used as input data for modelling approaches to access soft tissue structures, muscle forces, contact forces or to predict wear. Validation of such models is extremely challenging for the biomechanics community. One of the only ways validation can currently be achieved is direct comparison of the predicted forces against measured internal joint contact forces, but access to such data has been difficult. In attempt to generate a comprehensive dataset, to validate models and to investigate other factors driving the TKA kinematics, namely soft tissue loading and muscle forces, a study including six subjects with an instrumented knee implant [154] was performed. The measurement set up [37, 39] and data acquisition at the Institute for Biomechanics, the post processing of implant kinematics [38], motion capture [47, 48], force plate [98] and EMG data as well as data preparation for public release was part of this thesis. In addition to the data provided by the grand challenge [149], more subjects (six) were included and multiple repetitions of the most frequent daily activities, including knee bending activities and complete cycles of different gait activities, all with synchronised implant kinematics and internal joint forces, were assessed. The unique combination of an instrumented knee implant providing internal forces and the moving fluoroscope for kinematic assessment of gait activities will provide a base for a variety of scientific questions to better understand the function of the tibio-femoral joint during daily activities and towards improving knee implant design.

Chapter 8

Limitations and outlook

Despite the obvious possibilities that our new technology provides for a complete assessment of TKA kinematics, it still has some limitations. Major limitations included:

Walking with the moving fluoroscope can reduce gait speed due to technical limitations regarding maximal acceleration (slip of the wheels) or environmental factors, influencing the subject to reduce gait speed. However, it has been shown that walking with the moving fluoroscope is comparable to slow gait in the control condition. Possible improvements, namely optical tracking instead of the wire sensor attached to the knee, or a visual masking of the moving fluoroscope could be helpful to further reduce the influence of the moving fluoroscope. To achieve higher accelerations, a tooth rail system instead of the floor rubber-wheel interface could improve the tracking of normal gait speed in young subjects.

The assessment of patients with a good clinical outcome in this thesis does not allow an understanding whether kinematics could be a predictor for functional impairments like instability. Therefore, the clinical relevance of the kinematic differences found between different activities and implant design during gait activities remains unclear. However, the results of this thesis can be representative for the variations seen in good outcome subjects and could be used as norm data for comparison against bad outcome subjects with a clinical problem.

The number of subjects investigated in the presented studies is relatively low, especially when large variation between subjects was observed, as in the current thesis. Larger cohorts would allow better predictions of the general behaviour of an unconstrained design. However, despite the low numbers of subjects, the impact of characteristics of activity and implant design on the

implant kinematics could be demonstrated across the subjects as well as the influence of the activity and design within the subjects.

Condylar translations in medio-lateral direction were not analysed in this thesis due to reduced accuracy of single plane videofluoroscopy in the out of plane direction. The out of plane error of up to 3mm [37, 38] of the single plane fluoroscope is in the range of the expected small medio-lateral translations [36, 42]. Dynamic dual plane videofluoroscopic systems as described by Guan [36] would allow access to medio-lateral translation but are affected with more radiation exposure for the subjects. The small ranges of medio-lateral translation found in other studies investigating TKA kinematics or healthy knee kinematics during complete gait cycles [36, 42] showed that main translations occur in the A-P direction suggesting that in terms of translations, analysis in the sagittal plane for gait activities is sufficient.

Finally, a comparison to natural knee kinematics during complete gait activities including condylar motion, to evaluate which implant best mimics the natural knee kinematics, was not part of this thesis. Possibly, due to a more complex registration of bones instead of implant components with high contrast, there is a lack of knowledge in the literature. To close this gap and allow to assess the success of different implant designs to replicate the healthy knee kinematics during functional gait activities, the same activities as included in this thesis are currently investigated in an ongoing study, using the moving fluoroscope and subsequent 2D/3D registration based on CT models of the bones. To investigate the influence of limb alignment [163] on the healthy knee kinematics, the ongoing study includes neutral alignments as well as a varus and a valgus group. This study will for the first time provide a direct comparison of TKA kinematics to healthy knee kinematics throughout complete cycles of level walking, downhill walking and stair descent, investigated using the exact similar methodology. This reference data of healthy knee kinematics can then be used to evaluate the success of implant designs to replicate the healthy knee kinematics in knee bending as well as dynamic gait activities.

8.1 Further research and transfer to clinic/industry

To understand the impact of TKA kinematics during daily activities and its role in the mechanism leading to early failure [10] or unsatisfactory outcome in general [7], further studies are needed to investigate the influence of the kinematics on the clinical outcome and whether replication of the healthy knee kinematics is beneficial. Some ideas for further research are presented in the

following section:

In a further investigation, the kinematic behaviour of an implant could be related to the assessed external ground reaction forces and joint moments as well as to the internal forces and moments measured with the instrumented implant to understand the mechanisms leading to distinct kinematic behaviour when performing different activities.

The collected data in this thesis can be used as valuable input data for musculoskeletal modelling, to investigate the effect of the kinematics and internal forces on soft-tissue loading of collateral ligaments, or posterior-cruciate ligament (in cruciate-retaining implant designs). With such an approach, the influence of kinematics and joint forces on the surrounding tissues could be investigated in order to understand mechanisms, which could cause overloading [11, 168].
In addition, the influence of muscular contraction on TKA kinematics [165] could be analysed in order to understand the role of muscle contraction in guiding the kinematics. Modelling, based on the assessed datasets, could also improve wear [79, 80] prediction for the different gait activities to enhance longevity of implants and avoid failure due to excessive wear.
Finally, based on the CAMS-knee dataset, musculoskeletal models can be improved and validated, and specific models for TKA subjects might be developed [148, 167].

A comparison of the kinematics of bad outcome subjects to the kinematics of the good outcome subjects, investigated in the current thesis, could provide a crucial route to evaluate the potential of kinematic patterns as predictors for clinical outcome. It would be interesting to compare condylar motions for subjects with a feeling of instability [6, 10] to the good outcome subjects investigated within the current thesis.

In order to develop innovative implant designs, the results gained from an assessment with the moving fluoroscope can be used to verify the impact of a design feature *in vivo* during different functional activities. Furthermore, when a comparison to healthy knee kinematics is provided in future, this knowledge can then be used to choose the design to address patient specific needs.

Chapter 9

Conclusion

The presented doctoral thesis has investigated characteristics of activity and design and their role in governing *in vivo* TKA kinematics during daily activities. For the first time the TKA kinematics of different implant designs were analysed throughout complete cycles of level walking, downhill walking and stair descent. It has been shown, that TKA kinematics during dynamic gait activities cannot only be explained by knee flexion angle. The thesis therefore demonstrated the need to include gait activities with phases of loading and unloading combined with several changes in muscular activation in a complete assessment of TKA kinematics.
The results of this thesis showed the potential of design features to constrain and guide condylar motion. Highly constrained compartments resulted in less range of motion and smaller variations between subjects whereas unconstrained compartments led to larger ranges of motion and larger variation between the subjects, reflected in individual motion patterns. Other factors related to soft tissue structures or surgical alignment were identified to be responsible for individual implant motion in unconstrained compartments.
The gained knowledge can be used to further improve the functionality of TKA, not only in an attempt to replicate healthy knee kinematics but possibly also to choose or develop a design to address subject specific needs.

Finally, within the presented framework unique data sets were acquired for understanding the biomechanical factors driving the tibio-femoral kinematics during functional gait activities. The assessment of a comprehensive data set for public release, combining the moving fluoroscope with an instrumented knee implant, will provide a promising base for future research in knee biomechanics.

References

[1] D. T. Felson, Y. Zhang, M. T. Hannan, A. Naimark, B. Weissman, P. Aliabadi, and D. Levy. Risk factors for incident radiographic knee osteoarthritis in the elderly: the framingham study. *Arthritis Rheum*, 40(4):728–33, 1997.

[2] N. J. Manek, D. Hart, T. D. Spector, and A. J. MacGregor. The association of body mass index and osteoarthritis of the knee joint: an examination of genetic and environmental influences. *Arthritis Rheum*, 48(4):1024–9, 2003.

[3] M. A. Freeman, T. Sculco, and R. C. Todd. Replacement of the severely damaged arthritic knee by the iclh (freeman-swanson) arthroplasty. *J Bone Joint Surg Br*, 59(1):64–71, 1977.

[4] S. Kurtz, F. Mowat, K. Ong, N. Chan, E. Lau, and M. Halpern. Prevalence of primary and revision total hip and knee arthroplasty in the united states from 1990 through 2002. *J Bone Joint Surg Am*, 87(7):1487–97, 2005.

[5] P. Moonot, M. Shang, G. T. Railton, R. E. Field, and S. A. Banks. In vivo weight-bearing kinematics with medial rotation knee arthroplasty. *Knee*, 17(1):33–7, 2010.

[6] J. D. Blaha. The rationale for a total knee implant that confers anteroposterior stability throughout range of motion. *J Arthroplasty*, 19(4 Suppl 1):22–6, 2004.

[7] R. B. Bourne, B. M. Chesworth, A. M. Davis, N. N. Mahomed, and K. D. Charron. Patient satisfaction after total knee arthroplasty: who is satisfied and who is not? *Clin Orthop Relat Res*, 468(1):57–63, 2010.

[8] M. J. Dunbar, G. Richardson, and O. Robertsson. I can't get no satisfaction after my total knee replacement: rhymes and reasons. *Bone Joint J*, 95-B(11 Suppl A):148–52, 2013.

[9] O. Robertsson, M. Dunbar, T. Pehrsson, K. Knutson, and L. Lidgren. Patient satisfaction after knee arthroplasty: a report on 27,372 knees operated on between 1981 and 1995 in sweden. *Acta Orthop Scand*, 71(3):262–7, 2000.

[10] M. Pitta, C. I. Esposito, Z. Li, Y. Y. Lee, T. M. Wright, and D. E. Padgett. Failure after modern total knee arthroplasty: A prospective study of 18,065 knees. *J Arthroplasty*, 2017.

[11] S. Hofmann, G. Seitlinger, O. Djahani, and M. Pietsch. The painful knee after tka: a diagnostic algorithm for failure analysis. *Knee Surg Sports Traumatol Arthrosc*, 19(9):1442–52, 2011.

[12] T. F. Grieco, A. Sharma, G. M. Dessinger, H. E. Cates, and R. D. Komistek. In vivo kinematic comparison of a bicruciate stabilized total knee arthroplasty and the normal knee using fluoroscopy. *J Arthroplasty*, 2017.

[13] D. A. Dennis, R. D. Komistek, and M. R. Mahfouz. In vivo fluoroscopic analysis of fixed-bearing total knee replacements. *Clin Orthop Relat Res*, (410):114–30, 2003.

[14] H. E. Cates, R. D. Komistek, M. R. Mahfouz, M. A. Schmidt, and M. Anderle. In vivo comparison of knee kinematics for subjects having either a posterior stabilized or cruciate retaining high-flexion total knee arthroplasty. *J Arthroplasty*, 23(7):1057–67, 2008.

[15] T. Saari, J. Uvehammer, L. V. Carlsson, P. Herberts, L. Regner, and J. Karrholm. Kinematics of three variations of the freeman-samuelson total knee prosthesis. *Clin Orthop Relat Res*, (410):235–47, 2003.

[16] T. Pfitzner, P. Moewis, P. Stein, H. Boeth, A. Trepczynski, P. von Roth, and G. N. Duda. Modifications of femoral component design in multi-radius total knee arthroplasty lead to higher lateral posterior femorotibial translation. *Knee Surg Sports Traumatol Arthrosc*, 2017.

[17] J. Victor, S. Banks, and J. Bellemans. Kinematics of posterior cruciate ligament-retaining and -substituting total knee arthroplasty: a prospective randomised outcome study. *J Bone Joint Surg Br*, 87(5):646–55, 2005.

[18] H. P. Delport, S. A. Banks, J. De Schepper, and J. Bellemans. A kinematic comparison of fixed- and mobile-bearing knee replacements. *J Bone Joint Surg Br*, 88(8):1016–21, 2006.

[19] S. Yoshiya, N. Matsui, R. D. Komistek, D. A. Dennis, M. Mahfouz, and M. Kurosaka. In vivo kinematic comparison of posterior cruciate-retaining and posterior stabilized total knee arthroplasties under passive and weight-bearing conditions. *J Arthroplasty*, 20(6):777–83, 2005.

[20] M. T. LaCour, A. Sharma, C. B. Carr, R. D. Komistek, and D. A. Dennis. Confirmation of long-term in vivo bearing mobility in eight rotating-platform tkas. *Clin Orthop Relat Res*, 472(9):2766–73, 2014.

[21] X. Shi, B. Shen, J. Yang, P. Kang, Z. Zhou, and F. Pei. In vivo kinematics comparison of fixed- and mobile-bearing total knee arthroplasty during deep knee bending motion. *Knee Surg Sports Traumatol Arthrosc*, 22(7):1612–8, 2014.

[22] S. A. Banks, G. D. Markovich, and W. A. Hodge. In vivo kinematics of cruciate-retaining and -substituting knee arthroplasties. *J Arthroplasty*, 12(3):297–304, 1997.

[23] C. Belvedere, A. Leardini, F. Catani, S. Pianigiani, and B. Innocenti. In vivo kinematics of knee replacement during daily living activities: Condylar and post-cam contact assessment by three-dimensional fluoroscopy and finite element analyses. *J Orthop Res*, 35(7):1396–1403, 2017.

[24] G. Scott, M. A. Imam, A. Eifert, M. A. Freeman, V. Pinskerova, R. E. Field, J. Skinner, and S. A. Banks. Can a total knee arthroplasty be both rotationally unconstrained and anteroposteriorly stabilised? a pulsed fluoroscopic investigation. *Bone Joint Res*, 5(3):80–6, 2016.

[25] B. H. van Duren, H. Pandit, D. J. Beard, A. B. Zavatsky, J. A. Gallagher, N. P. Thomas, D. T. Shakespeare, D. W. Murray, and H. S. Gill. How effective are added constraints in improving tkr kinematics? *J Biomech*, 40 Suppl 1:S31–7, 2007.

[26] A. Shimmin, S. Martinez-Martos, J. Owens, A. D. Iorgulescu, and S. Banks. Fluoroscopic motion study confirming the stability of a medial pivot design total knee arthroplasty. *Knee*, 22(6):522–6, 2015.

[27] H. Iwaki, V. Pinskerova, and M. A. Freeman. Tibiofemoral movement 1: the shapes and relative movements of the femur and tibia in the unloaded cadaver knee. *J Bone Joint Surg Br*, 82(8):1189–95, 2000.

[28] V. Pinskerova, P. Johal, S. Nakagawa, A. Sosna, A. Williams, W. Gedroyc, and M. A. Freeman. Does the femur roll-back with flexion? *J Bone Joint Surg Br*, 86(6):925–31, 2004.

[29] S. Hamai, T. A. Moro-oka, N. J. Dunbar, H. Miura, Y. Iwamoto, and S. A. Banks. In vivo healthy knee kinematics during dynamic full flexion. *Biomed Res Int*, 2013:717546, 2013.

[30] P. Johal, A. Williams, P. Wragg, D. Hunt, and W. Gedroyc. Tibio-femoral movement in the living knee. a study of weight bearing and non-weight bearing knee kinematics using 'interventional' mri. *J Biomech*, 38(2):269–76, 2005.

[31] P. F. Hill, V. Vedi, A. Williams, H. Iwaki, V. Pinskerova, and M. A. Freeman. Tibiofemoral movement 2: the loaded and unloaded living knee studied by mri. *J Bone Joint Surg Br*, 82(8):1196–8, 2000.

[32] T. P. Andriacchi, J. O. Galante, and R. W. Fermier. The influence of total knee-replacement design on walking and stair-climbing. *J Bone Joint Surg Am*, 64(9):1328–35, 1982.

[33] A. Stacoff, I.A. Kramers-de Quervain, G. Luder, R. List, and E. Stüssi. Ground reaction forces on stairs: Effects of stair inclination and age. In *XIXth International Congress of Biomechanics*.

[34] A. S. McIntosh, K. T. Beatty, L. N. Dwan, and D. R. Vickers. Gait dynamics on an inclined walkway. *J Biomech*, 39(13):2491–502, 2006.

[35] A. N. Lay, C. J. Hass, and R. J. Gregor. The effects of sloped surfaces on locomotion: a kinematic and kinetic analysis. *J Biomech*, 39(9):1621–8, 2006.

[36] S. Guan, H. A. Gray, F. Keynejad, and M. G. Pandy. Mobile biplane x-ray imaging system for measuring 3d dynamic joint motion during overground gait. *IEEE Trans Med Imaging*, 35(1):326–36, 2016.

[37] R. List, B. Postolka, P. Schütz, M. Hitz, P. Schwilch, H. Gerber, S. J. Ferguson, and W. R. Taylor. A moving fluoroscope to capture tibiofemoral kinematics during complete cycles of free level and downhill walking as well as stair descent. *PLoS One*, manuscript under review, 2017.

[38] M. Foresti. *In vivo measurement of total knee joint replacement kinematics and kinetics during stair descent.* Phd thesis, 2009.

[39] M. S. Zihlmann, H. Gerber, A. Stacoff, K. Burckhardt, G. Szekely, and E. Stuessi. Three-dimensional kinematics and kinetics of total knee arthroplasty during level walking using single plane video-fluoroscopy and force plates: a pilot study. *Gait Posture*, 24(4):475–81, 2006.

[40] K. Burckhardt, G. Szekely, H. Notzli, J. Hodler, and C. Gerber. Submillimeter measurement of cup migration in clinical standard radiographs. *IEEE Trans Med Imaging*, 24(5):676–88, 2005.

[41] R. List, M. Foresti, H. Gerber, J. Goldhahn, P. Rippstein, and E. Stüssi. Three-dimensional kinematics of an unconstrained ankle arthroplasty: a preliminary in vivo videofluoroscopic feasibility study. *Foot Ankle Int*, 33(10):883–92, 2012.

[42] M. A. Lafortune, P. R. Cavanagh, 3rd Sommer, H. J., and A. Kalenak. Three-dimensional kinematics of the human knee during walking. *J Biomech*, 25(4):347–57, 1992.

[43] A. Cappozzo, U. Della Croce, A. Leardini, and L. Chiari. Human movement analysis using stereophotogrammetry. part 1: theoretical background. *Gait Posture*, 21(2):186–96, 2005.

[44] L. Chiari, U. Della Croce, A. Leardini, and A. Cappozzo. Human movement analysis using stereophotogrammetry. part 2: instrumental errors. *Gait Posture*, 21(2):197–211, 2005.

[45] U. Della Croce, A. Leardini, L. Chiari, and A. Cappozzo. Human movement analysis using stereophotogrammetry. part 4: assessment of anatomical landmark misplacement and its effects on joint kinematics. *Gait Posture*, 21(2):226–37, 2005.

[46] A. Leardini, L. Chiari, U. Della Croce, and A. Cappozzo. Human movement analysis using stereophotogrammetry. part 3. soft tissue artifact assessment and compensation. *Gait Posture*, 21(2):212–25, 2005.

[47] Renate List, Turgut Gülay, Mirjam Stoop, and Silvio Lorenzetti. Kinematics of the trunk and the lower extremities during restricted and unrestricted squats. *The Journal of Strength and Conditioning Research*, 27(6):1529–1538, 2013.

[48] P. Schütz, R. List, R. Zemp, F. Schellenberg, W. R. Taylor, and S. Lorenzetti. Joint angles of the ankle, knee, and hip and loading conditions during split squats. *J Appl Biomech*, 30(3):373–80, 2014.

[49] V. U. Fenner, H. Behrend, and M. S. Kuster. Joint mechanics after total knee arthroplasty while descending stairs. *J Arthroplasty*, 32(2):575–580, 2017.

[50] U. K. Trinler, F. Baty, A. Mundermann, V. Fenner, H. Behrend, B. Jost, and R. Wegener. Stair dimension affects knee kinematics and kinetics in patients with good outcome after tka similarly as in healthy subjects. *J Orthop Res*, 34(10):1753–1761, 2016.

[51] S. Koo and T. P. Andriacchi. The knee joint center of rotation is predominantly on the lateral side during normal walking. *J Biomech*, 41(6):1269–73, 2008.

[52] W. R. Taylor, R. M. Ehrig, G. N. Duda, H. Schell, P. Seebeck, and M. O. Heller. On the influence of soft tissue coverage in the determination of bone kinematics using skin markers. *J Orthop Res*, 23(4):726–34, 2005.

[53] K. Li, L. Zheng, S. Tashman, and X. Zhang. The inaccuracy of surface-measured model-derived tibiofemoral kinematics. *J Biomech*, 45(15):2719–23, 2012.

[54] C. Reinschmidt, A. J. vandenBogert, A. Lundberg, B. M. Nigg, N. Murphy, A. Stacoff, and A. Stano. Tibiofemoral and tibiocalcaneal motion during walking: external vs. skeletal markers. *Gait Posture*, 6(2):98–109, 1997.

[55] A. Barré, J. P. Thiran, B. M. Jolles, N. Theumann, and K. Aminian. Soft tissue artifact assessment during treadmill walking in subjects with total knee arthroplasty. *IEEE Trans Biomed Eng*, 60(11):3131–40, 2013.

[56] A. Barré. *Assessment of the soft tissue artifact on the lower limb using bi-plane fluoroscopy and stereophotogrammetry*. Thesis, 2014.

[57] A. Barré, R. Aissaoui, K. Aminian, and R. Dumas. Assessment of the lower limb soft tissue artefact at marker-cluster level with a high-density marker set during walking. *J Biomech*, 62:21–26, 2017.

[58] D. Solav, V. Camomilla, A. Cereatti, A. Barré, K. Aminian, and A. Wolf. Bone orientation and position estimation errors using cosserat point elements and least squares methods: Application to gait. *J Biomech*, 62:110–116, 2017.

[59] V. Richard, A. Cappozzo, and R. Dumas. Comparative assessment of knee joint models used in multi-body kinematics optimisation for soft tissue artefact compensation. *J Biomech*, 62:95–101, 2017.

[60] V. Bonnet, V. Richard, V. Camomilla, G. Venture, A. Cappozzo, and R. Dumas. Joint kinematics estimation using a multi-body kinematics optimisation and an extended kalman filter, and embedding a soft tissue artefact model. *J Biomech*, 62:148–155, 2017.

[61] B. M. Potvin, M. S. Shourijeh, K. B. Smale, and D. L. Benoit. A practical solution to reduce soft tissue artifact error at the knee using adaptive kinematic constraints. *J Biomech*, 62:124–131, 2017.

[62] A. Leardini, C. Belvedere, F. Nardini, N. Sancisi, M. Conconi, and V. Parenti-Castelli. Kinematic models of lower limb joints for musculo-skeletal modelling and optimization in gait analysis. *J Biomech*, 62:77–86, 2017.

[63] A. Cereatti, T. Bonci, M. Akbarshahi, K. Aminian, A. Barré, M. Begon, D. L. Benoit, C. Charbonnier, F. Dal Maso, S. Fantozzi, C. C. Lin, T. W. Lu, M. G. Pandy, R. Stagni, A. J. van den Bogert, and V. Camomilla. Standardization proposal of soft tissue artefact description for data sharing in human motion measurements. *J Biomech*, 62:5–13, 2017.

[64] M. Sangeux, A. Barré, and K. Aminian. Evaluation of knee functional calibration with and without the effect of soft tissue artefact. *J Biomech*, 62:53–59, 2017.

[65] J. Karrholm, S. Brandsson, and M. A. Freeman. Tibiofemoral movement 4: changes of axial tibial rotation caused by forced rotation at the weight-bearing knee studied by rsa. *J Bone Joint Surg Br*, 82(8):1201–3, 2000.

[66] R. D. Komistek, D. A. Dennis, and M. Mahfouz. In vivo fluoroscopic analysis of the normal human knee. *Clinical Orthopaedics and Related Research*, (410):69–81, 2003.

[67] M. Kozanek, A. Hosseini, F. Liu, S. K. Van de Velde, T. J. Gill, H. E. Rubash, and G. Li. Tibiofemoral kinematics and condylar motion during the stance phase of gait. *J Biomech*, 42(12):1877–84, 2009.

[68] D. A. Dennis, R. D. Komistek, M. R. Mahfouz, B. D. Haas, and J. B. Stiehl. Multicenter determination of in vivo kinematics after total knee arthroplasty. *Clin Orthop Relat Res*, (416):37–57, 2003.

[69] S. A. Banks, C. Lightcap, and J. D. Yamokoski. A robotic radiographic imaging platform for observation of dynamic skeletal motion and tomography. *Journal of Biomechanics*, 39:S446, 2006.

[70] E. S. Grood and W. J. Suntay. A joint coordinate system for the clinical description of three- dimensional motions: application to the knee. *J Biomech Eng*, 105(2):136–44., 1983.

[71] H. J. Woltring. 3-d attitude representation of human joints: a standardization proposal. *Journal of Biomechanics*, 27(12):1399–414., 1994.

[72] M. A. Freeman and V. Pinskerova. The movement of the normal tibio-femoral joint. *J Biomech*, 38(2):197–208, 2005.

[73] S. A. Banks and W. A. Hodge. 2003 hap paul award paper of the international society for technology in arthroplasty. design and activity dependence of kinematics in fixed and mobile-bearing knee arthroplasties. *J Arthroplasty*, 19(7):809–16, 2004.

[74] E. Most, J. Axe, H. Rubash, and G. Li. Sensitivity of the knee joint kinematics calculation to selection of flexion axes. *J Biomech*, 37(11):1743–8, 2004.

[75] D. G. Eckhoff, J. M. Bach, V. M. Spitzer, K. D. Reinig, M. M. Bagur, T. H. Baldini, and N. M. Flannery. Three-dimensional mechanics, kinematics, and morphology of the knee viewed in virtual reality. *J Bone Joint Surg Am*, 87 Suppl 2:71–80, 2005.

[76] D. G. Eckhoff, J. M. Bach, V. M. Spitzer, K. D. Reinig, M. M. Bagur, T. H. Baldini, D. Rubinstein, and S. Humphries. Three-dimensional morphology and kinematics of the distal part of the femur viewed in virtual reality. part ii. *J Bone Joint Surg Am*, 85-A Suppl 4:97–104, 2003.

[77] D. G. Eckhoff, T. F. Dwyer, J. M. Bach, V. M. Spitzer, and K. D. Reinig. Three-dimensional morphology of the distal part of the femur viewed in virtual reality. *J Bone Joint Surg Am*, 83-A Suppl 2(Pt 1):43–50, 2001.

[78] R. C. Wasielewski, R. D. Komistek, S. M. Zingde, K. C. Sheridan, and M. R. Mahfouz. Lack of axial rotation in mobile-bearing knee designs. *Clin Orthop Relat Res*, 466(11):2662–8, 2008.

[79] J. Fisher, H. McEwen, J. Tipper, L. Jennings, R. Farrar, M. Stone, and E. Ingham. Wear-simulation analysis of rotating-platform mobile-bearing knees. *Orthopedics*, 29(9 Suppl):S36–41, 2006.

[80] H. M. McEwen, P. I. Barnett, C. J. Bell, R. Farrar, D. D. Auger, M. H. Stone, and J. Fisher. The influence of design, materials and kinematics on the in vitro wear of total knee replacements. *J Biomech*, 38(2):357–65, 2005.

[81] H. M. McEwen, J. Fisher, A. A. Goldsmith, D. D. Auger, C. Hardaker, and M. H. Stone. Wear of fixed bearing and rotating platform mobile bearing knees subjected to high levels of internal and external tibial rotation. *J Mater Sci Mater Med*, 12(10-12):1049–52, 2001.

[82] S. Simmons, S. Lephart, H. Rubash, P. Borsa, and R. L. Barrack. Proprioception following total knee arthroplasty with and without the posterior cruciate ligament. *J Arthroplasty*, 11(7):763–8, 1996.

[83] M. A. Freeman and G. T. Railton. Should the posterior cruciate ligament be retained or resected in condylar nonmeniscal knee arthroplasty? the case for resection. *J Arthroplasty*, 3 Suppl:S3–12, 1988.

[84] L. D. Dorr, J. L. Ochsner, J. Gronley, and J. Perry. Functional comparison of posterior cruciate-retained versus cruciate-sacrificed total knee arthroplasty. *Clin Orthop*, (236):36–43, 1988.

[85] H. Takagi, S. Asai, A. Sato, M. Maekawa, H. Kawashima, and K. Kanzaki. Case series report of navigation-based in vivo knee kinematics in total knee arthroplasty with a gradually reducing femoral radius design. *Ann Med Surg (Lond)*, 17:33–37, 2017.

[86] P. Moonot, S. Mu, G. T. Railton, R. E. Field, and S. A. Banks. Tibiofemoral kinematic analysis of knee flexion for a medial pivot knee. *Knee Surg Sports Traumatol Arthrosc*, 17(8):927–34, 2009.

[87] R. Schmidt, R. D. Komistek, J. D. Blaha, B. L. Penenberg, and W. J. Maloney. Fluoroscopic analyses of cruciate-retaining and medial pivot knee implants. *Clin Orthop Relat Res*, (410):139–47, 2003.

[88] S. Guan, H. A. Gray, A. G. Schache, J. Feller, R. de Steiger, and M. G. Pandy. In vivo six-degree-of-freedom knee-joint kinematics in overground and treadmill walking following total knee arthroplasty. *J Orthop Res*, 35(8):1634–1643, 2017.

[89] S. A. Banks, B. J. Fregly, F. Boniforti, C. Reinschmidt, and S. Romagnoli. Comparing in vivo kinematics of unicondylar and bi-unicondylar knee replacements. *Knee Surg Sports Traumatol Arthrosc*, 13(7):551–6, 2005.

[90] S. A. Banks and W. A. Hodge. Accurate measurement of three-dimensional knee replacement kinematics using single-plane fluoroscopy. *IEEE Trans Biomed Eng*, 43(6):638–49, 1996.

[91] M. Foresti, H. Gerber, and E. Stuessi. Biomechanics of the knee by means of a two degrees of freedom automated video fluoroscope and instrumented stairs. In *8th International Symposium on Computer Methods in Biomechanics and Biomedical Engineering*.

[92] W. A. Hoff, R. D. Komistek, D. A. Dennis, S. M. Gabriel, and S. A. Walker. Three-dimensional determination of femoral-tibial contact positions under in vivo conditions using fluoroscopy. *Clin Biomech (Bristol, Avon)*, 13(7):455–472, 1998.

[93] G. Li, T. H. Wuerz, and L. E. DeFrate. Feasibility of using orthogonal fluoroscopic images to measure in vivo joint kinematics. *J Biomech Eng*, 126(2):314–8, 2004.

[94] T. A. Moro-oka, M. Muenchinger, J. P. Canciani, and S. A. Banks. Comparing in vivo kinematics of anterior cruciate-retaining and posterior cruciate-retaining total knee arthroplasty. *Knee Surgery, Sports Traumatology, Arthroscopy*, 15(1):93–9, 2007.

[95] Adrija Sharma, Filip Leszko, Richard D Komistek, Giles R Scuderi, Harold E Cates, and Fei Liu. In vivo patellofemoral forces in high flexion total knee arthroplasty. *Journal of biomechanics*, 41(3):642–648, 2008.

[96] J. D. Yamokoski and S. A. Banks. Does close proximity robot motion tracking alter gait? *Gait Posture*, 34(4):508–13, 2011.

[97] F. Liu, R. Komistek, W. Hamel, M. Mahfouz, and P. Gabriel. Automatically image controlled mobile fluoroscope system. *Journal of Biomechanics*, 39:S213, 2006.

[98] M. Zihlmann, R. List, H. Gerber, and E. Stuessi. Net moments of tka during level walking based on video-fluoroscopy coupled with force plate data. *Journal of biomechanics*, 39:S128–S129, 2006.

[99] Joyce L Chen, Virginia B Penhune, and Robert J Zatorre. The role of auditory and premotor cortex in sensorimotor transformations. *Annals of the New York Academy of Sciences*, 1169(1):15–34, 2009.

[100] Ervin Sejdić, Yingying Fu, Alison Pak, Jillian A Fairley, and Tom Chau. The effects of rhythmic sensory cues on the temporal dynamics of human gait. *PloS one*, 7(8):e43104, 2012.

[101] Natalie de Bruin, Cody Kempster, Angelica Doucette, Jon B Doan, Bin Hu, and Lesley A Brown. The effects of music salience on the gait performance of young adults. *Journal of music therapy*, page thv009, 2015.

[102] Jeffrey P Kaipust, Denise McGrath, Mukul Mukherjee, and Nicholas Stergiou. Gait variability is altered in older adults when listening to auditory stimuli with differing temporal structures. *Annals of biomedical engineering*, 41(8):1595–1603, 2013.

[103] M Pat Murray, A Bernard Drought, and Ross C Kory. Walking patterns of normal men. *J Bone Joint Surg Am*, 46(2):335–360, 1964.

[104] E. Stüssi and H.U. Debrunner. Parameter-analyse des menschlichen ganges. *Biomed Tech (Berl)*, 25:222–224, 1980. Stacoff: Ordner Treppe.

[105] A. Stacoff, C. Diezi, G. Luder, E. Stüssi, and I. A. Kramers-de Quervain. Ground reaction forces on stairs: effects of stair inclination and age. *Gait Posture*, 21(1):24–38, 2005.

[106] Giannis Giakas and Vasilios Baltzopoulos. Time and frequency domain analysis of ground reaction forces during walking: an investigation of variability and symmetry. *Gait Posture*, 5(3):189–197, 1997.

[107] R White, I Agouris, RD Selbie, and M Kirkpatrick. The variability of force platform data in normal and cerebral palsy gait. *Clinical biomechanics*, 14(3):185–192, 1999.

[108] MP Kadaba, HK Ramakrishnan, ME Wootten, J Gainey, G Gorton, and GVB Cochran. Repeatability of kinematic, kinetic, and electromyographic data in normal adult gait. *Journal of Orthopaedic Research*, 7(6):849–860, 1989.

[109] Inès A Kramers-de Quervain, Edgar Stüssi, and Alex Stacoff. Ganganalyse beim gehen und laufen. *Schweiz Z. Sportmed. Sporttraum*, 56:35–42, 2008.

[110] Inès A Kramers-de Quervain, Edgar Stüssi, Roland Müller, Tomas Drobny, Urs Munzinger, and Norbert Gschwend. Quantitative gait analysis after bilateral total knee arthroplasty with two different systems within each subject. *The Journal of arthroplasty*, 12(2):168–179, 1997.

[111] H. Abbasi-Bafghi, H. R. Fallah-Yakhdani, O. G. Meijer, H. C. de Vet, S. M. Bruijn, L. Y. Yang, D. L. Knol, B. J. Van Royen, and J. H. van Dieen. The effects of knee arthroplasty on walking speed: a meta-analysis. *BMC Musculoskelet Disord*, 13:66, 2012.

[112] Mrn P Kadaba, HK Ramakrishnan, and ME Wootten. Measurement of lower extremity kinematics during level walking. *Journal of orthopaedic research*, 8(3):383–392, 1990.

[113] Jacquelin Perry and Judith M Burnfield. Gait analysis: normal and pathological function. 1992.

[114] MP Murray, LA Mollinger, GM Gardner, and SB Sepic. Kinematic and emg patterns during slow, free, and fast walking. *Journal of Orthopaedic Research*, 2(3):272–280, 1984.

[115] Robert Riener, Marco Rabuffetti, and Carlo Frigo. Stair ascent and descent at different inclinations. *Gait Posture*, 15(1):32–44, 2002.

[116] R. Stagni, S. Fantozzi, A. Cappello, and A. Leardini. Quantification of soft tissue artefact in motion analysis by combining 3d fluoroscopy and stereophotogrammetry: a study on two subjects. *Clin Biomech (Bristol, Avon)*, 20(3):320–9, 2005.

[117] TP Andriacchi, JA Ogle, and JO Galante. Walking speed as a basis for normal and abnormal gait measurements. *Journal of biomechanics*, 10(4):261–268, 1977.

[118] T. P. Andriacchi, E. J. Alexander, M. K. Toney, C. Dyrby, and J. Sum. A point cluster method for in vivo motion analysis: applied to a study of knee kinematics. *J Biomech Eng*, 120(6):743–9., 1998.

[119] M. Akbarshahi, A. G. Schache, J. W. Fernandez, R. Baker, S. Banks, and M. G. Pandy. Non-invasive assessment of soft-tissue artifact and its effect on knee joint kinematics during functional activity. *J Biomech*, 43(7):1292–301, 2010.

[120] N. Wolterbeek, R. G. Nelissen, and E. R. Valstar. No differences in in vivo kinematics between six different types of knee prostheses. *Knee Surg Sports Traumatol Arthrosc*, 20(3):559–64, 2012.

[121] S. H. Hosseini Nasab, R. List, K. Oberhofer, S. F. Fucentese, J. G. Snedeker, and W. R. Taylor. Loading patterns of the posterior cruciate ligament in the healthy knee: A systematic review. *PLoS One*, 11(11):e0167106, 2016.

[122] K. Oberhofer, S. H. Hosseini Nasab, P. Schütz, B. Postolka, J. G. Snedeker, W. R. Taylor, and R. List. The influence of muscle-tendon forces on acl loading during jump landing: a systematic review. *Muscles Ligaments Tendons J*, 7(1):125–135, 2017.

[123] M. A. Freeman and V. Pinskerova. The movement of the knee studied by magnetic resonance imaging. *Clin Orthop Relat Res*, (410):35–43, 2003.

[124] M. Hajizadeh, R. List, M. O. Heller, R. M. Ehrig, P. Schütz, K. Oberhofer, B. Postolka, and W. R. Taylor. Interpretation of tibio-femoral kinematics critically depends upon the kinematic analysis approach: A survey and comparison of methodologies. in preparation.

[125] M. O. Heller, W. R. Taylor, C. Perka, and G. N. Duda. The influence of alignment on the musculo-skeletal loading conditions at the knee. *Langenbecks Arch Surg*, 388(5):291–7, 2003.

[126] Y. Kuroyanagi, S. Mu, S. Hamai, W. J. Robb, and S. A. Banks. In vivo knee kinematics during stair and deep flexion activities in patients with bicruciate substituting total knee arthroplasty. *J Arthroplasty*, 27(1):122–8, 2012.

[127] W. R. Taylor, P. Schütz, G. Bergmann, R. List, B. Postolka, M. Hitz, J. Dymke, P. Damm, G. Duda, H. Gerber, V. Schwachmeyer, S. H. Hosseini Nasab, A. Trepczynski, and I. Kutzner. A comprehensive assessment of the musculoskeletal system: The cams-knee data set. *J Biomech*, 2017.

[128] H. Gerber, M. Foresti, M. Zihlmann, and E. Stüssi. Method to simultaneously measure kinetic and 3d kinematic data during normal level walking using kistler force plates, vicon system and video-fluoroscopy. *Journal of Biomechanics*, 40(Supplement 2):S405–S405, 2007.

[129] R. List, H. Gerber, M. Foresti, P. Rippstein, and J. Goldhahn. A functional outcome study comparing total ankle arthroplasty (taa) subjects with pain to subjects with absent level of pain by means of videofluoroscopy. *Foot Ankle Surg*, 18(4):270–6, 2012.

[130] T. C. Pataky, M. A. Robinson, and J. Vanrenterghem. Region-of-interest analyses of one-dimensional biomechanical trajectories: bridging 0d and 1d theory, augmenting statistical power. *PeerJ*, 4:e2652, 2016.

[131] P. Moewis, G. N. Duda, T. Jung, M. O. Heller, H. Boeth, B. Kaptein, and W. R. Taylor. The restoration of passive rotational tibio-femoral laxity after anterior cruciate ligament reconstruction. *PLoS One*, 11(7):e0159600, 2016.

[132] C. W. Clary, C. K. Fitzpatrick, L. P. Maletsky, and P. J. Rullkoetter. The influence of total knee arthroplasty geometry on mid-flexion stability: an experimental and finite element study. *J Biomech*, 46(7):1351–7, 2013.

[133] A. Stacoff, I. A. Kramers-de Quervain, G. Luder, R. List, and E. Stüssi. Ground reaction forces on stairs. part ii: knee implant patients versus normals. *Gait Posture*, 26(1):48–58, 2007.

[134] R. M. Ehrig, W. R. Taylor, G. N. Duda, and M. O. Heller. A survey of formal methods for determining functional joint axes. *J Biomech*, 40(10):2150–7, 2007.

[135] H. Asano, A. Hoshino, and T. J. Wilton. Soft-tissue tension total knee arthroplasty. *J Arthroplasty*, 19(5):558–61, 2004.

[136] M. Schiraldi, G. Bonzanini, D. Chirillo, and V. de Tullio. Mechanical and kinematic alignment in total knee arthroplasty. *Ann Transl Med*, 4(7):130, 2016.

[137] M. Hitz, P. Schütz, M. Angst, W. R. Taylor, and R. List. Influence of the moving fluoroscope on gait patterns. *PLoS One*, 13(7):e0200608, 2018. Hitz, Marina Schütz, Pascal Angst, Michael Taylor, William R List, Renate eng PLoS One. 2018 Jul 13;13(7):e0200608. doi: 10.1371/journal.pone.0200608. eCollection 2018.

[138] J. W. Pritchett. Patients prefer a bicruciate-retaining or the medial pivot total knee prosthesis. *J Arthroplasty*, 26(2):224–8, 2011.

[139] N. Wolterbeek, E. H. Garling, B. J. Mertens, R. G. Nelissen, and E. R. Valstar. Kinematics and early migration in single-radius mobile- and fixed-bearing total knee prostheses. *Clin Biomech (Bristol, Avon)*, 27(4):398–402, 2012.

[140] M.A. Lafortune. *The use of intra-cortical pins to measure the motion of the knee joint during walking*. Phd thesis, 1984.

[141] P. Schütz, B. Postolka, H. Gerber, S. J. Ferguson, W. R. Taylor, and R. List. Knee implant kinematics are task dependent. *submitted*.

[142] D. Dennis, R. Komistek, G. Scuderi, J. N. Argenson, J. Insall, M. Mahfouz, J. M. Aubaniac, and B. Haas. In vivo three-dimensional determination of kinematics for subjects with a normal knee or a unicompartmental or total knee replacement. *J Bone Joint Surg Am*, 83-A Suppl 2 Pt 2:104–15, 2001.

[143] T. D. Szwedowski, W. R. Taylor, M. O. Heller, C. Perka, M. Muller, and G. N. Duda. Generic rules of mechano-regulation combined with subject specific loading conditions can explain bone adaptation after tha. *PLoS One*, 7(5):e36231, 2012.

[144] M. S. Thompson, M. N. Bajuri, H. Khayyeri, and H. Isaksson. Mechanobiological modelling of tendons: Review and future opportunities. *Proc Inst Mech Eng H*, 231(5):369–377, 2017.

[145] Y. Niki, Y. Takeda, K. Udagawa, H. Enomoto, Y. Toyama, and Y. Suda. Is greater than 145degrees of deep knee flexion under weight-bearing conditions safe after total knee arthroplasty?: a fluoroscopic analysis of japanese-style deep knee flexion. *Bone Joint J*, 95-B(6):782–7, 2013.

[146] Jr. Lombardi, A. V. Do new materials improve acetabular fixation and reduce wear? commentary on an article by david c. ayers, md, et al.: "radiostereometric analysis study of tantalum compared with titanium acetabular cups and highly cross-linked compared with conventional liners in young patients undergoing total hip replacement". *J Bone Joint Surg Am*, 97(8):e39, 2015.

[147] H. Boeth, G. N. Duda, M. O. Heller, R. M. Ehrig, R. Doyscher, T. Jung, P. Moewis, S. Scheffler, and W. R. Taylor. Anterior cruciate ligament-deficient patients with passive knee joint laxity have a decreased range of anterior-posterior motion during active movements. *Am J Sports Med*, 41(5):1051–7, 2013.

[148] F. Schellenberg, W. R. Taylor, A. Trepczynski, R. List, I. Kutzner, P. Schütz, G. N. Duda, and S. Lorenzetti. Evaluation of the accuracy of musculoskeletal simulation during squats by means of instrumented knee prostheses. *Journal of biomechanics*, in review, 2017.

[149] B. J. Fregly, T. F. Besier, D. G. Lloyd, S. L. Delp, S. A. Banks, M. G. Pandy, and D. D. D'Lima. Grand challenge competition to predict in vivo knee loads. *J Orthop Res*, 30(4):503–13, 2012.

[150] A. L. Kinney, T. F. Besier, D. D. D'Lima, and B. J. Fregly. Update on grand challenge competition to predict in vivo knee loads. *J Biomech Eng*, 135(2):021012, 2013.

[151] Z. Zhu and G. Li. An automatic 2d-3d image matching method for reproducing spatial knee joint positions using single or dual fluoroscopic images. *Comput Methods Biomech Biomed Engin*, 15(11):1245–56, 2012.

[152] B. Heinlein, F. Graichen, A. Bender, A. Rohlmann, and G. Bergmann. Design, calibration and pre-clinical testing of an instrumented tibial tray. *J Biomech*, 40 Suppl 1:S4–10, 2007.

[153] F. Graichen, R. Arnold, A. Rohlmann, and G. Bergmann. Implantable 9-channel telemetry system for in vivo load measurements with orthopedic implants. *IEEE Trans Biomed Eng.*, 54(2):253–61, 2007.

[154] I. Kutzner, B. Heinlein, F. Graichen, A. Bender, A. Rohlmann, A. Halder, A. Beier, and G. Bergmann. Loading of the knee joint during activities of daily living measured in vivo in five subjects. *J Biomech*, 43(11):2164–73, 2010.

[155] W. R. Taylor, E. I. Kornaropoulos, G. N. Duda, S. Kratzenstein, R. M. Ehrig, A. Arampatzis, and M. O. Heller. Repeatability and reproducibility of ossca, a functional approach for assessing the kinematics of the lower limb. *Gait Posture*, 32(2):231–6, 2010.

[156] R. M. Ehrig, M. O. Heller, S. Kratzenstein, G. N. Duda, A. Trepczynski, and W. R. Taylor. The score residual: a quality index to assess the accuracy of joint estimations. *J Biomech*, 44(7):1400–4, 2011.

[157] R. M. Ehrig, W. R. Taylor, G. N. Duda, and M. O. Heller. A survey of formal methods for determining the centre of rotation of ball joints. *J Biomech*, 39(15):2798–809, 2006.

[158] M. O. Heller, S. Kratzenstein, R. M. Ehrig, G. Wassilew, G. N. Duda, and W. R. Taylor. The weighted optimal common shape technique improves identification of the hip joint center of rotation in vivo. *J Orthop Res*, 29(10):1470–5, 2011.

[159] S. Kratzenstein, E. I. Kornaropoulos, R. M. Ehrig, M. O. Heller, B. M. Popplau, and W. R. Taylor. Effective marker placement for functional identification of the centre of rotation at the hip. *Gait Posture*, 36(3):482–6, 2012.

[160] R. List, M. Hitz, M. Angst, W. R. Taylor, and S. Lorenzetti. In-situ force plate calibration: 12 years' experience with an approach for correcting the point of force application. *Gait Posture*, 58:98–102, 2017.

[161] A.O. Perotto. *Anatomical Guide for the Electromyographer – the Limbs and Trunk*. Charles C Thomas Publisher LTD, 5 edition, 2011.

[162] O. M. Mahoney, T. L. Kinsey, A. Z. Banks, and S. A. Banks. Rotational kinematics of a modern fixed-bearing posterior stabilized total knee arthroplasty. *J Arthroplasty*, 24(4):641–5, 2009.

[163] G. Maderbacher, C. Baier, H. R. Springorum, F. Zeman, J. Grifka, and A. Keshmiri. Lower limb anatomy and alignment affect natural tibiofemoral knee kinematics: A cadaveric investigation. *J Arthroplasty*, 31(9):2038–42, 2016.

[164] G. Maderbacher, C. Baier, H. R. Springorum, H. Maderbacher, A. M. Birkenbach, A. Benditz, J. Grifka, and A. Keshmiri. Impact of axial component alignment in total knee arthroplasty on lower limb rotational alignment: An in vitro study. *J Knee Surg*, 30(4):372–377, 2017.

[165] M. G. Benedetti, F. Catani, T. W. Bilotta, M. Marcacci, E. Mariani, and S. Giannini. Muscle activation pattern and gait biomechanics after total knee replacement. *Clin Biomech (Bristol, Avon)*, 18(9):871–6, 2003.

[166] A. J. Johnson, S. F. Harwin, K. A. Krackow, and M. A. Mont. Alignment in total knee arthroplasty: Where have we come from and where are we going? *Surg Technol Int*, 21:183–8, 2011. Johnson, Aaron J Harwin, Steven F Krackow, Kenneth A Mont, Michael A eng 2012/04/17 06:00 Surg Technol Int. 2011 Dec;21:183-8.

[167] A. Navacchia, P. J. Rullkoetter, P. Schütz, R. B. List, C. K. Fitzpatrick, and K. B. Shelburne. Subject-specific modeling of muscle force and knee contact in total knee arthroplasty. *J Orthop Res*, 34(9):1576–87, 2016.

[168] S. J. Breugem and D. Haverkamp. Anterior knee pain after a total knee arthroplasty: What can cause this pain? *World J Orthop*, 5(3):163–70, 2014.

Appendix A

Appendix: Supplementary material

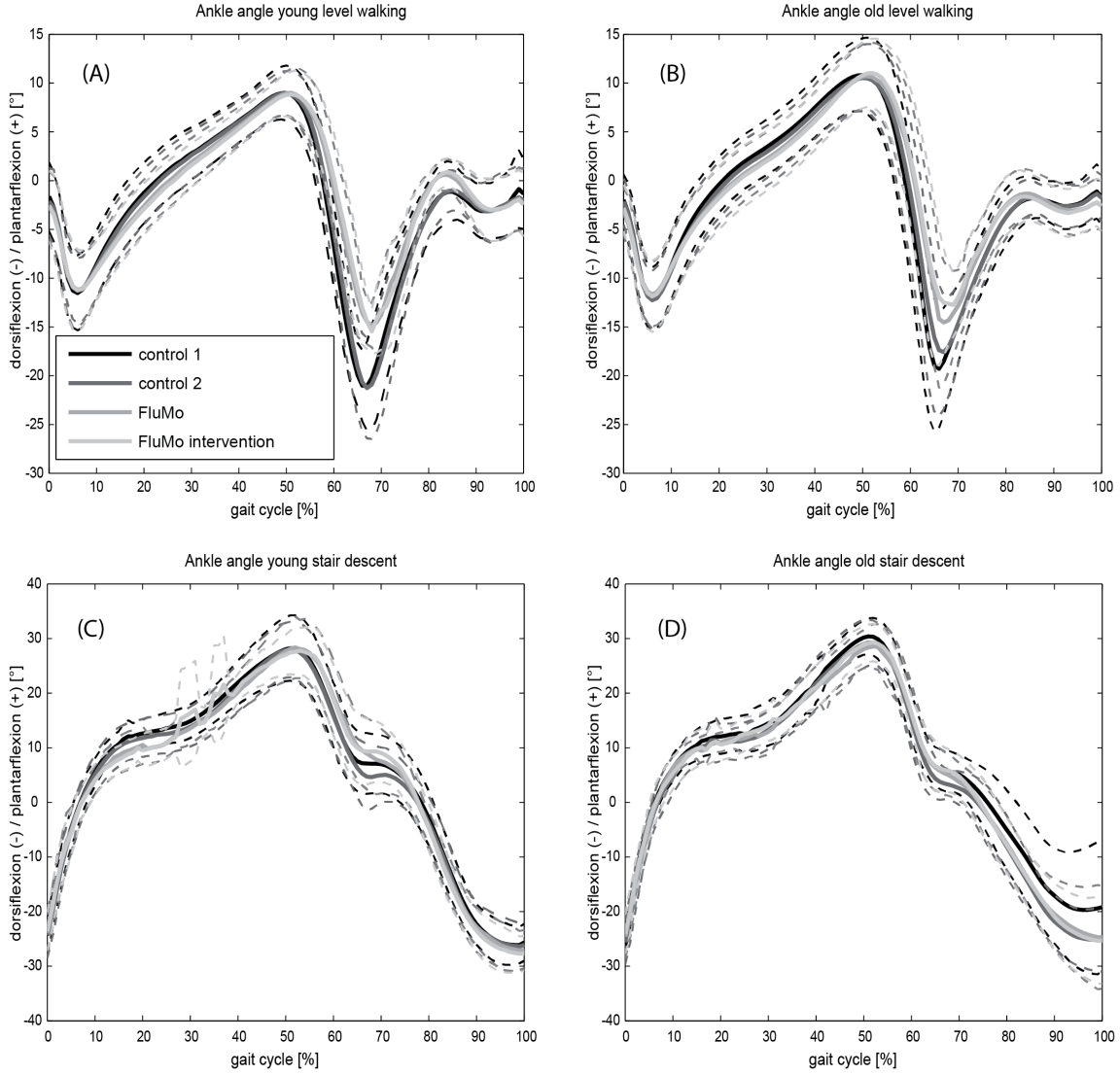

Figure A.1: Ankle sagittal plane movement. Mean and standard deviation of ankle sagittal plane movement in level gait (A, B) and stair descent (C, D) for the young (A, C) and elderly (B, D) age groups.

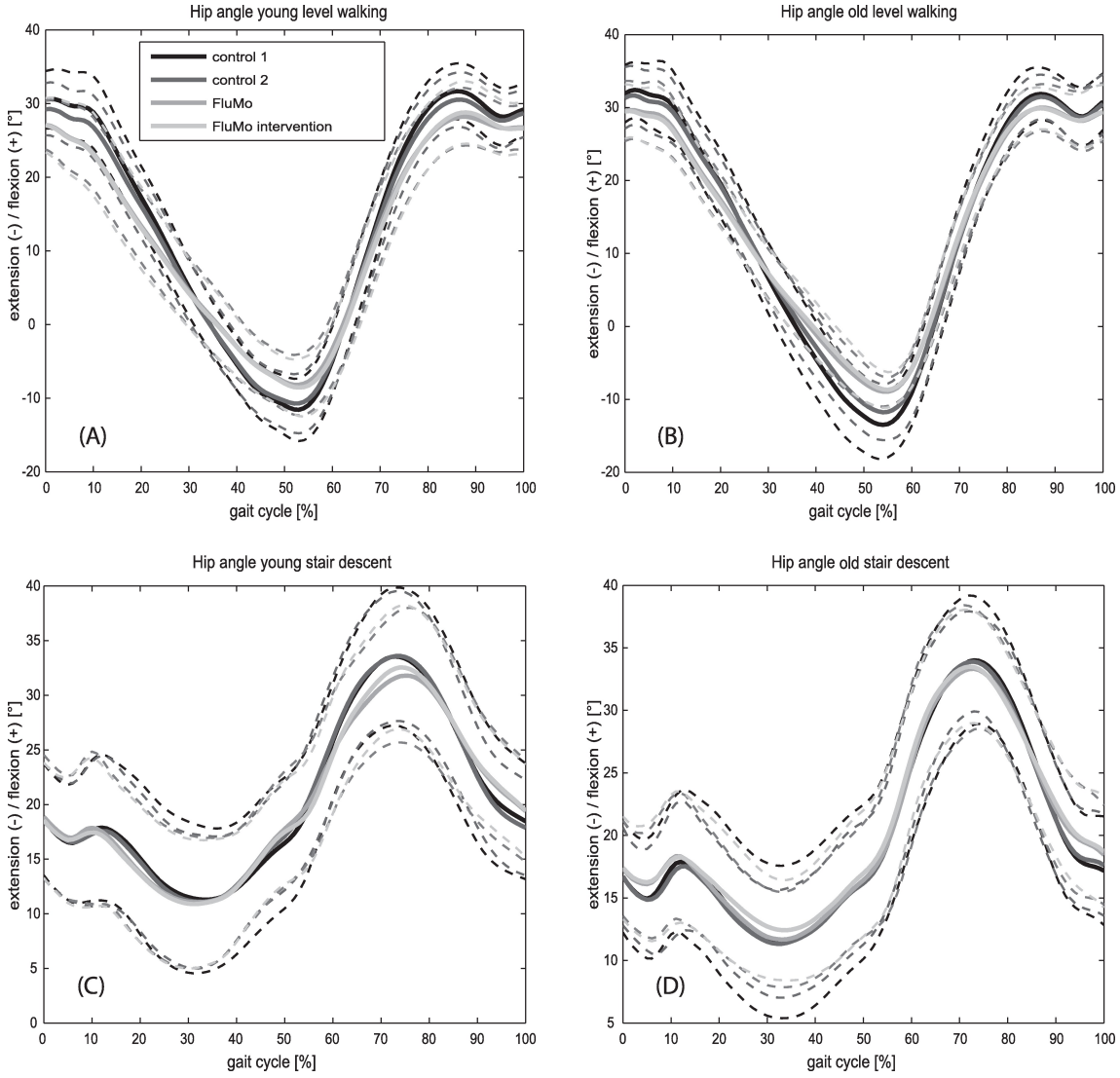

Figure A.2: Hip sagittal plane movement. Mean and standard deviation of hip flexion/extension in level gait (A, B) and stair descent (C, D) for the young (A, C) and elderly (B, D) age groups.

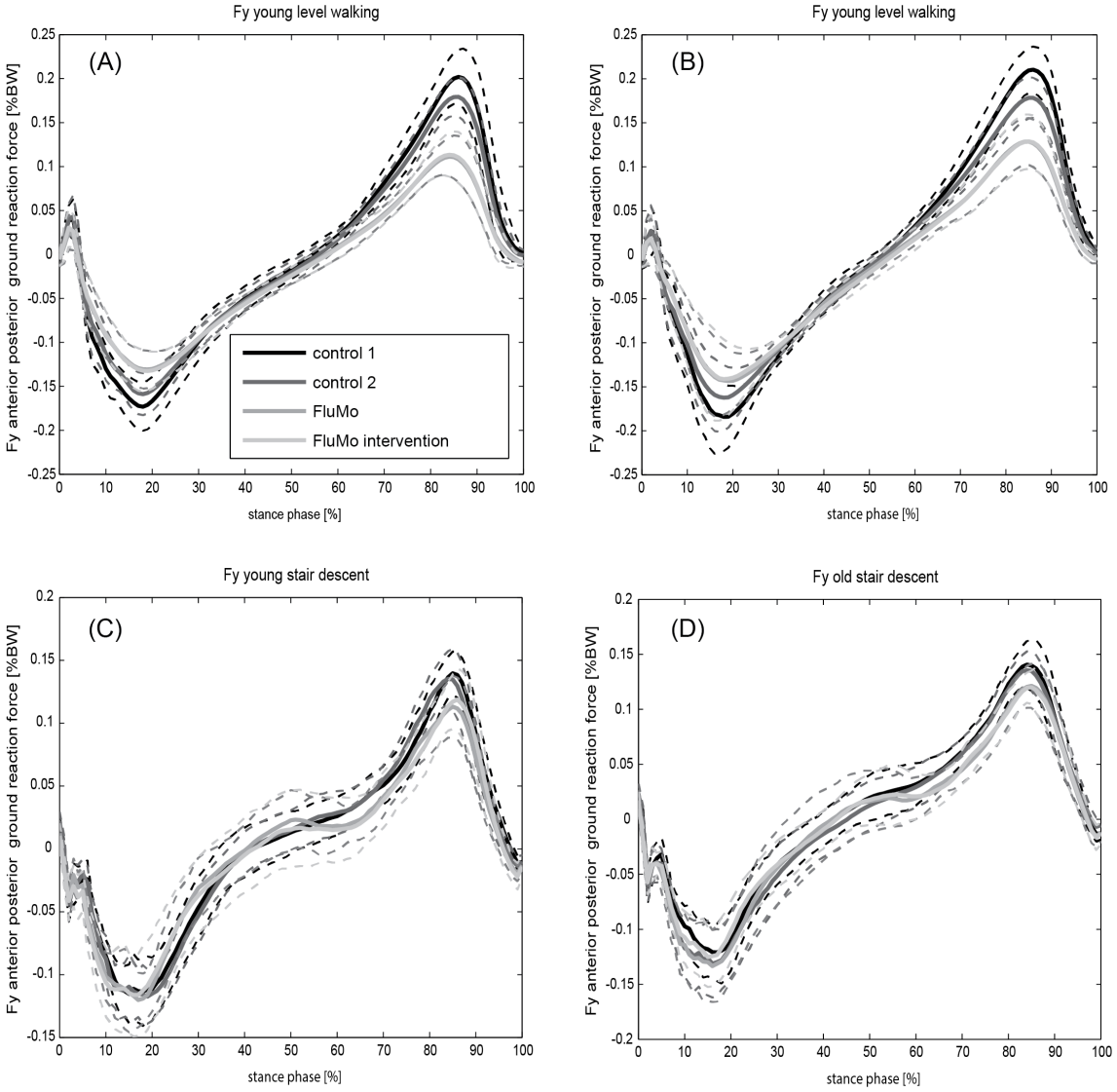

Figure A.3: Anterior-posterior ground reaction forces. Mean and standard deviation of anterior (negative) and posterior (positive) ground reaction forces (Fy) in level gait (A. B) and stair descent (C, D) for the young (A, C) and elderly (B, D) age groups.

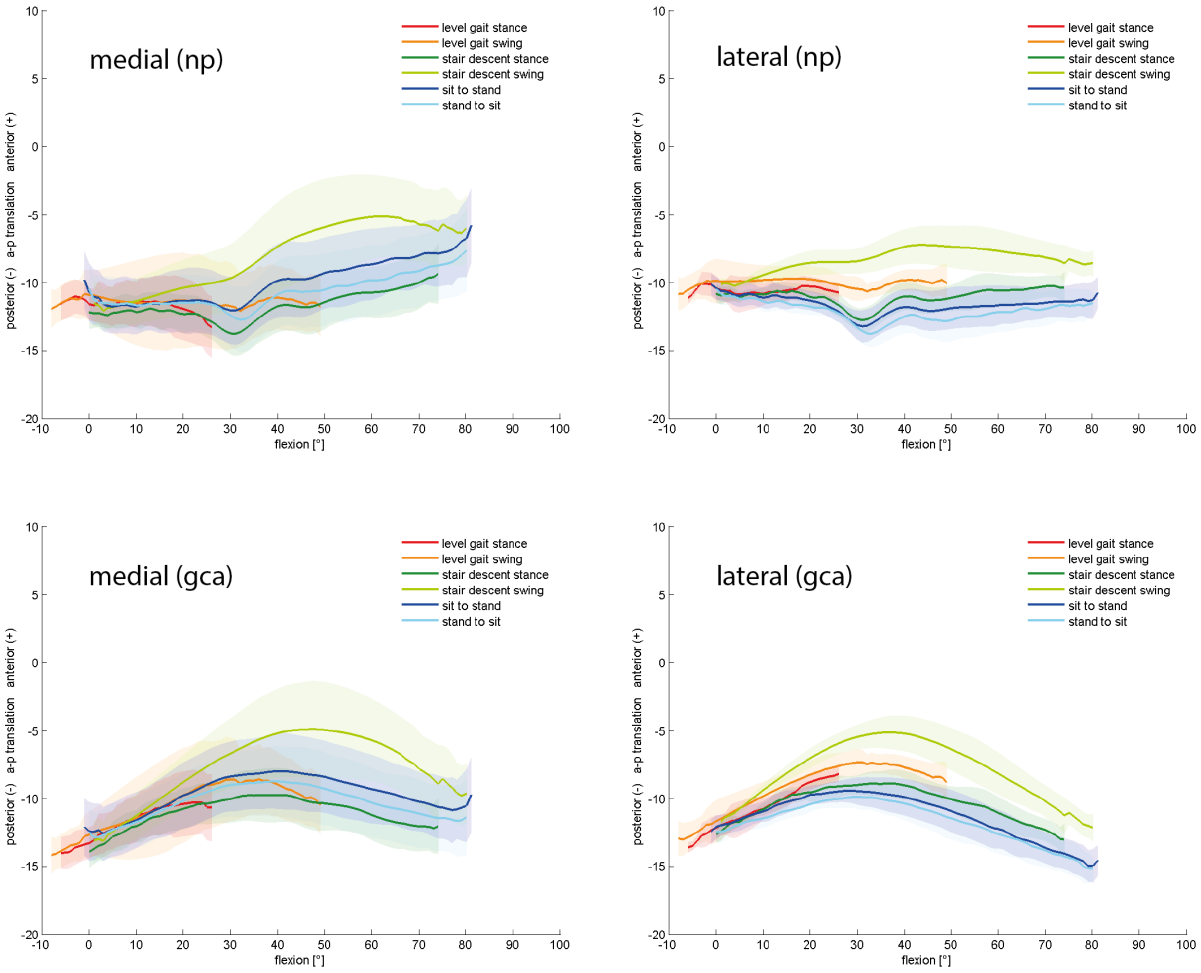

Figure A.4: Kinematic coupling of A-P translation and knee flexion for the medial and lateral condyle, mean and SD over all subjects: Nearest point approach (np) vs. geometric center axis (gca).